

**EFFECT OF PDLA ON CRYSTALLINITY,
MECHANICAL PROPERTIES AND HDT
OF PLA/NR BLENDS**



**A Thesis Submitted in Partial Fulfillment of the Requirements for the
Degree of Master of Engineering in Polymer Engineering
Suranaree University of Technology
Academic Year 2017**

ผลของพอลิดีแลคติกแอซิดต่อปริมาณผลึก สมบัติทางกลและอุณหภูมิโคงตัว
ด้วยความร้อนของพอลิเมอร์ผสมระหว่างพอลิแลคติกแอซิดและยางธรรมชาติ



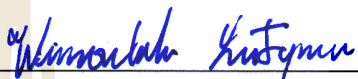
นางสาวชिरาภรณ์ พงศ์พุฒิพัชร

วิทยานิพนธ์นี้เป็นส่วนหนึ่งของการศึกษาตามหลักสูตรปริญญาวิศวกรรมศาสตรมหาบัณฑิต
สาขาวิชาวิศวกรรมพอลิเมอร์
มหาวิทยาลัยเทคโนโลยีสุรนารี
ปีการศึกษา 2560

**EFFECT OF PDLA ON CRYSTALLINITY, MECHANICAL
PROPERTIES AND HDT OF PLA/NR BLENDS**

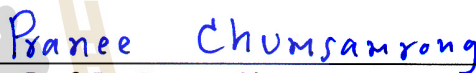
Suranaree University of Technology has approved this thesis submitted in fulfillment of the requirements for a Master's Degree.

Thesis Examining Committee




(Asst. Prof. Dr. Wimonlak Sutapun)

Chairperson



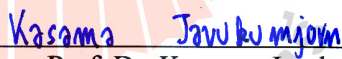
(Asst. Prof. Dr. Pranee Chumsamrong)

Member (Thesis Advisor)



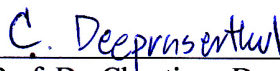
(Assoc. Prof. Dr. Yupaporn Raksakulpiwat)

Member



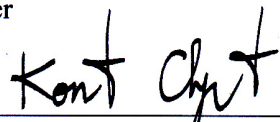
(Assoc. Prof. Dr. Kasama Jarukumjorn)

Member




(Asst. Prof. Dr. Chantima Deprasertkul)

Member



(Assoc. Prof. Ft. Lt. Dr. Kontorn Chamniprasart)



(Prof. Dr. Santi Maensiri)

Vice Rector for Academic Affairs
and Internationalization

Dean of Institute of Engineering

วชิราภรณ์ พงศ์วุฒิพัชร : ผลของพอลิดีแลคติกแอซิดต่อปริมาณผลึก สมบัติทางกลและ
อุณหภูมิโค้งตัวด้วยความร้อนของพอลิเมอร์ผสมระหว่างพอลิแลคติกแอซิดและยาง
ธรรมชาติ (EFFECT OF PDLA ON CRYSTALLINITY, MECHANICAL PROPERTIES
AND HDT OF PLA/NR BLENDS) อาจารย์ที่ปรึกษา : ผู้ช่วยศาสตราจารย์ ดร.ปราณี
ชุมสำโรง, 112 หน้า

ในการศึกษานี้พอลิเมอร์ผสมระหว่างพอลิแลคติกแอซิดกับยางธรรมชาติที่อัตราส่วนต่างๆ
คือ 95/5, 90/10, 85/15 และ 80/20 เปอร์เซ็นต์โดยน้ำหนัก เตรียมขึ้นโดยใช้เทคนิคผสมแบบหลอม
ด้วยเครื่องบดผสมภายใน ชิ้นงานทดสอบถูกขึ้นรูปด้วยเครื่องกดอัด สมบัติทางกล อุณหภูมิโค้งตัว
ด้วยความร้อน และสัณฐานวิทยาของพอลิเมอร์ผสมระหว่างพอลิแลคติกแอซิดและยางธรรมชาติถูก
ศึกษา พบว่า ค่าความต้านทานต่อแรงกระแทกและค่าความยืดสูงสุด ณ จุดขาด ของพอลิเมอร์ผสม
ระหว่างพอลิแลคติกแอซิดกับยางธรรมชาติเพิ่มขึ้นเมื่อเพิ่มปริมาณยางธรรมชาติจนถึง 15
เปอร์เซ็นต์โดยน้ำหนัก ในขณะที่ค่าความต้านแรงดึงและค่ามอดุลัสลดลง อุณหภูมิโค้งตัวด้วยความ
ร้อนของพอลิเมอร์ผสมลดลงเล็กน้อย ภาพถ่ายจากกล้องจุลทรรศน์อิเล็กตรอนแบบส่องกราด
(scanning electron microscopy, SEM) แสดงให้เห็นว่าพอลิแลคติกแอซิดกับยางธรรมชาติไม่เข้ากัน

ความต้านทานต่อแรงกระแทกแบบไอซอดที่มีการบากชิ้นงาน (notched) และไม่บากชิ้นงาน
(unnotched) และค่าความยืดสูงสุด ณ จุดขาดของพอลิเมอร์ผสมมีค่าสูงสุดเมื่อปริมาณยางธรรมชาติ
เท่ากับ 15 เปอร์เซ็นต์โดยน้ำหนัก [PLA/NR(85/15)] โดยมีค่าเท่ากับ 167.22 กิโลจูลต่อตารางเมตร
54.31 กิโลจูลต่อตารางเมตร และ 257.85 เปอร์เซ็นต์ ตามลำดับ ดังนั้นพอลิเมอร์ผสมระหว่างพอลิ
แลคติกแอซิดกับยางธรรมชาติที่อัตราส่วน 85/15 เปอร์เซ็นต์โดยน้ำหนักจึงถูกเลือกเพื่อมาศึกษาผล
ของพอลิดีแลคติกแอซิดต่อสมบัติทางกล สมบัติทางความร้อน และอุณหภูมิโค้งตัวด้วยความร้อน
ของพอลิเมอร์ผสมระหว่างพอลิแลคติกแอซิดและยางธรรมชาติ ปริมาณพอลิดีแลคติกแอซิดมีค่า
เป็น 1, 3 และ 5 เปอร์เซ็นต์โดยน้ำหนักของปริมาณพอลิแลคติกแอซิดในพอลิเมอร์ผสม ผลการ
ทดลองแสดงให้เห็นว่า ค่าความต้านทานต่อแรงกระแทกและค่าความยืดสูงสุด ณ จุดขาดของพอลิ
เมอร์ผสมลดลงเมื่อเพิ่มปริมาณพอลิดีแลคติกแอซิดแต่ยังคงสูงกว่าพอลิแลคติกแอซิด อุณหภูมิโค้ง
ตัวด้วยความร้อนของพอลิเมอร์ผสมที่เติมพอลิดีแลคติกแอซิดปริมาณ 1 เปอร์เซ็นต์โดยน้ำหนักของ
ปริมาณพอลิแลคติกแอซิด [PLA/NR/PDLA(1)] มีค่าสูงสุด ปริมาณผลึกและทรานซิชันทางความ
ร้อนของพอลิเมอร์ผสมระหว่างพอลิแลคติกแอซิด, ยางธรรมชาติ และพอลิดีแลคติกแอซิดถูก
ตรวจสอบโดยเครื่องดิฟเฟอเรนเชียลสแกนนิ่งแคลอริมิเตอร์ (differential scanning calorimeter DSC)
พบว่า ปริมาณผลึกของพอลิเมอร์ผสมระหว่างพอลิแลคติกแอซิด, ยางธรรมชาติ และพอลิดีแลคติก

แฉ็ดสูงกว่ำพอลิแลคติกแฉ็ด จากข้อมูลการให้ควมร้อนครั้งทีหนึ่ง พบว่า อุณหภูมิการตกผลึก (cold crystallization temperature, T_{cc}) ของพอลิเมอร์ผสมสูงกว่ำ T_{cc} ของพอลิแลคติกแฉ็ด อุณหภูมิการหลอมเหลว (melting temperature, T_m) ของพอลิแลคติกแฉ็ดในพอลิเมอร์ผสมมีค่าสูงขึ้ ยกเว้น T_{cc} ของพอลิเมอร์ผสม PLA/NR/PDLA(1) ไม่ปรากฏในการให้ควมร้อนครั้งทีหนึ่ง ข้อมูลจากการให้ควมร้อนครั้งทีสอง พบว่า อุณหภูมิเปลี่ยนสภาพแก้ว (glass transition temperature, T_g) ของเฟสพอลิแลคติกแฉ็ดในพอลิเมอร์ผสมเพิ่มขึ้นเมื่อใส่ยางธรรมชาติ T_{cc} ของพอลิเมอร์ผสมระหว่างพอลิแลคติกแฉ็ดกับยางธรรมชาติและพอลิดีแลคติกแฉ็ดต่ำกว่ำพอลิเมอร์ผสม PLA/NR(85/15) T_g และ T_m ของพอลิแลคติกแฉ็ดในพอลิเมอร์ผสมไม่มีการเปลี่ยนแปลงอย่างมีนัยสำคัญเมื่อเติมพอลิดีแลคติกแฉ็ด ภาพถ่ายจากกล้องจุลทรรศน์อิเล็กตรอนแบบส่องกราด แสดงให้เห็นว่า ขนาดของอนุภาคยางเพิ่มขึ้นเมื่อเติมพอลิดีแลคติกแฉ็ดลงไปนพอลิเมอร์ผสมระหว่างพอลิแลคติกแฉ็ดกับยางธรรมชาติ แผนภาพการกระเจิงรังสีเอกซ์ (Wide Angle X-ray Scattering, WAXS, patterns) ของพอลิเมอร์ผสมทีเติมพอลิดีแลคติกแฉ็ดแสดงพีคการกระเจิงของรังสีเอกซ์อันเนื่องมาผลึกสเตริโอคอมเพล็กซ์ (stereocomplex crystallite) ณ มุม 2θ เท่ากับ 10.5° , 18.5° และ 23.8° ความเข้มของพีคสูงขึ้เมื่อปริมาณพอลิดีแลคติกแฉ็ดเพิ่มขึ้น

เพื่อศึกษาผลของการอบอ่อนทีมีต่อสมบัติทางกล สมบัติทางควมร้อนและอุณหภูมิโก่งตัวทางควมร้อนของพอลิเมอร์ผสม ซึ้นทดสอบถูกนำไปอบในตู้อบลมร้อนทีอุณหภูมิ 100 องศาเซลเซียสเป็นเวลา 10, 30 และ 60 นาที พบว่า ค่าควมต้านแรงดึง ค่ามอดุลัส ค่าควมยืดสูงสุด ณ จุดขาดและค่าควมต้านทานต่อแรงกระแทกพอลิเมอร์ผสมหลังการอบอ่อนมีแนวโน้มลดลง อุณหภูมิโก่งตัวด้วยควมร้อนและปริมาณผลึกของพอลิแลคติกแฉ็ด พอลิเมอร์ผสมระหว่างพอลิแลคติกแฉ็ดกับยางธรรมชาติ และพอลิเมอร์ผสมระหว่างพอลิแลคติกแฉ็ดกับยางธรรมชาติทีเติมพอลิดีแลคติกแฉ็ดเพิ่มขึ้นเมื่อเวลาการอบอ่อนเพิ่มขึ้น อุณหภูมิการหลอมเหลวของพอลิแลคติกแฉ็ดในพอลิเมอร์ผสมสูงขึ้หลังจากผ่านการอบอ่อน ภาพถ่ายจากกล้องจุลทรรศน์อิเล็กตรอนแบบส่องกราด แสดงให้เห็นว่า ขนาดอนุภาคยางในพอลิเมอร์ผสมมีขนาดใหญ่ขึ้เมื่อเพิ่มเวลากการอบอ่อน

สาขาวิชา วิศวกรรมพอลิเมอร์

ปีการศึกษา 2560

ลายมือชื่อนักศึกษา จิราภรณ์

ลายมือชื่ออาจารย์ทีปรึกษา Pranee Chumsamrong

ลายมือชื่ออาจารย์ทีปรึกษาร่วม Wanpaporn Alf

WACHIRABHORN PONGPUTTHIPAT : EFFECT OF PDLA ON
CRYSTALLINITY, MECHANICAL PROPERTIES AND HDT OF PLA/NR
BLENDS. THESIS ADVISOR : ASST. PROF. PRANEE
CHUMSAMRONG, Ph.D., 112 PP.

POLY(LACTIC ACID)/NATURAL RUBBER/POLY(D-LACTIC ACID)/
STEREOCOMPLEX CRYSTALLITE/HDT/ANNEALING

In this study, polymer blends of poly(lactic acid) (PLA) and natural rubber (NR) at the ratios of 95/5, 90/10, 85/15 and 80/20 (wt%) were melt blended using an internal mixer. The test specimens were molded using a compression molding machine. Mechanical properties, heat distortion temperatures (HDT) and morphologies of PLA/NR blends were studied. It was found that the impact strength and elongation at break of PLA/NR blends increased with increasing NR content up to 15 wt%. While tensile strength and Young's modulus decreased. HDT of the PLA/NR blends was slightly decreased. SEM micrographs showed that PLA/NR blends were immiscible.

The highest unnotched, notched Izod impact strength and elongation at break were found for the blend containing 15 wt% NR [PLA/NR(85/15)] which were 167.22 kJ/m², 54.31 kJ/m² and 257.85%, respectively. Therefore, PLA/NR(85/15) was chosen to study the effect of poly(D-lactic acid) (PDLA) on mechanical, thermal properties and HDT of PLA/NR blend. The amounts of PDLA in PLA/NR (85/15) blend were 1, 3 and 5 wt% based on PLA content. The results showed that impact strength and elongation at break of PLA/NR(85/15) blend were decreased with increasing PDLA content. However, the values were higher than those of neat PLA. HDT of the blend with 1 wt% PDLA based on PLA content [PLA/NR-/PDLA(1)] was the highest value. The crystallinity (X_c) and thermal transitions of PLA/-

NR/PDLA blends were examined using differential scanning calorimeter (DSC). It was found that X_c of the PLA/NR/PDLA blends was higher than that of neat PLA. From first heating scan results, with an exception of the blend containing 1 %wt PDLA, cold crystallization temperature (T_{cc}) of the blends was higher than that of neat PLA. Melting temperature (T_m) of PLA in the blend was also shifted to higher temperature. T_{cc} of PLA phase did not find in PLA/NR/PDLA(1). From DSC second heating scan results, glass transition temperature (T_g) of PLA was increased with adding NR into PLA. T_{cc} of PLA/NR/PDLA blends were lower than PLA/NR(85/15). T_g and T_m of PLA in the blends did not significantly change with adding PDLA. SEM micrographs revealed the increment in average diameter of NR particles in the blend containing PDLA. Wide angle x-ray scattering patterns of PLA/NR/PDLA blends exhibited scattering peaks of stereocomplex crystallite at $2\theta = 10.5^\circ$, 18.5° and 23.8° . These scattering peaks become sharper with increasing PDLA content.

To study the effects of annealing treatment on the properties of the blends, the blend specimens were annealed in an air oven at 100°C for 10, 30 and 60 minutes. The tensile strength, Young's modulus, elongation at break and impact strength of the blends after annealing treatment tended to decrease. HDTs and X_c of PLA, PLA/NR(85/15) and PLA/NR/PDLA blends increased with an increase of annealing time. SEM micrographs exhibited the domain NR droplets size tended to increase when the annealing time was increased.

School of Polymer Engineering

Academic Year 2017

Student's Signature Wachirabhorn

Advisor's Signature Pranee Chumsamrong

Co-Advisor's Signature Prasanna

ACKNOWLEDGEMENTS

I gratefully acknowledge the financial supports from Suranaree University of Technology and Center of Excellence on Petrochemical and Materials Technology. I am grateful to all the faculty and staff members of the School of Polymer Engineering and the Center for Scientific and Technological Equipment of Suranaree University of Technology for their help and assistance throughout the period of this study.

I am sincerely grateful to Dr. Siritwat Soontaranon and staff members of the Siam Photon Laboratory of the Synchrotron Light Research Institute for suggestion and all their help.

First and foremost, I would like to express my sincere gratitude to my thesis advisor, Asst. Prof. Dr. Pranee Chemsamrong, for her excellent supervision, inspiring guidance, support and kindness and encouragement throughout the period of the study. Moreover, I would like to thank Assoc. Prof. Dr. Yupaporn Raksakulpiwat, my co-advisors for advices during my research work. In addition, I wish to express my gratitude to Asst. Prof. Dr. Wimonlak Sutapun, Assoc. Prof. Dr. Kasama Jarukumjorn and Asst. Prof. Dr. Chantima Deeprasertkul for their valuable suggestions and guidance given as committee members.

Wachirabhorn Pongputthipat

TABLE OF CONTENTS

	Page
ABSTRACT (THAI).....	I
ABSTRACT (ENGLISH).....	III
ACKNOWLEDGEMENT.....	V
TABLE OF CONTENTS.....	VI
LIST OF TABLE.....	XI
LIST OF FIGURES.....	XIII
SYMBOLS AND ABBREVIATIONS.....	XVIII
CHAPTER	
I INTRODUCTION.....	1
1.1 Background.....	1
1.2 Research objectives.....	6
1.3 Scope and limitation of the study.....	6
II LITERATURE REVIEW.....	7
2.1 Toughness and toughness improvement of PLA.....	7
2.1.1 Toughness improvement of PLA by blending with natural rubber and its derivatives.....	8

TABLE OF CONTENTS (Continued)

	Page
2.1.2 Toughness improvement of PLA by blending with synthetic rubber.....	9
2.2 Crystallization of PLA.....	10
2.2.1 Crystallization and degree of crystallinity of PLA.....	11
2.2.2 Effect of nucleating agent on crytallization of PLA.....	15
2.2.2.1 Organic nucleating agent.....	16
2.2.2.2 Inorganic nucleating agent.....	18
2.2.3 Effect of heat treatment on crytallization of PLA.....	20
2.3 Heat distortion temperature (HDT) and HDT enhancement for PLA.....	21
2.3.1 Enhancing HDT of PLA by increasing crystallinity and crystallization rate.....	23
2.3.2 Enhancing HDT of PLA by the addition of high stiffness filler or polymers.....	26
III EXPERIMENTAL.....	31

TABLE OF CONTENTS (Continued)

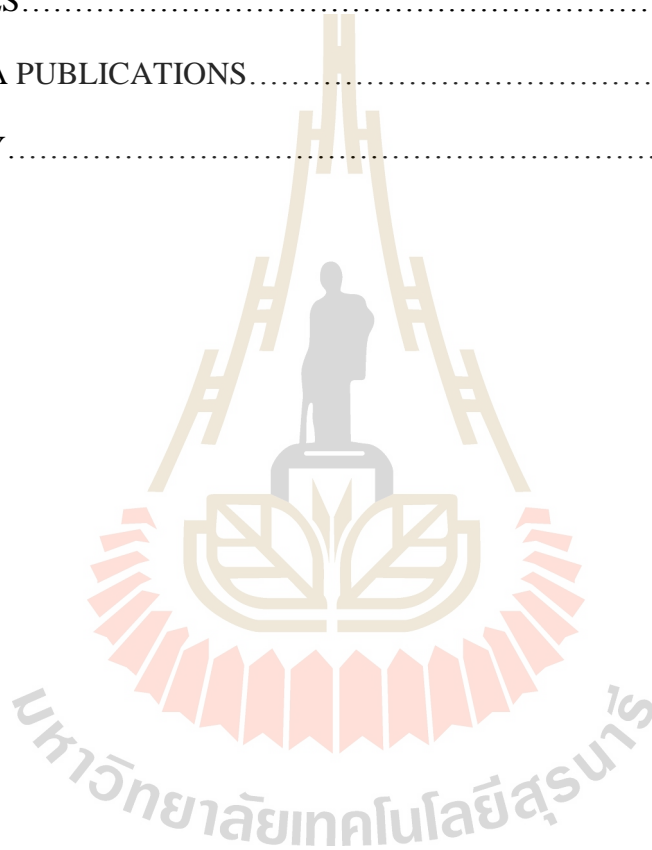
	Page
3.1	Materials.....31
3.2	Experimental.....31
3.2.1	Blends preparation.....31
3.2.3	Characterization of PLA and the blends.....33
3.2.3.1	Tensile testing.....33
3.2.3.2	Unnotched and notched Izod impact testing.....33
3.2.3.3	Heat distortion temperature.....33
3.2.3.4	Differential scanning calorimetry.....33
3.2.3.5	Scanning electron microscopy.....34
3.2.3.6	Wide angle X-ray scattering.....34
IV	RESULTS AND DISCUSSION.....35
4.1	Effect of NR content on mechanical, thermal and morphological properties of PLA.....35
4.1.1	Mechanical properties.....35
4.1.1.1	Tensile properties.....35
4.1.1.2	Impact properties.....37
4.1.2	Heat distortion temperature38
4.1.3	Morphological property.....41

TABLE OF CONTENTS (Continued)

	Page
4.2	Effect of PDLA content on thermal, mechanical and morphological properties of PLA/NR blend.....44
4.2.1	Mechanical properties.....44
4.2.1.1	Tensile properties.....44
4.2.1.2	Impact properties.....46
4.2.2	Heat distortion temperature.....48
4.2.3	Morphological property.....51
4.2.4	Thermal properties.....55
4.2.5	WAXS patterns of PLA, PDLA and the blends.....62
4.3	Effect of annealing time on mechanical, thermal and morphological properties of PLA/NR/PDLA blends.....64
4.3.1	Mechanical properties.....64
4.3.1.1	Tensile Properties64
4.3.1.2	Impact properties.....68
4.3.3	Heat distortion temperature properties.....70
4.3.4	Morphological property.....71
4.3.5	Thermal properties.....79

TABLE OF CONTENTS (Continued)

	Page
V CONCLUSIONS	86
REFERENCES.....	89
APPENDIX A PUBLICATIONS.....	100
BIOGRAPHY.....	112



LIST OF TABLES

Table	Page
1.1 Polylactic acid (PLA) typical properties.....	3
2.1 Glass transition temperature (T_g) and change of specific heat at T_g (ΔC_p), melting peak temperature (T_m) and enthalpy (ΔH_m) and crystallization peak temperature (T_c) and enthalpy (ΔH_c) for different molecular weight of PLLA samples during a DSC cycle of heating-cooling-heating between 0 and 220°C at 10°C/min.....	13
3.1 Blend Compositions.....	32
4.1 Mechanical properties and HDT of PLA and PLA/NR blend at various NR contents.....	40
4.2 Mechanical properties and HDT of PLA, PLA/NR(85/15) and PLA/NR/PDLA blends.....	50
4.3 Diameters of NR particles in the PLA/NR(85/15) and PLA/NR/PDLA blends.....	54
4.4 DSC first heating results of PLA, PLA/NR(85/15) and PLA/NR/PDLA blends.....	59
4.5 DSC second heating results of PLA, PLA/NR(85/15) and PLA/NR/PDLA blends.....	61
4.6 Diameters of NR particles in the PLA/NR(85/15) and.....	74

LIST OF TABLES (Continued)

Table	Page
4.7 DSC first heating results of PLA, PLA/NR/PDLA blends before and after annealing treatment.....	85



LIST OF FIGURES

Figure	Page
1.1 Lactic acid isomers.....	2
2.1 Differential scanning calorimetry thermograms of amorphous PLLA and PDLLA (heating rate 10°C/min).....	10
2.2 DSC thermal cycles of PLLA 200 kDa (first heating, cooling, and second heating at ±10°C/min).....	11
2.3 XRD patterns of PLA pellet and PLA film.....	14
2.4 Heat distortion temperature test geometry.....	21
4.1 Stress-strain curves of PLA and PLA/NR blends at various NR contents.....	36
4.2 Tensile strength and Young's modulus PLA and PLA/NR blends at various NR contents.....	36
4.3 Elongation at break of PLA and PLA/NR blends at various NR Contents.....	37
4.4 Izod impact strength of PLA, PLA/NR blends at various NR contents.....	38
4.5 Heat distortion temperatures of PLA and PLA/NR blends at various NR content.....	39
4.6 SEM micrographs at 500x magnification of impact fractured surface of PLA (a), PLA/NR (95/5) (b), PLA/NR (90/10) (c),	

LIST OF FIGURES (Continued)

Figure	Page
PLA/NR (80/15) (d) and PLA/NR (80/20) (e).....	42
4.7 SEM micrographs at 500x magnification of tensile fractured surface of PLA (a), PLA/NR (95/5) (b),PLA/NR (90/10) (c), PLA/NR (80/15) (d) and PLA/NR(80/20) (e).....	43
4.8 Stress-strain curves of PLA, PLA/NR(85/15) and PLA/NR/PDLA blends.....	45
4.9 Tensile strength and Young's modulus of PLA, PLA/NR(85/15) and PLA/NR/PDLA blends.....	45
4.10 Elongation at break of PLA, PLA/NR(85/15) and PLA/NR/PDLA blends.....	46
4.11 Izod impact strength of PLA, PLA/NR(85/15) and PLA/NR/PDLA blend.....	47
4.12 HDT of PLA, PLA/NR(85/15) and PLA/NR/PDLA blends.....	49
4.13 SEM micrographs at 300x magnification of tensile fractured surface of PLA/NR(85/15) (a), PLA/NR/PDLA (1) (b), PLA/NR/PDLA (3) (c) and PLA/NR/PDLA (5) (d).....	51
4.14 SEM micrographs at 1,000x magnification of freeze-fractured surfaces of PLA/NR(85/15) (a), PLA/NR/PDLA (1) (b), PLA/NR/PDLA (3) (c) and PLA/NR/PDLA (5) (d).....	53
4.15 DSC thermograms of PLA, PLA/NR(85/15) and PLA/NR/PDLA	

LIST OF FIGURES (Continued)

Figure	Page
blend with various contents of PDLA (the first heating, heating rate 5°C/min).....	.58
4.16 DSC thermograms of PLA, PLA/NR(85/15) and PLA/NR/PDLA blend with various contents of PDLA (the second heating, heating rate 5 °C/min).....	60
4.17 WAXS patterns of PDLA, PLA, PLA/NR(85/15) and PLA/NR/PDLA blend with various contents of PDLA.....	63
4.18 Stress-strain curve of PLA, PLA/NR(85/15), PLA/NR/PDLA blends before and after annealing treatment.....	65
4.19 Tensile strength of PLA, PLA/NR(85/15), PLA/NR/PDLA blends before and after annealing treatment.....	66
4.20 Modulus of PLA, PLA/NR(85/15), PLA/NR/PDLA blends before and after annealing treatment.....	66
4.21 Elongation at break of PLA, PLA/NR(85/15), PLA/NR/PDLA blends before and after annealing treatment.....	67
4.22 Unnotched Izod impact strength of PLA, PLA/NR(85/15), PLA/NR/PDLA blends before and after annealing treatment.....	69
4.23 Notched Izod impact strength of PLA, PLA/NR(85/15), PLA/NR/PDLA blends before and after annealing treatment.....	69
4.24 HDT of PLA, PLA/NR(85/15), PLA/NR/PDLA blends before and	

LIST OF FIGURES (Continued)

Figure	Page
after annealing treatment.....	70
4.25 SEM micrographs at 300x magnification of tensile fractured surface of (a) PLA/NR(85/15), (b)PLA/NR/PDLA(1), (c) PLA/NR/PDLA(3) and PLA/NR/PDLA(5) blends before and after annealing treatment.....	72
4.26 SEM micrographs at 1,000x magnification of freeze-fractured surfaces of PLA/NR(85/15) with various annealing time: (a) 0 min, (b) 10 min, (c) 30 min and (d) 60 min.....	75
4.27 SEM micrographs at 1,000x magnification of freeze-fractured surfaces of PLA/NR/PDLA(1) with various annealing time: (a) 0 min, (b) 10 min, (c) 30 min and (d) 60 min.....	76
4.28 SEM micrographs at 1,000x magnification of freeze-fractured surfaces of PLA/NR/PDLA(3) with various annealing time: (a) 0 min, (b) 10 min, (c) 30 min and (d) 60 min.....	77
4.29 SEM micrographs at 1,000x magnification of freeze-fractured surfaces of PLA/NR/PDLA(5) with various annealing time: (a) 0 min, (b) 10 min, (c) 30 min and (d) 60 min.....	78
4.30 DSC thermograms of neat PLA with various annealing time (the first heating, heating rate 5°C/min).....	80
4.31 DSC thermograms of PLA/NR(85/15) with various annealing	

LIST OF FIGURES (Continued)

Figure		Page
	time (the first heating, heating rate 5°C/min).....	81
4.32	DSC thermograms of PLA/NR/PDLA(1) with various annealing time (the first heating, heating rate 5°C/min).....	82
4.33	DSC thermograms of PLA/NR/PDLA(3) with various annealing time (the first heating, heating rate 5°C/min).....	83
4.34	DSC thermograms of PLA/NR/PDLA(5) with various annealing time (the first heating, heating rate 5°C/min).....	84

SYMBOLS AND ABBREVIATIONS

%	=	Percent
°C	=	Degree Celsius
ΔH_c	=	Crystallization enthalpy
ΔH_m	=	Melting enthalpy
μm	=	Micrometer
X_c	=	Degree of crystallinity
α	=	Alpha
D_i	=	Diameter of the particle
D_n	=	Number averaged diameter
g	=	Gram
kJ	=	Kilojoule
n_i	=	Total number of diameter particle
m^2	=	Square meters
min	=	Minute
MPa	=	Megapascal
M_v	=	Viscosity average molecular weight
GPa	=	Gigapascal
rpm	=	Revolution per minute
wt	=	Weight

CHAPTER I

INTRODUCTION

1.1 Background

For more than 50 years, global production and consumption of plastics have continued to rise. An estimated 299 million tons of plastics were produced in 2013, representing a 4 percent increase over 2012, and confirming an upward trend over the past years. The high consumption of those traditional non-biodegradable polymers in various fields causes tremendous environmental problems. Environmental protection drives attention in order to increase recycling of non-biodegradable polymer and focus on development of bio-based biodegradable polymers to replace petroleum-based non-biodegradable polymers.

Poly(lactic acid) (PLA) is an economically bio-based polymer which accomplishes large scale production since 2001 (Lunt, 1998; Vink et al., 2003). It is potential polymer for replacing petroleum-based polymer due to its biodegradability and biocompatibility (Garlotta, 2001; Ikada and Tsuji, 2000).

The monomer of PLA is lactic acid (2-hydroxy propanonic acid), LA, that exists in the two optical isomers, L (+) and D (-) as shown in Figure 1.1. It can be obtained by petrochemical synthesis or fermentation process. Commercial PLA grades however are usually based on an L-rich mixture as the majority of bacteria used in fermentation processes produce L-lactic acid predominantly. Due to purification issues, they typically comprise a minimum of 1–2% D units (Xavier, 2010).

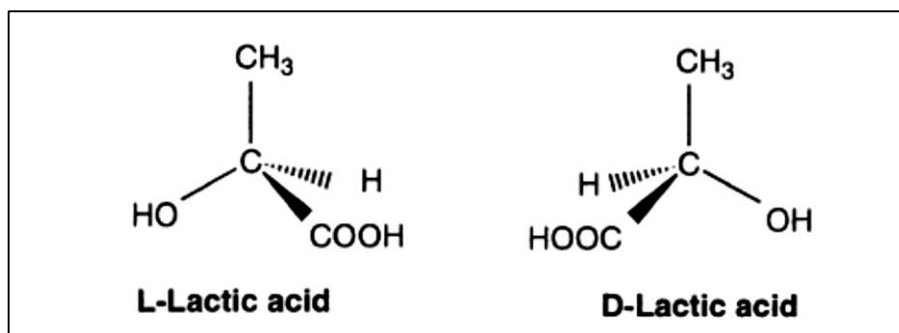


Figure 1.1 Lactic acid isomers (O dian, 2004).

Polymers with high L-lactic levels can be used to produce crystalline polymers, while the higher D-lactic materials (>15%) are more amorphous. There are several methods which can be employed for the production of polylactic acid. The main methods include direct condensation polymerization and ring opening polymerization. PLA has been widely used in industrial applications, such as automotive, medical applications, especially in food packaging applications. It exhibits the environmental friendliness, good clarity, high strength and modulus. Typical properties of PLA are shown in Table 1.1. Although PLA possess many desired properties it has some disadvantages, such as poor impact strength, weakness of heat-resistance and slow crystallization.

To achieve high toughness PLA, natural rubber (NR) has been one of desirable impact modifiers. (Bitinis et al., 2011; Juntuek et al., 2011; Pongtanayut et al., 2013). The rubber particles behave as stress concentrators enhancing the fracture energy absorption of brittle polymers and ultimately result in a material with improve toughness (Pongtanayut et al., 2013). NR exhibits a unique combination of tough-ness, flexibility and biodegradability that together with its low cost makes it an ideal candidate to improve toughness of PLA.

Table 1.1 Polylactic acid (PLA) typical properties. (Prospector materials database, 2015).

Properties	Typical Value	Test Method
Physical		
Density (g/cm ³)	1.24	ASTM D792
Melt Index (210°C,2.16 kg),g/10min	6-70	ASTM D1238
Mechanical		
Tensile Modulus (psi)	293000- 514000	ASTM D638
Tensile Strength (psi)	7080 - 8150	ASTM D638
Elongation at break (%)	0.50 - 9.2	ASTM D638
Notched Izod Impact (ft·lb/in)	0.30-0.88	ASTM D256
Thermal		
Deflection Temperature Under Load 66 psi (°C)	49.5-55	ASTM D648
Glass Transition Temperature (°C)	44-62	DSC
Melting Temperature (°C)	157-170	DSC
Peak Crystallization Temperature (°C)	130-164	ASTM D3418

NR is a renewable resource derived from a milky colloidal suspension or latex found in the sap of some plants. The major commercial source of natural latex used to produce rubber is the Para rubber tree, *Hevea brasiliensis*. Bitinis et al. (2011) reported that the ductility of PLA has been significantly improved by blending with NR. The elongation at break improved from 5% for neat PLA to 200% by adding 10 wt% NR. The ductility of PLA has been significantly improved by blending with NR. The amount of NR at 10 % weight seems to give optimum property.

Crystallization behaviors such as crystallization kinetics, crystal structure and arrangement of crystallites have a profound effect on the physical and mechanical properties of biodegradable polymers. Battezzore et al. (2011) reported that the incorporation of talc in PLA not only accelerated the crystallization rate of PLA but also improved the thermal and mechanical properties of PLA. Moreover, the crystallization rate increased slightly as the talc content in the PLA/talc blends

increased. It was found that the crystallinity of PLA/montmorillonite (MMT) nanocomposites increased remarkably at the MMT loadings higher than 5 wt%. The crystallization behavior of PLA was altered significantly in the presence of MMT (Ublekov et al., 2012). Yokohara et al. (2008) realized that crystallization of PLA was improved by the incorporation of poly(butylenes succinate) (PBS). PBS droplet acted as a nucleating agent for PLA and could be responsible for the pronounced cold crystallization of PLA/PBS blends. The presence of poly(ϵ -caprolactone) (PCL) in PLA was noted to accelerate the growth of crystallites and to increase the number of crystallites for the PLA matrix, indicating that PCL is an effective nucleating agent for PLA crystallization (Lopez et al., 2006).

One interesting attribute of PLA is the ability of enantiomeric blends of poly(L-lactic acid) (PLLA) and poly(D-lactic acid) (PDLA) to form a stereocomplex with high crystal stability and crystallization ability (Chen et al., 2005). PLA stereocomplex is formed from the stereoselective interaction between PLLA and PDLA. It has improves thermal resistance, and mechanical properties of PLLA or PDLA. These improvements arise from the strong interaction between the L- and D-lactyl unit sequences, which is based on $\text{CH}_3 \cdots \text{C}=\text{O}$ interactions of stereoselective van der Waals forces (Ikada et al, 1987). In the 1980s, it was found that an equivalent mixture of PLLA and PDLA formed a stereocomplex. The stereocomplex has a melting temperature ($T_m=230^\circ\text{C}$) that was approximately 50°C higher than the T_m of either PLLA or PDLA (Ikada et al., 1987).

Yamane and Sasai (2003) investigated the thermal property and non-isothermal crystallization behavior of PLLA blended with a small amount of PDLA (1–5 wt%). Low molecular weight PDLA ($\text{MW} = 1.2 \times 10^5$) isolated in the matrix of PLLA did

not form a stereocomplex crystallite with a surface area large enough to act as a nucleation site. On the other hand, high molecular weight PDLA ($M_w = 2.6 \times 10^5$ and 4.5×10^5) chains formed a large stereocomplex crystallite. With increasing PDLA content, stereocomplex crystallites were more easily formed and acted as nucleation sites, which effectively increased the number of PLLA spherulites, and therefore, the overall crystallization rate. Tsuji et al. (2006) studied the isothermal and non-isothermal crystallization behavior of blends of PLLA with 0.1–10 wt% PDLA ($M_w = 5.2 \times 10^4$). The addition of PDLA was shown to increase the number of spherulites in isothermal experiments but did not modify the crystal growth rate or the mechanical properties of crystallized films. Overall, the crystallization half-time was reduced only when 10% of PDLA was used and the reduction was around 50% in the optimal crystallization temperature range. Smaller PDLA concentration resulted in no change or increased crystallization half-time.

Heat distortion temperature (HDT) of PLA is only 54–60 °C. Therefore, it is not suitable for some applications, for example, microwavable trays and hot-fill applications and also transportation. There are several ways to improve the HDT of polymers. Forming crosslink in polymer and improving the glass transition of polymer are the effective methods for increasing the HDT value. In addition, the easy way to increase the HDT value of polymer is to increase the crystallinity of polymer with loading fillers or nucleating agent (Tang et al., 2012; Shi et al., 2012; Harris et al., 2008; Yu et al., 2012). Zou et al. (2012) investigated the crystallization and thermal behavior of PLLA blend with a small amount of PDLA (1–5 wt%). The higher PDLA content was in PLLA matrix, the faster crystallization rate was had, which revealed that PDLA was an effective nucleating agent for PLLA. The stereocomplex crystallites

was consistent with the increased content of the PDLA and annealed time. The complexed materials showed high heat distortion temperature (HDT), high T_m and high crystallinity.

In this research, the changes of mechanical and thermal properties of PLA/NR blend through the presence of PDLA were investigated. Crystallinity and HDT of PLA/NR was expected to be increased after the addition of PDLA.

1.2 Research objectives

The main objectives of this research are as below:

- (1) To study the mechanical properties, morphologies and HDT of PLA/NR blends.
- (2) To study the effect of PDLA content on mechanical, thermal, and morphological properties of PLA/NR blends.
- (3) To study the effect of annealing treatment on mechanical, thermal, and morphological properties of PLA/NR/PDLA blends.

1.3 Scope and limitation of the study

In this research, mechanical and thermal properties of PLA/NR blends at various ratios of 95/5, 90/10, 85/15 and 80/20 wt% were studied. All PLA/NR blends were prepared using an internal mixer and the test specimens were molded by a compression molding machine. PLA/NR blends were characterized by tensile and impact test. PLA/NR blend that showed the highest impact strength was chosen to study the effect of PDLA content on mechanical and thermal properties of PLA/NR blends. PDLA content was varied from 1, 3 and 5 wt% based on the amount of PLA. The influence of annealing treatment was also studied.

CHAPTER II

LITERATURE REVIEW

PLA is a biodegradable polymer derived from renewable resources. PLA provides good strength and easy processability with perfect degradable in most products. However, PLA suffers from low heat distortion temperature (HDT), because its T_g is only 54-60°C and low toughness. Thus, in order to broaden the applications of PLA, material properties have to be improved. One of frequent methods used in improvement of PLA toughness is the addition of rubber material into PLA matrix (Bitinis et al., 2011; Juntuek et al., 2011; Pongtanayut et al., 2013). There are several methods to improve HDT of PLA such as the addition of crystal nucleating agent, blending PLA with a high HDT polymer and the addition of natural fiber and inorganic filler. In this work, the effects of PDLA content and annealing treatment on the toughness and thermal properties of PLA toughened by NR were studied.

2.1 Toughness and toughness improvement of PLA

Toughness is the ability of a material to absorb energy and plastically deform without fracturing.

The toughness can be investigated by the mechanical testing such as impact and tensile testing. Impact toughness of material reflects the degree of energy absorption from the beginning mechanical load to final fracture (Kim and Michler, 1998). In the case of tensile tests, toughness is related to the area under the stress - strain curve.

The elongation at break is also used to represent the toughness. In general, the toughness increased with increasing elongation at break.

The brittleness characteristics of PLA limit its application in various fields thus there is a need for PLA toughness. Blending with rubber materials is one of the dominant methods.

2.1.1 Toughness improvement of PLA by blending with natural rubber and its derivatives

Juntuek et al. (2012) researched on the effect of glycidyl methacrylate-grafted natural rubber on physical properties of polylactic acid and natural rubber blends. The ratio of PLA/NR blend was 95/5, 90/10, 85/15 and 80/20 wt%. It was found that the impact strength of PLA, PLA/NR blends increased with increasing NR content up to 10% (w/w). To study the effect of NR-g-GMA content and % grafting on mechanical properties of PLA/NR blends, PLA content was fixed at 90 wt % according to the highest impact strength of PLA/ NR (90/10). The NR-g -GMA was varied at 0.2, 1, 3 and 5 wt %. The impact strength of PLA/NR blends increased dramatically with increasing NR-g-GMA content to 1% (w/w). The impact strength of PLA/NR blend with NR-g-GMA content of 1% was 54.24 kJ/m², which is about 2.5 times higher than that of neat PLA. This was the result from an improvement in compatibility between PLA and NR. With increasing NR-g-GMA content to 3 and 5% (w/w), impact strength of PLA/NR blends was slightly decreased to 51.34 and 49.27 kJ/m², respectively. However, these values were still higher than that of neat PLA and PLA/NR blend without NR-g-GMA.

Pongtanayut et al. (2013) studied effect of rubber on mechanical properties and thermal properties of PLA/NR and PLA/ENR Blends. PLA/NR and

PLA/ENR were prepared at various compositions from 0-30% by weight. The results showed that ductility of PLA has been significantly improved by blending with NR. The amount of NR at 10% weight seemed to give optimum property. At high content of NR, it seemed to suffer tensile properties. In the case of the addition of ENR, it reduced crystallization ability, thermal resistance and tensile properties of the blend.

Bitinis et al. (2011) investigated structure and properties of polylactide/natural rubber blends. The ratio of PLA/NR was 95/5, 90/10, 80/20 wt%. PLA/NR was prepared using an internal mixer. The rubber phase was uniformly dispersed in the continuous PLA matrix with a droplet size range from 1.1 to 2.0 μm . The ductility of PLA had been significantly improved by blending with NR. The elongation at break improved from 5% for neat PLA to 200% by adding 10 wt% NR.

2.1.2 Toughness improvement of PLA by blending with synthetic rubber

Zhao et al. (2013) studied effect of ultrafine full-vulcanized powdered rubber (EA-UFPR) on mechanical properties of PLA. To achieve good dispersion of EA-UFPR in PLA, a master batch of the blends with 30 wt% EA-UFPR was first prepared using a co-rotating twin-screw extruder. Then, the master batch was diluted with PLA in the same manner to obtain a weight percentage of 0.5, 1, 3 and 5 wt% UFPR in PLA matrix. The results showed that impact strength of PLA/EA-UFPR blend increased with increasing EA-UFPR content. The elongation at break of blend reached the maximum with the addition of 3 wt% EA-UFPR. The tensile strength of blend slightly decreased with an increase of EA-UFPR.

Petchwattana et al. (2012) investigated the utilization of ultrafine acrylate rubber particles as a toughening agent for poly(lactic acid). The concentration

of the acrylate rubber was varied at 0.1, 0.3, 0.5, 0.7, 1.0, 3.0, 5.0, 7.0 and 10 wt%. Each formulation was melt blended by using a conical co-rotating twin screw extruder. Specimens of the acrylate rubber-modified PLA were finally injection molded. The results showed that the impact strength and elongation at break of acrylate rubber-modified PLA increased with increasing acrylate rubber content.

Yu et al. (2014) studied on the toughness improvement of polylactide by melt blending with bio-based poly(ester)urethane(TPU). PLA/TPU were prepared at various compositions from 0-20% by weight. The results showed that the notched izod impact strength was improved after adding the TPU. The impact strength of PLA/TPU blends increased with increasing TPU content up to 15% (w/w)

2.2 Crystallization of PLA

PLA can be either an amorphous or a semicrystalline polymer, depending on the stereochemistry and thermal history. PLLA and PDLA are semicrystalline polymer, while atactic polymer, poly(D,L-lactic acid) (PDLLA) is amorphous (Robertson,2012). The T_g of semicrystalline PLA is approximately 50 to 60°C and the T_m ranges from 130 to 180°C, depending on the degree of crystallinity and molecular weight (MW) of the polymer. Commercial PLA is normally a PLLA and PDLLA copolymer and has a semicrystalline structure with high MW (above 100 kDa) (Lim et al., 2008).

Despite the fact that PLA is a semi-crystalline polymer, almost no crystallization proceeds under fast cooling such as a practical molding condition (Kawamoto et al., 2007). The low crystallization rate of PLA results in poor heat resistance and severely limits the range of application of PLA.

2.2.1 Crystallization and degree of crystallinity of PLA

Typical differential scanning calorimetry (DSC) analysis of thermal behavior of two amorphous PLAs are shown in Figure 2.1. PDLLA (Mw = 70 kDa) sample that is intrinsically amorphous and PLLA (Mw = 200 kDa) that was quenched to the amorphous state by fast cooling at $-100^{\circ}\text{C}/\text{min}$ after melting. In both cases, the T_g is evident and is located at about 65°C .

The initial amorphous PLLA presents a broad crystallization peak in the range $100\text{--}160^{\circ}\text{C}$ centered at about 132°C with crystallization enthalpy (ΔH_c) = 38 J/g , followed by melting at 182°C with melting enthalpy (ΔH_m) = 38 J/g . As determined by the equal values of the crystallization and melting enthalpies, the fast quenching produced a fully amorphous material.

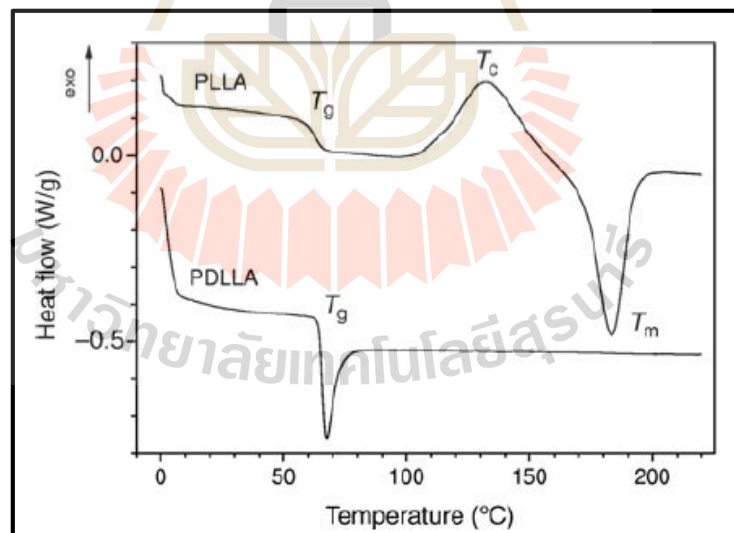


Figure 2.1 Differential scanning calorimetry thermograms of amorphous PLLA and PDLLA (heating rate $10^{\circ}\text{C}/\text{min}$) (Auras et al., 2010).

Figure 2.2 refers to a commercial PLLA (L210 from Boehringer, Ingelheim, Germany) with a molecular weight of 200 kDa, subjected to the following three DSC runs at 10°C/min: (i) heating from 0 to 220°C, (ii) cooling from 220 to 0°C, and finally (iii) heating from 0 to 220°C. The initially crystalline polymer presented a T_g at 73 °C and melted at 192°C. During cooling, apparently no crystallization developed and the following thermal run on the initially amorphous materials showed glass transition (at $T_g = 64^\circ\text{C}$), crystallization (at $T_c = 127^\circ\text{C}$), and melting (at $T_m = 181^\circ\text{C}$) (Auras et al., 2010).

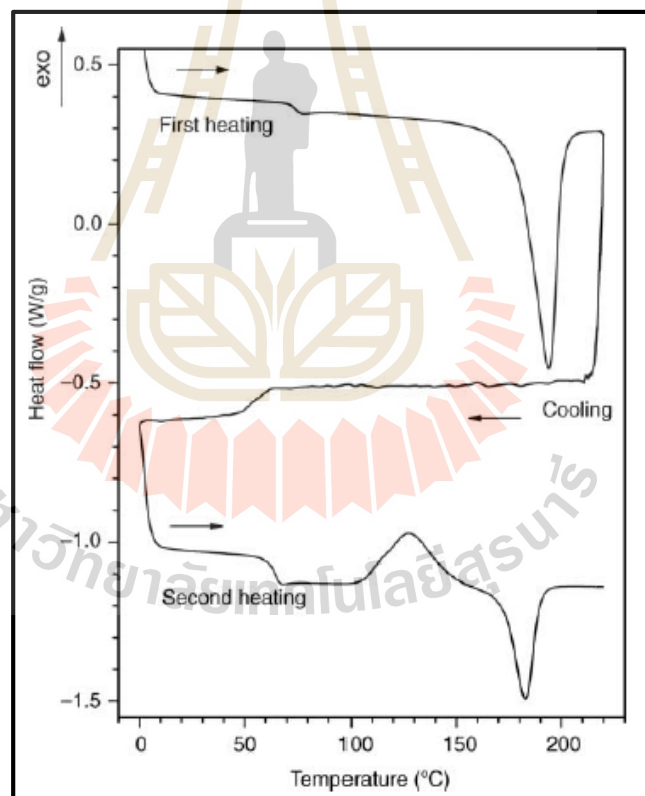


Figure 2.2 DSC thermal cycles of PLLA 200 kDa (first heating, cooling, and second heating at $\pm 10^\circ\text{C}/\text{min}$) (Auras et al., 2010).

Table 2.1 lists T_g , T_m , T_c , ΔH_c , and ΔH_m of various molecular weight PLLA samples, namely, 2, 30, and 200 kDa, respectively. The crystallinity content (X) has been evaluated from the DSC data according to the following equation:

$$X\% = 100(\Delta H_m - \Delta H_c)/\Delta H_m^0 \quad (2.1)$$

where ΔH_m and ΔH_c are the melting and the crystallization enthalpies, respectively, and ΔH_m^0 is melting enthalpy of 100% crystalline PLA (93.6 J/g) (Auras et al., 2010).

Table 2.1 Glass transition temperature (T_g) and change of specific heat at T_g (ΔC_p), melting peak temperature (T_m) and enthalpy (ΔH_m) and crystallization peak temperature (T_c) and enthalpy (ΔH_c) for different molecular weight of PLLA samples during a DSC cycle of heating–cooling–heating between 0 and 220°C at 10°C/min (Auras et al., 2010).

First Heating					
Mw (kDa)	T_g (°C)	ΔC_p (J/(g K))	T_m (°C)	ΔH_m (J/g)	X (%)
2	58	0.17	147	48	51
30	79	0.06	171	68	73
200	73	0.22	192	67	72
Cooling					
Mw (kDa)	T_c (°C)	ΔH_c (J/g)	T_g (°C)	ΔC_p (J/(g K))	
2	-	-	39	0.56	
30	96	21	50	0.32	

Table 2.1 Glass transition temperature (T_g) and change of specific heat at T_g (ΔC_p), melting peak temperature (T_m) and enthalpy (ΔH_m) and crystallization peak temperature (T_c) and enthalpy (ΔH_c) for different molecular weight of PLLA samples during a DSC cycle of heating–cooling–heating between 0 and 220°C at 10°C/min (Cont.) (Auras et al., 2010).

Cooling							
Mw (kDa)	T_c (°C)	ΔH_c (J/g)	T_g (°C)	ΔC_p (J/(g K))			
200	-	-	55	0.50			
Second Heating							
Mw(kDa)	T_g (°C)	ΔC_p (J/(g K))	T_c (°C)	ΔH_c (J/g)	T_m (°C)	ΔH_m (J/g)	X (%)
2	43	0.54	107	9	142	9	0
30	55	0.32	97	21	174	50	31
200	64	0.51	127	25	181	26	1

The X-ray diffraction patterns of PLA (Figure 2.3) show that the film of this polymer exhibits no peaks, showing an amorphous nature. On the other hand, X-ray results for PLA pellet show that this polymer seems to be semi-crystalline, presenting a peak located at 19.4°, characteristic of PLA (Almeida et al., 2012). The difference between these XRD results is probably due to the type of polymer molding used in each case. The films obtained by solution casting, which does not favor the formation of

orderly polymer chains by curing the chains approximation, and thus inhibits the development of crystallinity (Santos and Tavares, 2014).

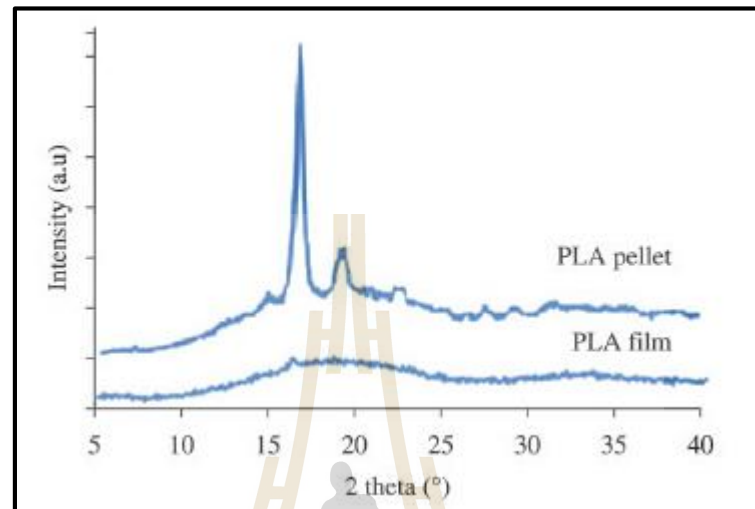


Figure 2.3 XRD patterns of PLA pellet and PLA film (Santos and Tavares, 2014).

2.2.2 Effect of nucleating agent on crystallization of PLA

Crystallization behaviors such as crystallization kinetics, crystal structure and arrangement of crystallites have a profound effect on the physical and mechanical properties of biodegradable polymers (Maiti et al., 2002; Gagnon et al., 1992; Tang et al., 2011; Shi et al., 2012); therefore, study of crystallization behaviors of PLA is of great importance because crystallization influences not only the crystal structure of PLA but also the final physical and mechanical properties of PLA products.

Increasing the crystallinity of PLA, which can be achieved by enhancing its crystallization, has been regarded as an effective mean to improve the thermal resistance and has attracted considerable interest in recent years (Xin-Feng et al., 2013; Li HB et al., 2007).

Nucleation is the onset of a phase transition in a small region of a medium. The phase transition can be the formation of a tiny bubble in a liquid, dirt, filler or the polymer itself in polymer melt. Homogeneous nucleation and heterogeneous nucleation are two main types of nucleation models. Nucleation normally occurs at nucleation sites on surfaces contacting the liquid or vapor. Suspended particles or minute bubbles also provide nucleation sites this is called heterogeneous nucleation. Nucleation without preferential nucleation sites is homogeneous nucleation.

Nucleation agents are additives finely dispersed into the polymer at low concentration to seed crystals during solidification from the melt. They are dispersed in the melt and remain solid at crystallization temperature, so a large number of small crystals are formed around them (Hadi et al., 2002). Nucleating agent is often used to accelerate crystallization by increasing nucleation density and increase the crystallinity of the amorphous and semi-crystalline polymer. Many nucleating agents have been investigated including low molecular weight organic compound nucleating agent, inorganic nucleating agent and polymeric nucleating agent

2.2.2.1 Organic nucleating agent

Most of the nucleating agents reported for PLA are organic materials, such as N, N'-ethylenebis (1,2-hydroxystearamide) (EBH), triphenyl phosphate (TTP) and low molecular weight aliphatic amides .

Nam et al. (2006) detected that N, N'-ethylenebis (12-hydroxystearamide) (EBH) which crystallized at very early stage of PLA crystallization acted as an effective nucleating agent to improve the crystallization of PLA. As a result, typical spherulites formed at the interface between PLA and EBH, and the overall crystallization rate was increased by the addition of EBH.

Jing et al. (2011) reported the effect of N-aminophthalimide compound (NA-S) on the crystallization behavior and morphology of poly(lactic acid). The isothermal crystallization behavior was studied with DSC. The sample was heated from 20 to 185°C at a rate of 10°C/min, held for 5 min, and then cooled down to a particular crystallization temperature and held for 30 min, finally heated to 185°C with the same heating rate. When the level of NA-S was 1 and 0.5%, at the temperature above 120°C, the rates of crystallization at each temperature were increased compared with pure PLA, and the half crystallization times are shortened.

Zhaobin et al. (2011) found that the crystallization rate and crystallinity of PLA were significantly increased with addition of ethylenebis(hydroxystearamide) (EBH). The isothermal crystallization halftime at 105°C was decreased from 18.8 minutes for neat PLA to 2.8 minutes for PLA with 1.0 wt% of EBH. The crystallinity of PLA with 1.0 wt% EBH was about 35% after 5-minute annealing at 105°C.

Xing et al. (2012) studied effect of N, N'-ethylenebis(1,2-hydroxystearamide) (EBH) and N, N'-ethylenebisstearamide (EBSA) on the crystallization behavior of PLLA. The results showed that the crystallization rate of PLLA was significantly improved with the addition of EBH and EBSA, and EBH showed a stronger effect than that of EBSA. The hydrogen bond interaction between hydroxyl groups in EBH and the carbonyl groups in PLLA may be responsible for the stronger effect of EBH on the nucleating ability and crystallization kinetics of PLLA.

Polymeric nucleating agents are often thermoplastic crystalline and semi-crystalline polymers. They act as sites or nuclei for initiating polymer crystallization (Xu et al., 2005). The small amount of crystallites formed at the

cooling process, in which polymer dispers particles would act as nuclei, accelerates the crystallization during heating process (Yokohara et al., 2008).

Yokohara et al. (2008) realized that crystallization of PLA was improved by the incorporation of poly(butylenes succinate) (PBS) even in the molten state. It was found molten PBS droplets act as crystallization nuclei for PLA. Furthermore, the PLA crystallites generated during the quench operation are responsible for the enhancement of the cold-crystallization behavior for the blends.

Ahmed et al. (2014) studied thermal properties of stereo-complexed polylactide films. Poly(L-lactide) (PLLA) and Poly(D-lactide) (PDLA) blended films (PLLA/PDLA) were prepared (5/95; 25/75; 50/50, and 75/25) by solvent casting method. Blend of PLLA and PDLA led to the formation of stereocomplex (SC) which was evidenced by differential scanning calorimetry. PLLA/PDLA results a stereocomplex which remains unmelted above T_m of PLLA and the peak value of 222°C was demonstrated by 50/50 PDLA/ PLLA blend due to ideal SC formation. The T_m of the blend increased with increasing PDLA content. The crystallization temperature (T_c) also increased with increase in PDLA content

2.2.2.2 Inorganic nucleating agent

Besides low molecular weight organic compounds, many inorganic materials such as talc, montmorillonite, SiO_2 , and CaCO_3 can also be used as nucleating agents for accelerating the crystallization process and increasing the crystallinity of PLA. Generally, improvement of crystallization rate of polymer can be achieved by mixing of talc that has nucleation effect in polymer matrix. Kolstad (1996) found that talc was an effective nucleating agent for PLA. When 2–21 wt% of talc was

added to poly (91% L-lactide-co-9% meso-lactide), it was found that the best effect was achieved at 6 wt% talc, resulting in the 500-fold increase in nucleation density.

Ublekov et al. (2012) reported the effect of organophilic clay concentration on nonisothermal crystallization, poly(L-lactic acid) (PLLA)/montmorillonite (MMT) nanocomposites. The nanocomposites with 0, 1, 3, 5, 7 and 9 wt% of montmorillonite (MMT) were prepared. The results showed that the crystallinity of PLLA/montmorillonite (MMT) nanocomposites increased remarkably at the MMT loadings higher than 5 wt%, and the crystallization behavior of PLLA was altered significantly in the presence of MMT. Thermal measurements revealed that in neat PLLA, PLLA 1 wt% MMT, and PLLA 3 wt% MMT nanocomposites, cold crystallization took place. In nanocomposites with 5, 7, and 9 wt% clay loading, the heat of cold crystallization disappeared. This phenomenon had to be attributed to hindered PLLA chains movement in the clay galleries. In nanocomposite samples containing 1 and 3 wt% of clay, the reduced mobility of PLLA chains led to decreased enthalpy of cold crystallization.

Buzarovska et al. (2012) researched on the effect of titanium dioxide (TiO_2) on thermal properties and degradation of poly(L-lactic acid)/titanium dioxide nanocomposites. The nanocomposites with 0.5, 1, 2, 5, and 10 wt% of TiO_2 were produced by solution casting method. The degree of crystallinity (X_c) of the PLLA/ TiO_2 films was increased with the increase of TiO_2 content (up to 5 wt% of TiO_2).

Liao et al. (2007) investigated the isothermal cold crystallization kinetics of poly-(lactide)/nucleating agents using DSC. Three nucleating agents (CaCO_3 , TiO_2 , and BaSO_4 , content from 0.5–2.0 wt%) were blended with PLLA.

After adding a nucleating agent, the crystallinity of PLA increased when compared with pure PLA. Moreover, nucleating agents BaSO₄ and TiO₂ had better effects on the crystallinity than CaCO₃.

Shakoor et al. (2014) studied the crystallization behavior of talc as a nucleating agent in poly(lactic acid) composites. The composites with 0, 10, 20 and 30 wt% of talc were prepared. The DSC heating scans showed that the cold crystallization temperature (T_c) was reduced from 127°C for the pure PLA to 96°C for the PLA/talc composites demonstrating a nucleating effect by the talc filler. The pure PLA was found to be essentially amorphous with a crystallinity of only 2%, whereas the crystallinity increased to 25% after addition of talc.

2.2.3 Effect of heat treatment on crystallization of PLA

It is well known that semi-crystalline polymers generally change their physical and mechanical properties when they are heated to elevated temperatures between glass transition temperature and melting temperature, then maintaining the temperature for a time before slowly cooling plastics down. The heat treatment results in a reorganization of the structure leading to a state of order with a lower free energy.

Tábi et al (2010) focuses on the crystalline structure of injection moulding grade poly(lactic acid) (PLA) and the effect of crystalline structure on the processing. The research is induced by the significant differences in crystallinity of the pure PLA resin, and the injection moulded product. The specimens for WAXD were placed on a glass plate in a vented oven for annealing at 80, 100, 120°C for 10, 20, 30, 40, 50 and 60 minutes. To analyse the effect of the different crystalline content PLA specimens, they were annealed at different temperatures for different time periods as mentioned before. The transparency of the samples changed from transparent to nearly

totally white as the crystallinity increased. This observation was verified by WAXD analysis. The results showed that the un-annealed PLA had no crystallinity, but one significant peak appeared at 16.3° for the specimens annealed at 80°C . The intensity of the peak increased gradually as a function of annealing time at 80°C and this peak also shifted to 16.6° for the specimen annealed at 120°C for 10 minutes. Three more peaks appeared at 14.8 , 19.0 and at 22.3° for samples annealed at higher temperatures, which indicated higher crystallinities.

Zou et al. (2012) examined effect of annealed time and PDLA content on crystallization of poly(L-lactide acid) using DSC. The concentration of PDLA was varied at 0, 1 and 5 wt% (the specimens code P0, P1, P5). The specimens were annealed at 120°C for 10 min. The glass transition temperature was around 55°C in all the samples. The melting peak from the PLLA was presented around 153°C , while the stereocomplex melting peaks was around 210°C . The area of the melting endotherm for the stereocomplex increased with the amount of PDLA in the PLLA matrix increased. The degree of crystallinity of three specimens was increased with the addition of the contents of PDLA. The crystallinity increased from 11.6% to 42.8%.

2.3 Heat distortion temperature (HDT) and HDT enhancement for PLA

Heat distortion temperature (HDT) is the temperature at which a polymer or plastic sample deforms under a specified load. It can be determined by the test procedure outlined in ASTM D648. The test specimen is loaded in three-point bending in the edgewise direction. A load used for testing is either 0.455 MPa or 1.82 MPa, and the temperature is increased at $2^\circ\text{C}/\text{min}$ until the specimen deflects 0.25 mm. It is used to

determine short-term heat resistance. It distinguishes between materials that are able to sustain light loads at high temperatures and those that lose rigidity over a narrow temperature range. Figure 2.4 shows the HDT test geometry.

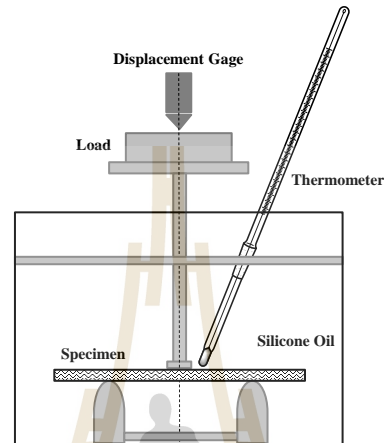


Figure 2.4 Heat distortion temperature test geometry

Although PLA has many advantages such as high tensile strength and modulus, the disadvantage of low heat deflection temperature (HDT) dramatically limits its market potential. For example, the molded PLA parts could be deformed during transportation or under operation because the ambient temperature was higher than HDT of PLA, which is about 55-60°C. Moreover, PLA typically cannot take the heat of hot-filling. Therefore, improvements in HDT must be done in order to widen its applications.

Factors that can affect the HDT of polymers include glass transition temperature, stiffness and degree of crystallinity. HDT will be increased when degree of crystallinity is increased. This was because the crystallization will hold polymer chains together and make mobility more difficult. Moreover, forming crosslink in

polymer can improve HDT of polymer because crosslink point restricts mobility of polymer chains.

There are several methods to improve HDT of PLA such as the addition of crystal nucleating agent, adding high thermal stability filler and blending with a high thermal stability polymer.

2.3.1 Enhancing HDT of PLA by increasing crystallinity and crystallization rate

Degree of crystallinity is a major important factor that affect HDT of semi-crystalline polymers. The increase of crystallinity can improve the stiffness of polymers. It is very difficult to improve HDT of PLA without increasing its crystallinity (Harris et al., 2008). The easy way to increase the HDT value of PLA is to increase the crystallinity of PLA by the addition of nucleating agent. Nucleating agent could help increase nuclei density, reduce spherulite size thus increases overall crystallization rate. Furthermore, the combination of annealing and nucleating agents is another way to increase the crystallinity. It was found that annealing treatment and incorporation of a nucleating agent greatly improved the crystallinity of PLA (Harris and Lee, 2008). This phenomena resulted in a reorganization of the structure leading to a state of ordered.

Harris et al. (2008) investigated the mechanical properties improvements of PLA by increasing the overall material crystallinity. The addition of just 2% of EBH had a considerable effect on both the isothermal and nonisothermal crystallization behavior, as shown by the lower cold crystallization temperatures and lower crystallization half-times. The highly crystalline samples formed by these methods were shown enhanced flexural stiffness, strength, and HDT.

Yu et al. (2012) examined the effect of talc on the mechanical and thermal properties of polylactide. Talc was treated with 0.3% of 3-aminopropyltriethoxysilane. The composites with 0, 2.5, 5, 10, 15, 20 and 25 wt% of treated talc powder were prepared. The results showed that crystallization rate and crystallinity were increased with the addition of talc content. This resulted in an enhancement of HDT.

Shi et al. (2012) studied effect of heat treatment on the heat distortion temperature of poly(lactic acid)/bamboo fiber(BF)/talc hybrid biocomposites. BF and talc loaded in PLA were prepared in internal mixer. These composites were compression molded at 180°C into sheets for subsequent measurements. For the heat treatment, samples were hold at 110, 120 and 130°C for 30 min. After the heat treatment and with loading BF and talc simultaneously, HDT value of PLA/20 wt % BF/20 wt % talc was about 94.5°C, which was much higher than that of PLA/20 wt % BF and PLA/20 wt % talc, which was only loaded one filler. This was due to the synergism of BF and talc in PLA composites. Transcrystallization was observed during heat treatment of PLA composite with loading BF and talc simultaneously and no similar phenomenon in other PLA composites. In some case, improvement in HDT of PLA composite was due to the effect of crystallinity. However, the formation of transcrystallization was the main effect on HDT of PLA composites.

Chen et al. (2015) examined effect of heat treatment on the thermal properties of ramie fabric-reinforced PLA biocomposites. The laminated biocomposites with 0, 9, 16, 24 and 38 wt% of ramie fabric (RF) were prepared through hot compression molding followed by direct cooling (without heat treatment) or meltcrystallized in another hot-press process at 115°C for 1 h followed by natural cooling to obtain highly crystallized samples (with heat treatment). The results showed

that the HDT of neat PLA without heat treatment is 53°C. With the addition of RF, the HDT of PLA/RF biocomposites were improved by only 1.5–5.5°C. After heat treatment HDT of neat PLA was up to 100°C. It is mainly because the increased degree of crystallinity promotes the improvement of HDT in PLA biocomposites. Moreover, PLA biocomposites with reinforcing fabric and after heat treatment show an even greater increase of HDT. The addition of RFs promotes the faster and larger growing of PLA crystals around ramie fibers compared to the growing of crystals in neat PLA with heat treatment. The higher the ramie proportion, the greater will be the increase of the HDT of PLA. The HDT of PLA/24 wt% RF biocomposite is about 149.3°C.

Tang et al. (2012) studied the crystallization behavior and mechanical properties of polylactic acid in the presence of a crystal nucleating agent. Polylactic acid (PLA)/ N, N'-ethylenebis (1,2-hydroxystearamide) (EBH) blend were prepared by melt extrusion. The weight ratio of PLA and EBH was kept at 99/1 and annealed at 105°C for 1, 2, 5, 10 and 20 min. The isothermal crystallization halftime at 105°C was decreased from 18.8 minutes for neat PLA to 2.8 minutes for PLA with 1.0 wt% of EBH. The crystallinity of PLA with 1.0 wt% EBH was about 35% after 5 minute annealing at 105°C. The HDT of PLA/EBH blend was much higher than that of neat PLA after annealing. The HDT could be increased from 51°C to 93°C. The HDT of both neat PLA and the blend was increased with the increase of the annealed time. This improvement is mainly due to the increase of crystallinity.

Zou et al. (2012) examined effects of poly(d-lactic acid)(PDLA) on the thermal properties of poly(l-lactic acid)(PLLA). The concentration of PDLA was varied at 0, 1 and 5 wt% (the specimens code P0, P1, P5). The specimen for HDT testing was annealed at 120°C for 10, 30, 60 min. The HDT of PLLA/PDLA increased with

increasing annealed time and PDLA content (up to 105°C). The high heat resistance might also be due to the increased crystallinity of the specimens. After annealing the HDT of specimen coded P5 was about 50°C higher than that of pure PLLA. This improvement was mainly because that PLLA was mixed with PDLA to form stereocomplex.

Wootthikanokkhan et al. (2013) evaluated effects of annealing on thermomechanical properties of PLA composites containing three different types of additives; namely: kenaf fiber (20 pph), Cloisite30B nanoclay (5 pph), and hexagonal boron nitrile (h-BN; 5 pph). The composites were prepared using a twin screw extruder before molding. They found that HDT value of the neat PLA specimen rapidly increased from 53.2 to 99.7°C after annealing. In addition, the HDT values of the annealed PLA composites were also slightly greater than that of the annealed neat PLA. The highest HDT value is 128°C, which was obtained by annealing PLA/kenaf fiber (20 pph) composite. The second highest HDT value (111°C) was obtained from the annealed PLA/h-BN specimen. The use of Cloisite30B as an additive for PLA also led to an increase in HDT value of the polymer from 57 to 103°C after annealing. These improvements were caused by two possible factors, that was, crystallinity of PLA increased after annealing and the different capability of the additives for reinforcing PLA.

2.3.2 Enhancing HDT of PLA by the addition of high stiffness filler or polymers

Stiffness is defined as ability of material to resist deformation under load. The HDT is a measure of the stiffness of a material when the temperature increases. Stiffness of PLA can be improved by blending with high stiffness polymers or adding reinforcing fillers which generally much more stiff than PLA matrix.

Kim et al. (2005) studied the thermal properties of cassava and pineapple flours-filled PLA bio-composites. The PLA was blended with 10, 20, 30 and 40 wt% of cassava and pineapple flours. In addition, to enhance interfacial adhesion, 3% maleic anhydride-PLA (MAPLA) was incorporated into the 30% filler loading. The results showed that the HDT of the PLA bio-composite increased from 56.8 to 66.3°C and to 69.7°C, respectively. In addition, the HDT of the PLA/pineapple flour/ MAPLA and PLA /destarched cassava flour/MAPLA composites was increased to 70.6 and 82.2 °C, respectively. The increase in HDT after the addition of MAPLA could be due to better chemical bonding between the PLA matrix and flour.

Serizawa et al. (2006) examined kenaf fiber reinforced poly(lactic acid) used for electronic products. Kenaf fiber was crushed to below 5 mm (average length of about 3 mm) and the crushed kenaf fiber was referred to as C-kenaf. The composites with 0, 10, 15 and 20 wt% of C-kenaf were prepared. All test pieces were annealed at 100°C for 4 h. The results showed that the heat resistance and modulus of PLA were greatly improved by the addition of kenaf fiber. The distortion temperature under a 1.8 MPa load of the PLA/C-kenaf composites increased with increasing C-kenaf fiber content.

Lee et al. (2009) investigated the effect of kenaf fiber on thermal properties of poly(lactic acid) (PLA)/ kenaf bio-composites. Kenaf fibers were treatment with 1, 3 and 5 parts per hundred (pph) of 3-glycidoxypropyl trimethoxy silane (GPS). The biocomposites with 0, 10, 30, 50, and 70 wt% of untreated and treated kenaf fiber were prepared. The results showed that HDT of PLA/kenaf fiber bio-composites was increasing with increasing kenaf loading. The HDT of PLA increase from 57°C to 160°C. The HDT values of GPS treated biocomposites were a little higher than values

of untreated biocomposites. This was attributable to the improved interfacial adhesion and higher crystallinity of the biocomposites.

Teng et al. (2011) investigated the thermal properties of polylactide grafted vapor-grown carbon nanofiber (VGCF)/polylactide nanocomposites. The nanocomposites with 0, 1, 3, 5, 7 and 10 wt% of PLA–VGCF were prepared. The results showed that the HDTs of the nanocomposites were increased with the increasing VGCF contents. The high HDT was caused by the interfacial interaction due to the improved wettability of the VGCF when compounding with PLA matrix. In the presence of 10 wt% PLA–VGCF, the HDT of the PLA/PLA–VGCF nanocomposite was 139°C, enhanced 135.59% compare to that of the neat PLA (59°C). SEM images revealed that the PLA-grafted VGCF exhibited superior dispersion and interfacial adhesion in a PLA matrix. The high aspect ratio of nano-scaled VGCF allows it to readily form network structures to transfer the load, resulting in more effective enhancement of the heat distortion temperature of PLA nanocomposites.

Shih et al. (2011) examined effect of banana fiber (BF) on thermal properties of polylactic acid (PLA)/banana fiber (BF). Banana fibers were treated with 4% NaOH solution for 45 min. And subsequently treated using a silane coupling agent (triethoxy-vinylsilane) to obtain the modified banana fiber (MBF). The composites with 20, 40, 60 wt% of MBF were prepared. The addition of 40 wt% of BF into the composite increased the HDT of pure PLA from 62°C to 139°C. This could be attributed to good adhesion in between treated fiber and high thermal stability of banana fiber.

Wang et al. (2012) reported the influence of compatibilizer on heat resistance of poly(lactic acid)/polycarbonate (PC) blend. The PLA/PC/epoxy compatibilizer (EP) (50/50/10 phr) ternary blends with tetrabutylammonium bromide catalyst (TBAB)

loading at 0.5 and 1 phr were prepared. The HDT of PLA/PC/EP ternary blends increased considerably with 10 phr EP due to rigid interphase formation. However, the drastic rise in the HDT with increasing catalyst content indicated that the improved interfacial adhesion due to accelerated ring opening of the epoxide with the carboxylic end of PLA was achieved.

Wang et al. (2012) researched on the effect poly(butylene succinate-co-lactate) compatibilizer (PBSL) content on heat resistance of PLA/PC (50/50) blend was also studied by varying PBSL content from 5 to 20 phr. The non-isothermal cooling behaviors of the ternary systems cooled from the molten state at 220°C. The T_g of PLA component remained unchanged, broadening of PC glass transition with T_g peak shifting to lower temperature were also clearly observed in the cooling scans. The HDT of the PLA/PC blend with 5 phr PBSL up to 94.8°C, which was nearly 20% increase compared with the unmodified blend (80.3°C). The increased in HDT could be due to the improvement in interfacial adhesion between PC and PLA.

Guo et al. (2015) were studied effect of polyoxymethylene (POM) on thermal mechanical properties of poly(lactic acid)/polyoxymethylene blends. The ratio of PLA/POM blends were 75/25, 65/35, 60/40, 50/50, 40/60, and 25/75 (w/w). The authors reported that crystallization rate and crystallinity of the blends were increased with increasing POM content. As a result, HDT of the blends increased with an increase of POM content and was greater than that of neat PLA. The HDT was barely raised by adding 25 and 35 wt% POM and started to noticeably increase when the addition of POM larger than 40 wt%. The HDT of PLA was increased from 65.5°C to 133°C which is nearly 2-fold by adding 50 wt% POM. TEM photomicrographs confirmed that PLA/POM blend was immiscible as they formed distinct phases, the observed nano-

sized interpenetrating structure implied complex interaction on molecular level between these two polymers, which would greatly affect HDTs properties of the blends.



CHAPTER III

EXPERIMENTAL

3.1 Materials

Poly(lactic acid) (PLA, 4043D) was supplied by NatureWorks LLC. PDLA with a molecular weight of 100,000 g/mol was purchased from department of chemistry, Chiang Mai University. Natural rubber (STR 5L) was supplied by P. J. Rubber Co., Ltd.

3.2 Experimental

3.2.1 Blends preparation

PLA/NR blends with various ratio (i.e; 95/5, 90/10, 85/15 and 80/20 wt%) were prepared using an internal mixer (Haake Rheomix, 3000P) at the temperature of 170°C with a rotor speed of 60 rpm for 10 min. PLA/NR blends were characterized by tensile and impact test. The blend that showed the highest impact strength was chosen to study the effect of PDLA content on mechanical and thermal properties of PLA/NR blends. Blends containing 1, 3, 5 wt% PDLA base on amount of PLA were prepared using an internal mixer (Haake Rheomix, 3000P). PLA and PDLA were dried at 70°C for 4 hours in an oven before blending. The compositions in percentage by weight (wt%) of all blends are shown in Table 3.1.

Table 3.1 Blend Compositions

Code	PLA (wt%)	NR (wt%)	PDLA (wt%)
PLA	100	-	-
PLA/NR (95/5)	95	5	-
PLA/NR (90/10)	90	10	-
PLA/NR (85/15)	85	15	-
PLA/NR (80/20)	80	20	-
PLA/NR/PDLA (1)	84.15	15	0.85 (1)
PLA/NR/PDLA (3)	82.45	15	2.55 (3)
PLA/NR/PDLA (5)	80.75	15	4.25 (5)

^a The weight percentage of PDLA based on the amount of PLA in the blends.

3.2.2 Specimen preparation

All specimens were produced using a compression molding machine (Labtech, LP20-B) at 170°C and the pressure of 100 MPa.

Tensile specimens were prepared according to ASTM D638. The thickness, the width at narrow section, the overall width and the gage length of specimens were 4 mm, 3.18 mm, 9.53 mm and 7.62 mm respectively.

Unnotched and notched Izod impact strength test specimens were molded according to ASTM D256. The specimens have a width of 12.7 mm, a length of 64 mm and a depth of 4 mm. The specimen was notched using engine lathe machine with a notch angle of 45° having a radius of 0.25 mm and a depth of 2.54 mm. The depth of specimens after notched mark was 10.20±0.05 mm.

HDT test specimen were conformed to the ASTM D648 standard. The specimens were a 127 mm in length, 13 mm in depth and 3 mm in width.

To observe the effects of annealing treatment on the properties of the blends, HDT bars, tensile and impact specimens were annealed in an air oven at 100°C

for 10, 30 and 60 min.

3.2.3 Characterization of PLA and the blends

3.2.3.1 Tensile testing

Tensile properties of PLA, PLA/NR blends, and PLA/NR/PDLA blends were obtained according to ASTM D638. The tensile properties of samples were determined using a universal testing machine (Instron, 5565) with a load cell of 5 kN and crosshead speed of 10 mm/min.

3.2.3.2 Unnotched and notched Izod impact testing

Unnotched and notched izod impact strength of PLA, PLA/NR blends, PLA/NR/PDLA blends were performed according to ASTM D256 in Izod mode using an impact testing machine (Instron CEAST 9050).

3.2.3.3 Heat distortion temperature (HDT)

The heat distortion temperature of PLA, and PLA/NR, PDLA/PLA/NR blends were measured using a HDT/VICAT manual heat deflection tester (model HDV1). The test procedure was conformed to the ASTM D648 standard. The loading pressure was 0.455 MPa (66 psi) and samples were heated at a rate of 2°C/min from room temperature.

3.2.3.4 Differential scanning calorimetry (DSC)

Thermal properties of PLA, and PLA/NR, PLA/NR/PDLA blends was characterized using a differential scanning calorimeter (DSC204F1). The sample with a weight between 5 and 10 mg was put in an aluminum pan and sealed with an aluminum cover. The sample was heated from 25°C to 200°C at the rate of 5°C/min (the first heating) and kept for 2 min at 200°C to remove the previous thermal history.

Subsequently, the sample was cooled to 25°C at the rate of 5°C/min (cooling) and heated again to 200°C at the rate of 5°C/min (the second heating).

3.2.3.5 Scanning electron microscopy (SEM)

Morphological properties of PDLA, PLA, PLA/NR and PLA/NR/PDLA blends were observed using a scanning electron microscope (JEOL, JSM6010). Acceleration voltage of 15 keV was used to collect SEM images of the samples. The tensile fractured surface of specimens were coated with gold before analysis.

3.2.3.6 Wide angle X-ray scattering (WAXS)

Wide-angle X-ray scattering (WAXs) patterns of PDLA, PLA, PLA/NR and PLA/NR/PDLA blends were obtained from a Small/Wide Angle X-ray Scattering (SAXS) beamline constructed at the Siam Photon Laboratory of the Synchrotron Light Research Institute (SLRI), Thailand. The samples were performed using the x-ray energy of 9 keV, the exposure time of 60 second in the angular region (2θ) of 0° - 40°.

CHAPTER IV

RESULTS AND DISCUSSION

In this chapter, the experimental results on PLA/NR and PLA/NR/PDLA blends were reported and discussed.

4.1 Effect of NR content on mechanical, thermal and morphological properties of PLA

4.1.1 Mechanical properties

4.1.1.1 Tensile properties

Tensile stress-strain curves of PLA and PLA blends are shown in Figure 4.1. PLA showed brittle fracture. The addition of NR into PLA matrix changed the brittle fracture of PLA to a ductile fracture with a formation of neck while stretching. Tensile strength and Young's modulus of PLA, PLA/NR blends with various contents of NR are shown in Figure 4.2. Modulus and tensile strength of PLA/NR decreased with increasing NR content. The reduction in these mechanical properties was due to the result of the rubbery nature of NR. Also, the reduced PLA phase in the blend and the poor interfacial adhesion between PLA and NR (see Figure 4.6 (a) – (e) in section 4.1.3) were the reasons for a decrease in tensile strength and Young's modulus.

Elongation at break of PLA and PLA/NR blends is shown in Figure 4.3. Elongation at break was increased from 18.54% for neat PLA to 257.85% for PLA/NR (85/15). The softness and flexibility of NR would increase the elongation

of the blend. When NR content up to 20% (wt/wt), elongation at break of PLA/NR blends was decreased. The decrease in elongation at break of PLA/NR blends at high NR content was de to the enlargement of the NR particles caused by the coalescence of NR phase.

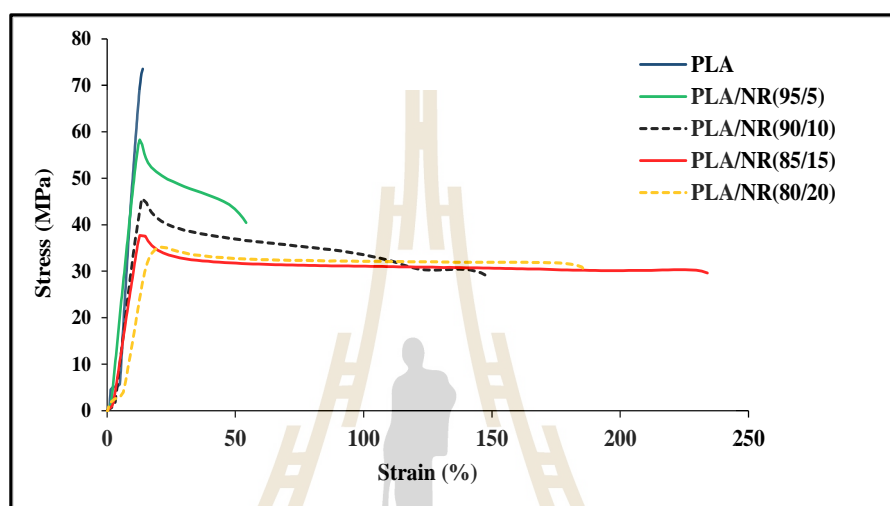


Figure 4.1 Stress-strain curves of PLA and PLA/NR blends at various NR contents.

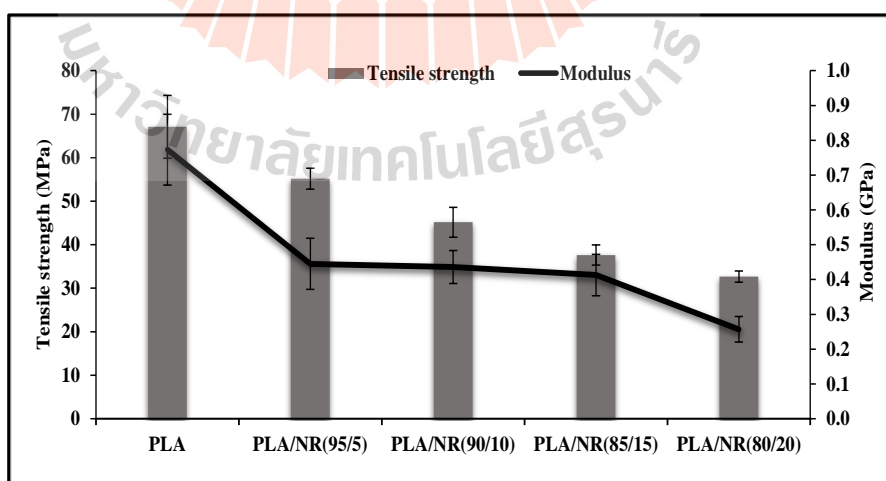


Figure 4.2 Tensile strength and Young's modulus of PLA and PLA/NR blends at various NR contents.

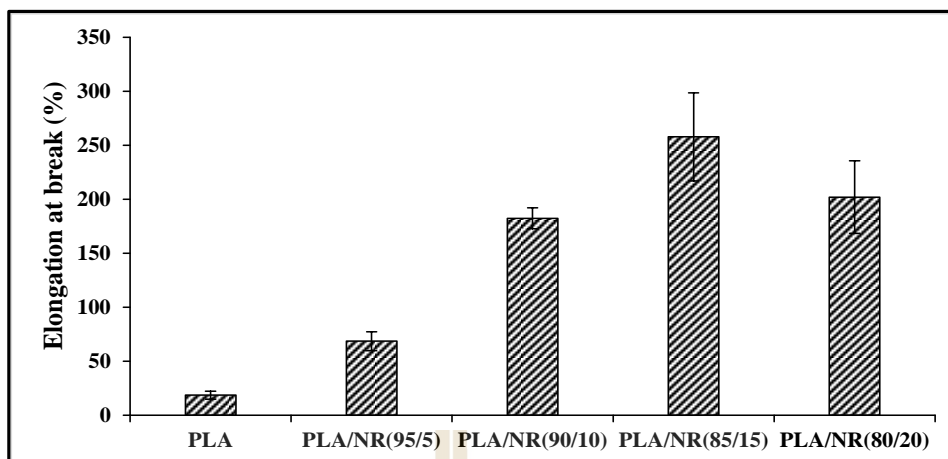


Figure 4.3 Elongation at break of PLA and PLA/NR blends at various NR contents.

4.1.1.2 Impact properties

Figure 4.4 shows the unnotched and notched Izod impact strength of PLA, PLA/NR blends at various NR contents. Notched condition was designed to reduce the toughness of materials. In the other words, the notched condition gives much lower absorbed energy to the samples. Hence, notch specimen is better measure the resistance of the polymer to crack propagation and it is can determine how resistant the specimen absorbs energy when given some defects on it. The unnotched and notched Izod impact strength of neat PLA were 21.16 and 2.91 kJ/m², respectively. Impact strength of PLA/NR blends increased with increasing NR content up to 15 wt%. When NR content was 15 wt%, unnotched and notched izod impact strength of the PLA/NR blend were 173.34 and 46.95 kJ/m², respectively. The high flexibility of NR resulted in more energy absorption. However, when NR content was increased to 20 wt%, unnotched and notched Izod impact strength of PLA/NR blend were decreased to 139.09 and 28.05 kJ/m², respectively. The decrease in impact strength of PLA/NR blends at high NR content (20 wt%) might be due to coalescence of NR phase in the

blend as shown in Figure 4.6 (b-e) in section 4.1.3. However, the value were still higher than those of neat PLA .The summaries of tensile strength, modulus, elongation at break and impact strength of PLA and PLA/NR blend at various NR contents are shown in Table 4.1.

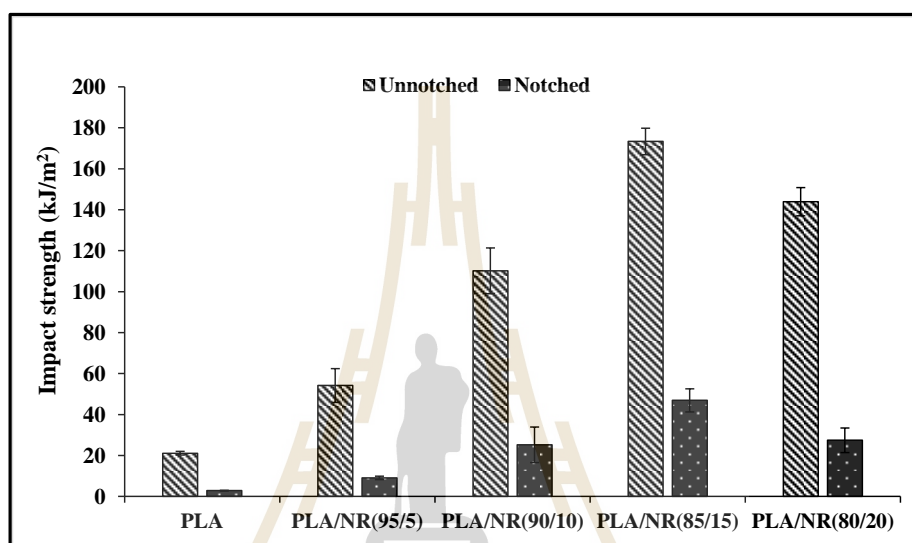


Figure 4.4 Izod impact strength of PLA, PLA/NR blends at various NR contents.

4.1.2 Heat distortion temperature

Heat distortion temperatures of neat PLA and PLA/NR blends PLA, PLA/NR(95/5), PLA/NR(90/10), PLA/NR(85/15) and PLA/NR(80/20) are 55.0, 55.0, 54.0, 54.5 and 53.0°C, respectively as listed in Table 4.1 and plotted in Figure 4.5. The HDTs slightly decreased as NR content increased. The decrease of HDT of PLA/NR blends could be resulted from soft NR phase.

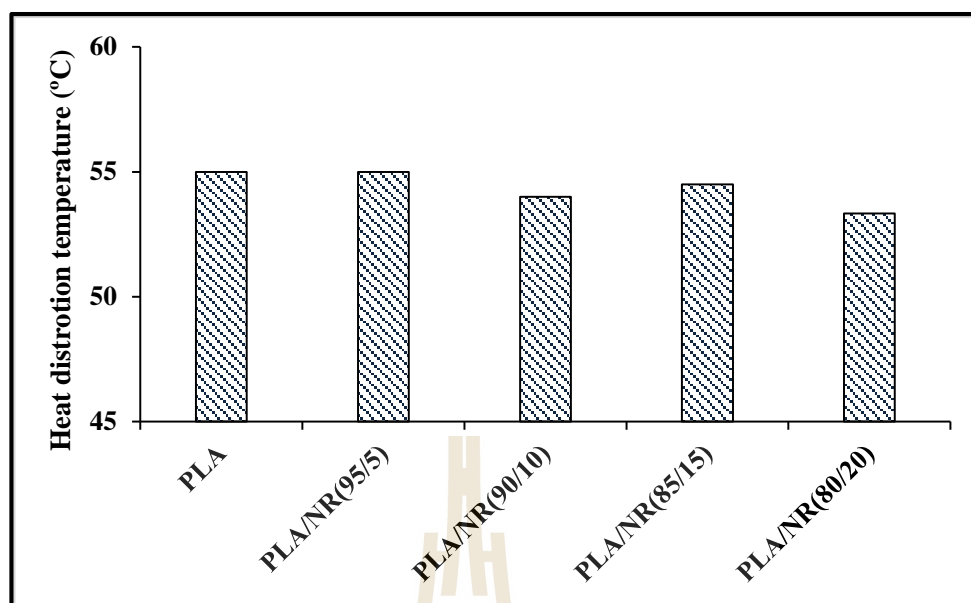


Figure 4.5 Heat distortion temperatures of PLA and PLA/NR blends at various NR content.

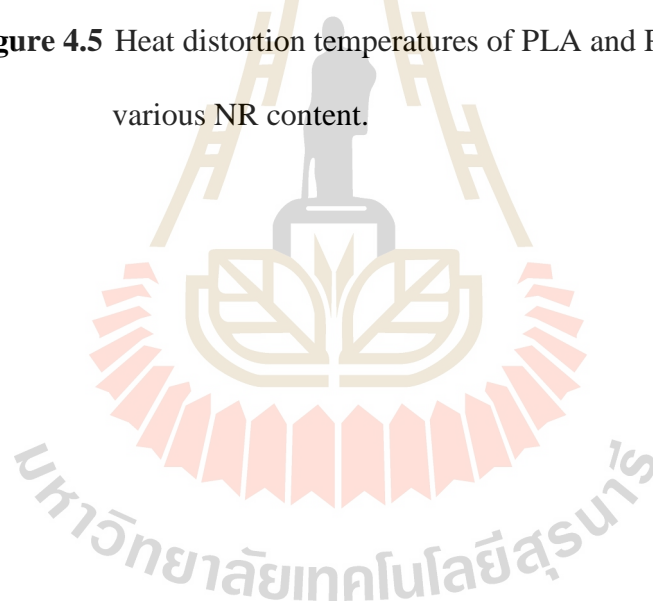


Table 4.1 Mechanical properties and HDT of PLA and PLA/NR blend at various NR contents.

Sample	Tensile strength (MPa)	Modulus (GPa)	Elongation at break (%)	Izod impact strength (kJ/m ²)		HDT (°C)
				Unnotched	Notched	
PLA	67.11 ± 7.23	0.83 ± 0.10	18.54 ± 3.66	21.16 ± 0.94	2.85 ± 0.15	55.0
PLA/NR(95/5)	55.15 ± 2.42	0.52 ± 0.07	68.54 ± 8.64	56.19 ± 13.98	9.12 ± 0.83	55.0
PLA/NR(90/10)	45.15 ± 3.43	0.44 ± 0.04	182.35 ± 9.67	110.16 ± 11.15	25.22 ± 8.65	54.0
PLA/NR(85/15)	37.63 ± 2.30	0.35 ± 0.06	257.85 ± 40.83	173.34 ± 6.49	46.95 ± 5.65	54.5
PLA/NR(80/20)	32.65 ± 1.29	0.31 ± 0.04	201.99 ± 33.66	143.94 ± 6.87	27.44 ± 5.99	53.3

4.1.3 Morphological property

SEM micrographs of impact fractured surface of PLA and PLA/NR blends with various contents of NR are shown in Figure 4.6. Neat PLA exhibits a typical fractured surface of a brittle material with rather a smooth surface with no plastic deformation. The micrographs of PLA/NR blends are shown in Figure 4.6 (b) – (e), all the PLA/NR blends showed phase separated morphology. The difference in polarity of PLA and NR led to a phase separation. This indicated that PLA/NR blends were immiscible blend. The phase morphology apparently showed poor interfacial adhesion evident by the empty spherical grooves on the surface. The droplet size of rubber was increased with the increasing of NR content. This generally occurred in an immiscible binary polymer blend, where the size of dispersed phase increased with an increase the amount the minor phase in the blend. This was due to the coalescence phenomena.

Figure 4.7 (a-e) shows SEM micrographs of tensile fractured surface of PLA and PLA/NR blends with various contents of NR. The smooth fracture surface of neat PLA clearly revealed a typical brittle fracture as shown in Figure 4.7 (a). The addition of the rubber led to a large plastic deformation with a formation of neck. It was clearly shown by the elongated deformed plastic on the fractured surface shown in Figure 4.7 (b) – (c). The SEM micrographs of tensile fracture surface supported the explanation about the increasing in elongation at break.

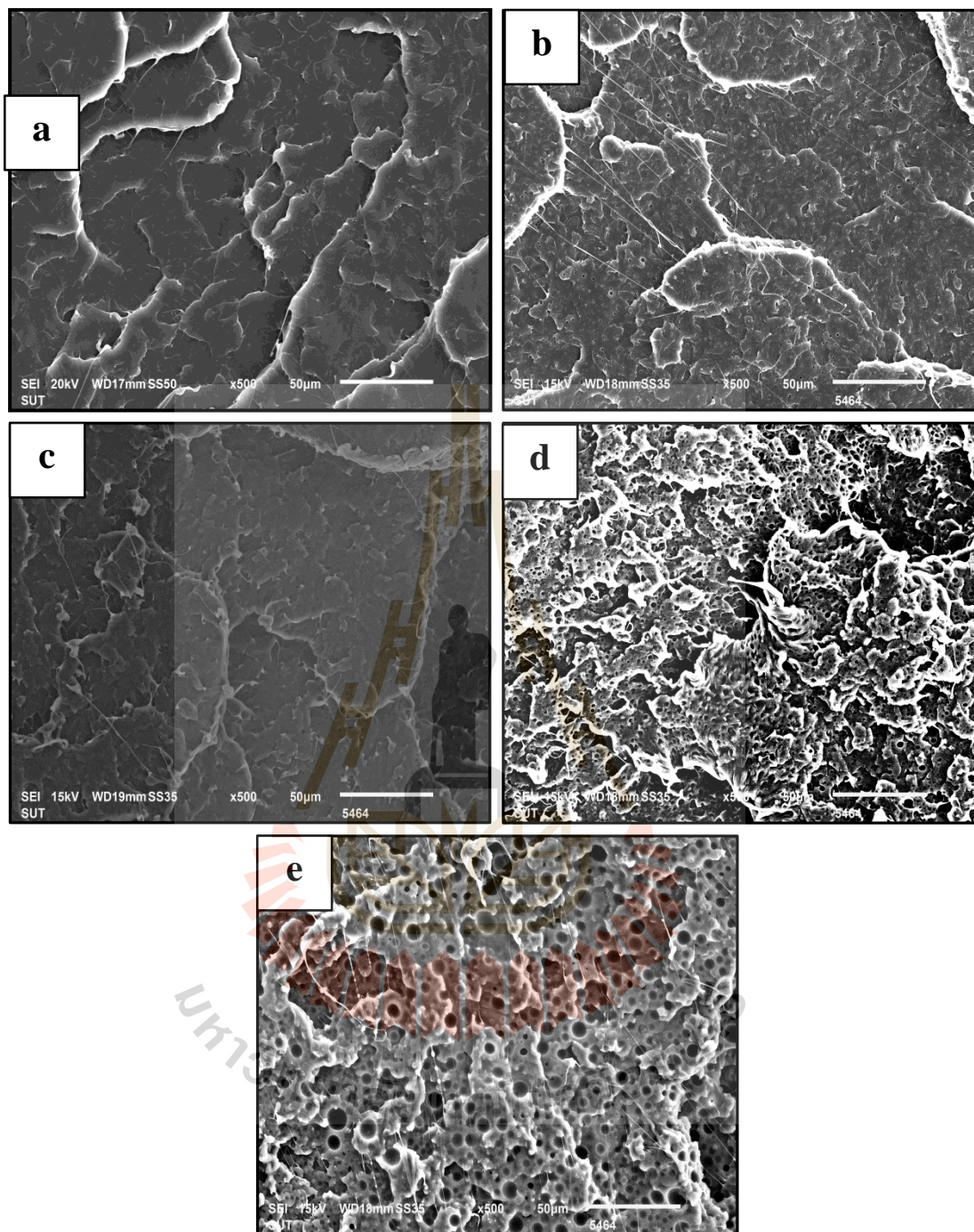


Figure 4.6 SEM micrographs at 500x magnification of impact fractured surface of PLA (a), PLA/NR (95/5) (b), PLA/NR (90/10) (c), PLA/NR (80/15) (d) and PLA/NR (80/20) (e).

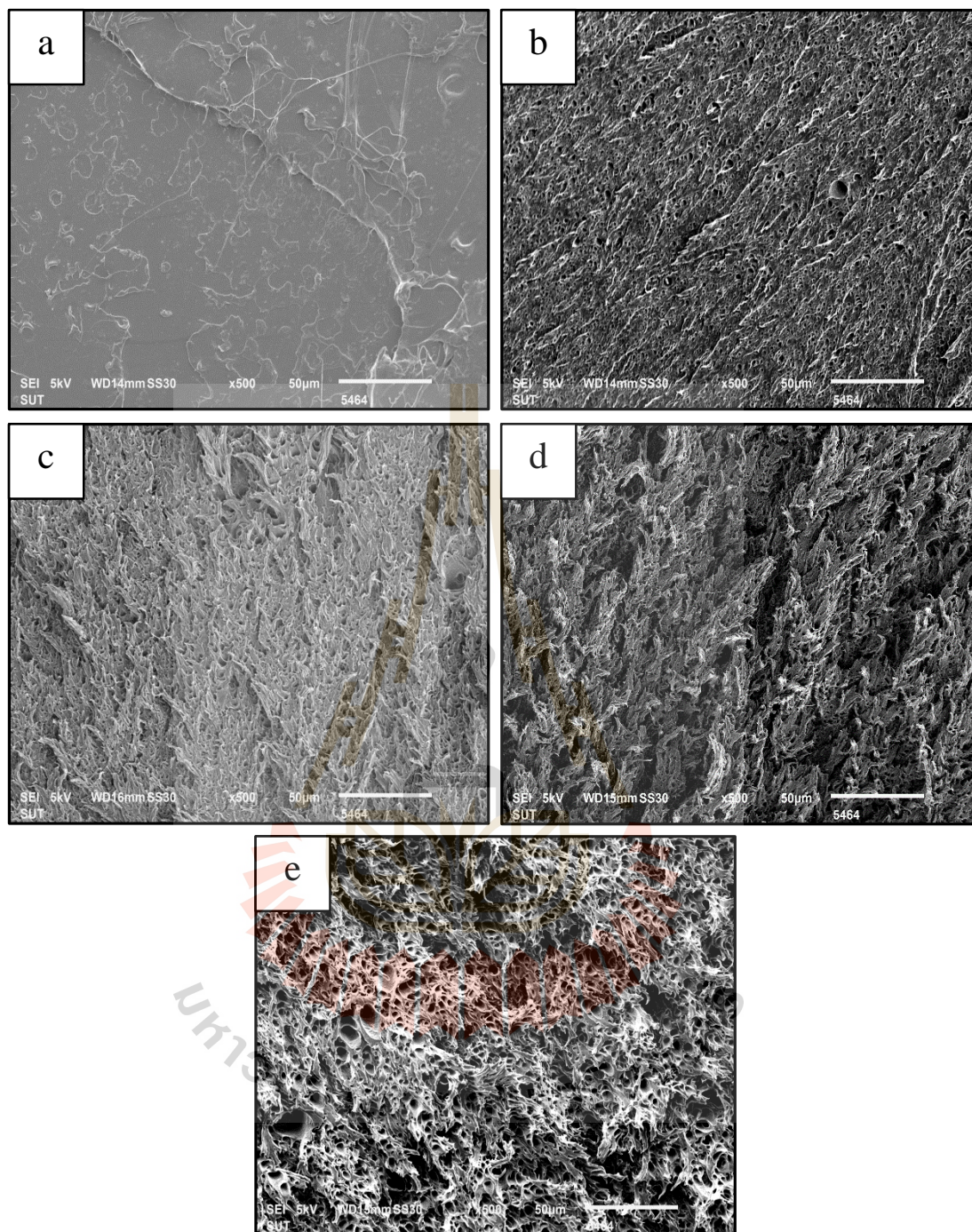


Figure 4.7 SEM micrographs at 500x magnification of tensile fractured surface of PLA (a), PLA/NR (95/5) (b), PLA/NR (90/10) (c), PLA/NR (80/15) (d) and PLA/NR(80/20) (e).

4.2 Effect of PDLA content on thermal, mechanical and morphological properties of PLA/NR blend

To study the effect of PDLA content on mechanical properties of PLA/NR blends, NR content was fixed at 15 wt% according to the highest impact strength of PLA/NR (85/15) blend. The total amount of PLA and PDLA in the blend was kept constant at 85 wt% and the PDLA content in the blends was designed to be 1, 3 and 5 wt% based on the amount of PLA. Therefore, the ratios of PLA to PDLA were 84.15/0.85, 82.45/2.55 and 80.75/4.25 wt%. The addition of small amount of PDLA with $M_w \approx 170,000$ g/mol was expected to act as a crystal nucleating agent for PLA phase in the PLA/NR blend.

4.2.1 Mechanical properties

4.2.2.1 Tensile properties

Tensile stress-strain curves of PLA, PLA/NR(85/15) and PLA/NR/PDLA blends are shown in Figure 4.8. The ductility of PLA/NR(85/15) in the presence of PDLA was lower than that of PLA/NR(85/15) in the absence of PDLA. Figure 4.9 presents the tensile strength and Young's modulus of PLA, PLA/NR(85/15) and PLA/NR/PDLA blends at various PDLA contents. Modulus of PLA/NR(85/15) blend was increased from 0.35 GPa to 0.47 GPa by adding 1 wt% PDLA based on the amount of PLA. This indicated that PDLA slightly enhanced stiffness of PLA/NR(85/15) blends. The addition of PDLA to PLA/NR(85/15), tensile strength of the blend insignificantly changed compared to PLA/NR(85/15). However, tensile strength and modulus of all PLA/NR/PDLA blends were lower than those of neat PLA.

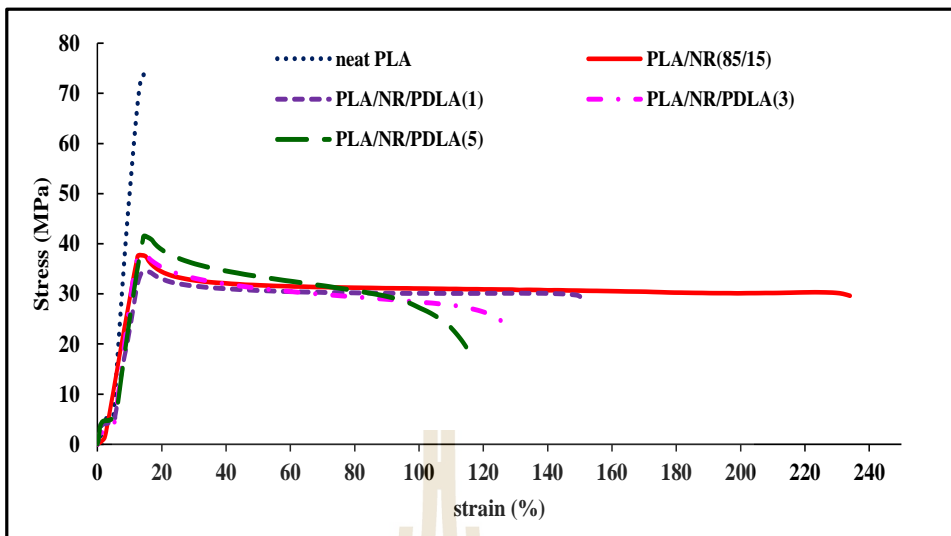


Figure 4.8 Stress-strain curves of PLA, PLA/NR(85/15) and PLA/NR/PDLA blends .

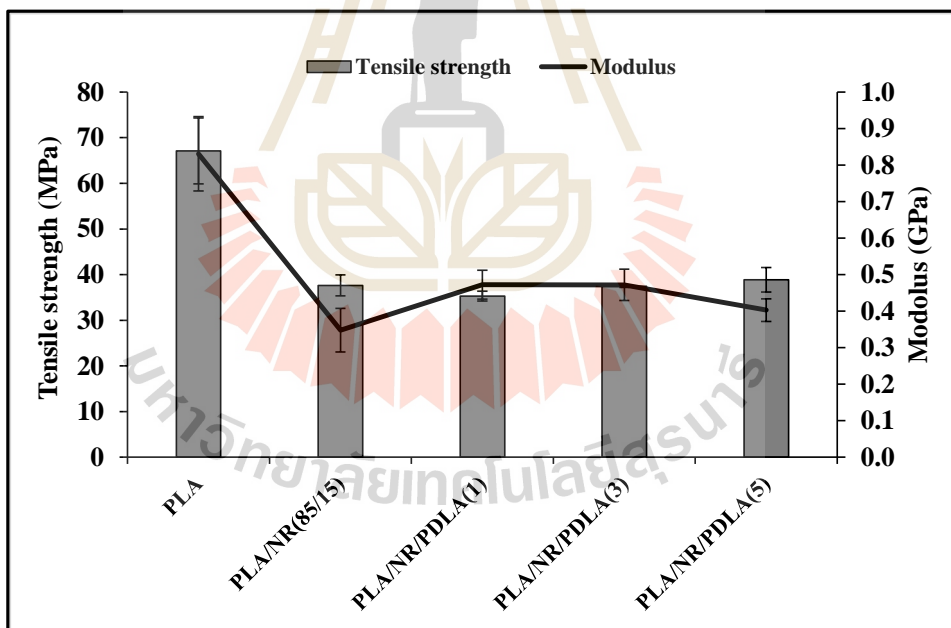


Figure 4.9 Tensile strength and Young’s modulus of PLA, PLA/NR(85/15) and PLA/NR/PDLA blends.

Elongation at break of PLA, PLA/NR and PLA/NR/PDLA blends is shown in Figure 4.10. Elongation at break was decreased with increasing PDLA content. The lowest elongation at break of $115.81 \pm 8.18\%$ was found for PLA/NR/PDLA(5). However, it was still significantly higher than that of neat PLA. The decrease of elongation at break at high PDLA content could be due to an increase of the number of large NR particles leading to poor interfacial adhesion between PLA matrix and NR droplets. These reasons were confirmed by NR particles size measurement from SEM micrographs in section 4.2.4.

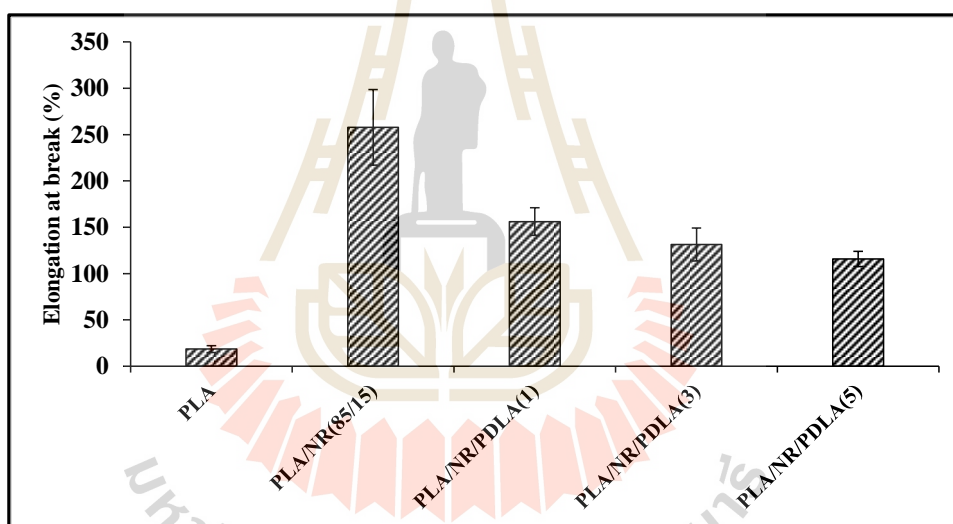


Figure 4.10 Elongation at break of PLA, PLA/NR(85/15) and PLA/NR/PDLA blends.

4.2.1.2 Impact properties

Figure 4.11 shows the unnotched and notched Izod impact strength of the PLA, PLA/NR and PLA/NR/PDLA blends. The unnotched and notched Izod impact strength were 20.70 and 2.91 kJ/m² for neat PLA and 173.34 and 46.95

kJ/m^2 for PLA/NR (85/15), respectively. After the addition of PDLA, the decrease in impact strength with increasing PDLA content was obtained. At 1 wt% PDLA based on the amount of PLA, impact strength was higher than at 3 and 5 wt% PDLA. The domain sizes of NR particle in PLA/NR(85/15) blend at 3 and 5 wt% PDLA were much larger than at 1 wt% PDLA. Also poor distribution of NR particles was observed in section 4.2.3. The decrease in impact strength of PLA/NR(85/15) at 3 and 5 wt% PDLA content might be due to the appearance of some large domain size as shown by SEM micrographs. There are many factors that affect the performance of rubber on toughness of polymer such as interfacial adhesion between rubber particles and matrix,

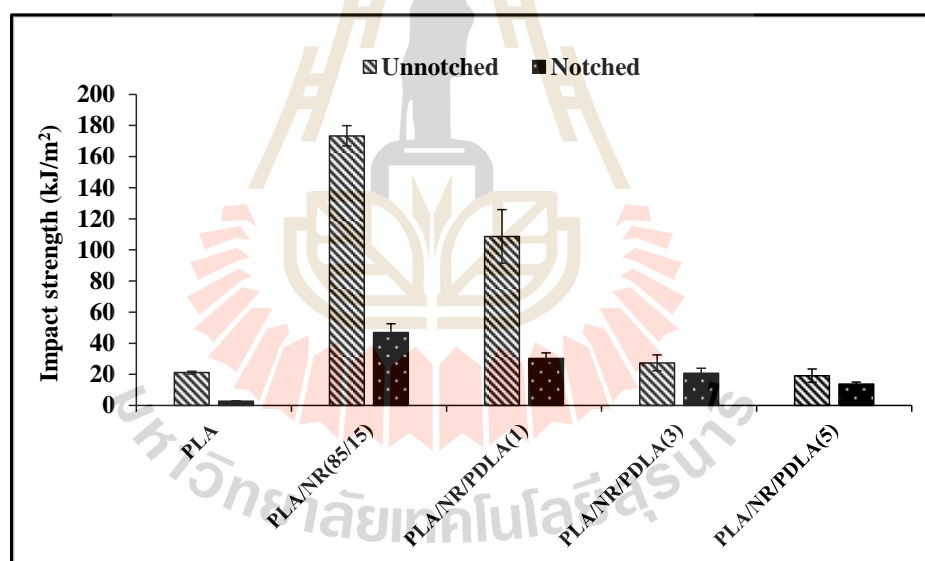


Figure 4.11 Izod impact strength of PLA, PLA/NR(85/15) and PLA/NR/PDLA blend.

rubber particle size, type and concentration of rubber. A large NR particle size and poor interfacial adhesion between rubber particles and matrix would result in poor mechanical properties in the blends. The summaries of tensile strength, modulus,

elongation at break and impact strength of PLA, PLA/NR and PLA/NR/PDLA blends are shown in Table 4.2

4.2.2 Heat distortion temperature

Heat distortion temperature (HDT) is another important thermal property from the view of practical application, thus the HDT of neat PLA, PLA/NR and PLA/NR/PDLA blends were examined. The improvements in crystallinity can result in the enhancement of HDT (Harris and Lee., (2007), Yu et al., (2011)). Figure 4.12 shows the HDTs of PLA, PLA/NR(85/15) and PLA/NR/PDLA blends. The HDT of neat PLA was 55°C which corresponds to T_g of neat PLA. The HDT of an amorphous polymer is around its T_g (Guo, 2012). The HDT of PLA/NR(85/15) blend was increased from 55°C to 61.8°C by adding 1 wt% PDLA based on the amount of PLA. This improvement of HDT is mainly due to the increase of crystallinity of PLA (see section 4.2.5). The crystallinity increase amorphous phase was decreased. Thus, HDT of amorphous and semi-crystalline polymer was improved. On the other hand, there was almost no change in HDT when the PDLA content based on the amount of PLA was above 1 wt %. This was because the X_c of PLA phase in PLA/NR/PDLA blends did not improve when added PDLA was above 1 %wt. This could be because the large NR particles in PLA/NR/PDLA(3) and PLA/NR/PDLA(5) inhibited crystallization of PLA matrix. Therefore, the increase in PDLA content had no observable effect on the HDT of PLA/NR blend. The HDT values of the PLA/NR(85/15) and PLA/NR/PDLA blend with various contents of PDLA are listed in Table 4.2.

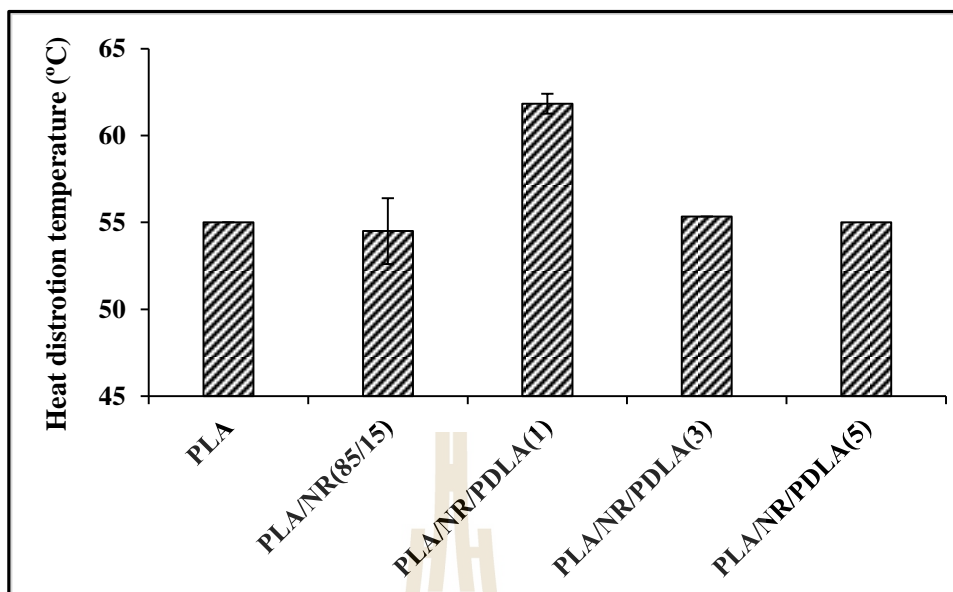


Figure 4.12 HDT of PLA, PLA/NR(85/15) and PLA/NR/PDLA blends.

Table 4.2 Mechanical properties and HDT of PLA, PLA/NR(85/15) and PLA/NR/PDLA blends.

Sample	Tensile strength (MPa)	Modulus (GPa)	Elongation at break (%)	Izod impact strength (kJ/m ²)		HDT (°C)
				Unnotched	Notched	
PLA	67.11 ± 7.23	0.83 ± 0.10	18.54 ± 3.66	21.16 ± 0.94	2.85 ± 0.15	55.0
PLA/NR(85/15)	37.63 ± 2.30	0.35 ± 0.06	257.85 ± 40.83	173.34 ± 6.49	46.95 ± 5.65	54.5
PLA/NR/PDLA(1)	35.30 ± 2.30	0.47 ± 0.03	156.14 ± 14.83	108.68 ± 17.22	30.20 ± 3.59	61.8
PLA/NR/PDLA(3)	37.44 ± 0.21	0.47 ± 0.04	131.43 ± 17.79	27.38 ± 5.07	20.71 ± 2.18	55.3
PLA/NR/PDLA(5)	38.87 ± 2.66	0.40 ± 0.03	115.81 ± 8.18	19.18 ± 4.21	13.71 ± 1.38	55.0

4.2.3 Morphological property

Figure 4.13 (a-e) shows SEM micrographs of tensile fractured surface of PLA/NR(85/15) blends with increasing PDLA contents from 1 to 5% wt. The tensile fractured surface of PLA/NR(85/15) without PDLA showed longer fibrils than those of all PLA/NR/PDLA blends. This could be used as evidence of a reduction in elongation at break of all PLA/NR/PDLA blends.

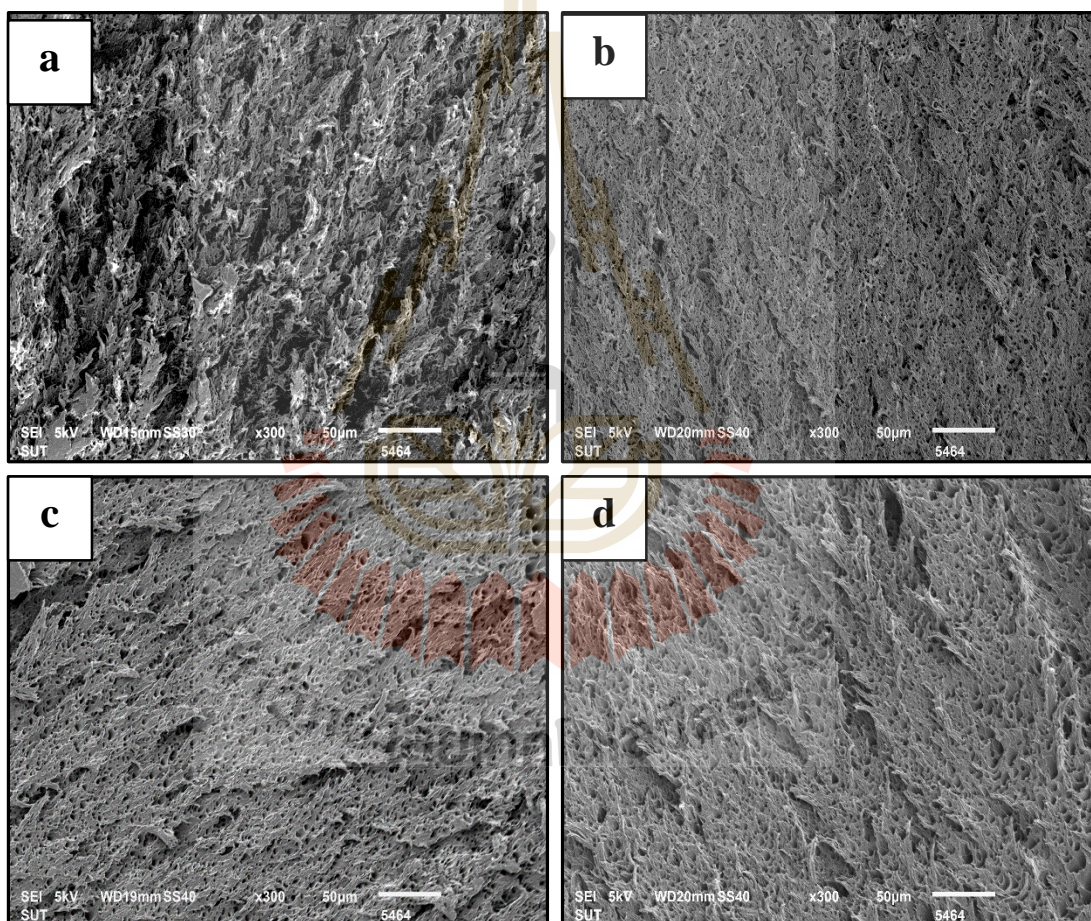


Figure 4.13 SEM micrographs at 300x magnification of tensile fractured surface of PLA/NR(85/15) (a), PLA/NR/PDLA (1) (b), PLA/NR/PDLA (3) (c) and PLA/NR/PDLA (5) (d).

SEM micrographs of freeze-fractured surfaces of PLA and PLA/NR blends containing difference PDLA contents are shown in Figure 4.14. All the blends showed phase separated morphology where the rubber particles formed spherical dispersed with low interfacial adhesion with the PLA matrix. The incorporation of 1 wt% PDLA had no influence on the domain NR droplets size, dispersion and size distribution of rubber particle. The domain droplets size of NR particles in PLA/NR/PDLA blend at 3 wt% and 5 wt% of PDLA were increased, and poor dispersion and poor size distribution of rubber particle could be observed. The results indicated that the size of the NR phase increased upon increasing the amount of PDLA. The increase of NR droplets size in PLA/NR/PDLA(3) and PLA/NR/PDLA(5) blends could be due to the increased viscosity and elasticity of the PLA phase induced by the formation of stereocomplex crystallites (Zhang et al, 2017, Dai et al, 2016). The micrographs of PLA/NR(85/15) and PLA/NR/PDLA(1) showed spherical NR particles evenly dispersed in PLA and the dispersion of the particle size was narrow (see figure 4.15 (a)-(d) in section 4.2.3). Figure 4.14 (d) and (c) shows the representative morphology of PLA/NR/PDLA(3) and PLA/NR/PDLA(5) blends respectively. The blends clearly shows phase separated morphology. NR droplets were dispersed randomly in the PLA matrix.

The diameter of rubber particle in the blends was measured from SEM micrographs of freeze-fractured surfaces of PLA and its blends (Figure 4.14) .The number averaged diameter, D_n was calculated from a minimum of 200 particles according to the following equations:

$$D_n = \frac{\sum_i N_i D_i}{\sum_i N_i} \quad (4.1)$$

where D_i is the diameter of particle and N_i is the total number of particles having diameter, D_i (Wu et al., 2010).

The average particle diameter of NR in the PLA/NR/PDLA blends are shown in Table 4.3. The average diameter of NR particles was increased from 3.03 to 3.54 μm when PDLA content was increased from 1 to 5%wt. The occurrence of larger NR particles occurred which resulted in a decrease in elongation at break and impact strength of PLA/NR/PDLA blend.

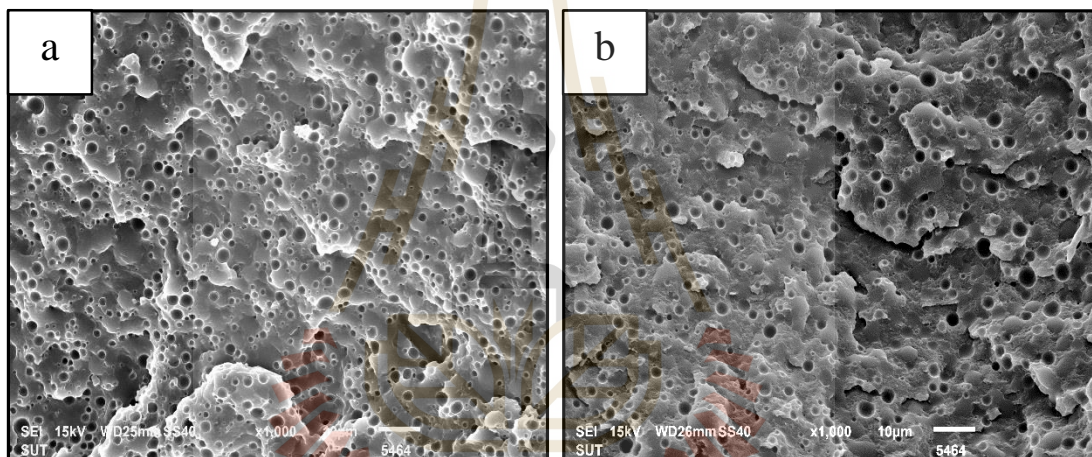


Figure 4.14 SEM micrographs at 1,000x magnification of freeze-fractured surfaces of PLA/NR(85/15) (a), PLA/NR/PDLA (1) (b), PLA/NR/PDLA (3) (c) and PLA/NR/PDLA (5) (d).

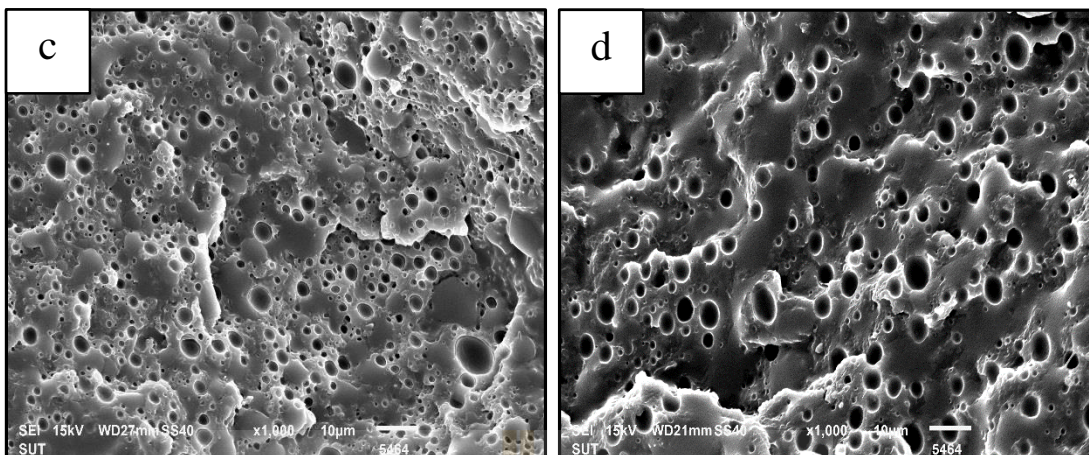


Figure 4.14 SEM micrographs at 1,000x magnification of freeze-fractured surfaces of PLA/NR(85/15) (a), PLA/NR/PDLA (1) (b), PLA/NR/PDLA (3) (c) and PLA/NR/PDLA (5) (d) (continued).

Table 4. 3 Diameters of NR particles in the PLA/NR(85/15) and PLA/NR/PDLA blends.

Samples	Average particle diameter (D_n) (μm)	Minimum particle diameter (μm)	Maximum particle diameter (μm)
PLA/NR(85/15)	3.03 ± 1.06	1.08	8.43
PLA/NR/PDLA(1)	3.34 ± 1.07	1.30	7.65
PLA/NR/PDLA(3)	3.30 ± 1.00	0.80	8.00
PLA/NR/PDLA(5)	3.54 ± 1.08	1.71	8.25

4.2.4 Thermal properties

In this section, the effects of PDLA on thermal properties in particular cold crystallization temperature (T_{cc}), crystallinity (X_c), glass transition temperature (T_g) and melting temperature (T_m) are discussed. The thermal properties were examined by differential scanning calorimetry (DSC). The DSC data of neat PLA, PLA/NR(85/15) and PLA/NR/PDLA blends were obtained from first and second heating scans. The first heating scan gave original crystalline state of the PLA in the molded sample that related to the mechanical properties (Feng et al., 2013). While second heat evaluated the inherent properties of the material. The crystallinity (X_c) of the blend samples can be calculated based on the enthalpy value of a 100% crystalline PLA from the following equation:

$$\%Crystallinity = X_c = 100 \times \frac{\Delta H_m - \Delta H_c}{\Delta H_m^\infty} \quad (4.2)$$

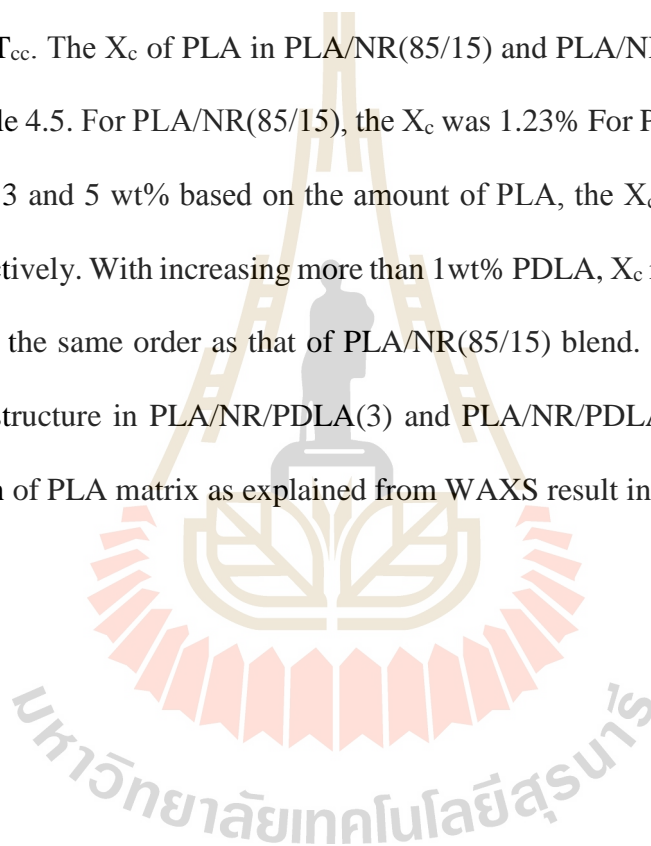
where ΔH_m is the measured endothermic enthalpy of melting and ΔH_c is the cold crystallization exothermic enthalpy during the heating scans. The theoretical melting enthalpy of 100% crystalline PLA was taken to be $\Delta H_m^\infty = 93.6$ J/g (Tang et al., 2012).

DSC results from first heating scan of PLA, PLA/NR(85/15) and PLA/NR/PDLA blend with various contents of PDLA are shown in Figure 4.16 and thermal characteristics data are summarized in Table 4.4. The endothermic peak appeared in DSC thermogram of PLA/NR(85/15) and PLA/NR/PDLA blend with various contents of PDLA (see figure 4.16) close to T_g was attributed to the enthalpy relaxation effects reflecting the thermal history of the samples (Celli and Scandola, 1992). The T_{cc} of PLA phase in neat PLA, PLA/NR(85/15), PLA/NR/PDLA(3)

and PLA/NR/PDLA(5) are 98.6, 104.1, 102.4 and 104.8°C respectively. T_{cc} of PLA phase appeared in PLA/NR(85/15), PLA/NR/PDLA(3) and PLA/NR/PDLA(5) are higher than that of neat PLA. This result suggested that NR particles impeded the orderly arrangement of the PLA molecular chains. The double melting temperature found in PLA, PLA/NR(85/15) and PLA/NR/PDLA blend with various contents of PDLA were observed. The presence of two melting peaks in PLA phase related to the melting of the α' and α phases. The peak at the lower temperature is related to the melting of the α' form, while the second peak corresponds to the melting of the α form. The two processes, the melting of the α' form and the recrystallization into the α form can be considered as the α' - α phase transition (Pan et al., 2007). T_{cc} of PLA phase did not found in PLA/NR/PDLA(1) and the blend also showed a single T_m peak. It should be because PLA phase in the PLA/NRPDLA(1) was completely crytallized during sample preparation which confirmed by an increase of the X_c from 1.80% for PLA/NR(85/15) blend to 25.25% for PLA/NR/PDLA(1). This result suggested that only 1 wt% of PDLA could enhanced crystallization for PLA matrix.

During second heating scan, T_g of PLA matrix increased from 53.9°C to 59.4°C. The X_c of PLA phase in PLA/NR(85/15) was lower than that of neat PLA. Moreover, the T_{cc} and T_m of PLA phase in PLA/NR(85/15) were significantly higher than that of neat PLA. This could be due to the addition of NR into PLA may interrupted the movement of polymer chains and hinder diffusion of PLA molecular chains to the surface of the nucleus in the blends. This result suggested that NR particles impeded the orderly arrangement of the PLA molecular chains. The crystallization kinetic of PLA could be affected by the presence of NR. However, T_g and T_m of PLA phase in PLA/NR blend did not change after PDLA was added into the

blends. The T_{cc} of PLA phase obtained from second heating scan of PLA/NR(85/15), PLA/NR/PDLA(1), PLA/NR/PDLA(3) and PLA/NR/PDLA(5) are 114.8, 112.9, 113.8 and 112.9 °C respectively. DSC results showed that the T_{cc} appeared in all PLA/NR/PDLA blends were lower than that appeared in PLA/NR(85/15). It is known that the lower T_{cc} initiates faster crystallization. The introduction of a small amount of PDLA could promote the crystallization capability of PLA phase in PLA/NR(85/15) blend by reducing the T_{cc} . The X_c of PLA in PLA/NR(85/15) and PLA/NR/PDLA blends were shown in Table 4.5. For PLA/NR(85/15), the X_c was 1.23%. For PLA/NR(85/15) blend containing 1, 3 and 5 wt% based on the amount of PLA, the X_c were 3.82, 1.63 and 1.23%, respectively. With increasing more than 1wt% PDLA, X_c reached around 1.2%, which was of the same order as that of PLA/NR(85/15) blend. This may be because the network structure in PLA/NR/PDLA(3) and PLA/NR/PDLA(5) blends inhibited crystallization of PLA matrix as explained from WAXS result in section 4.2.5



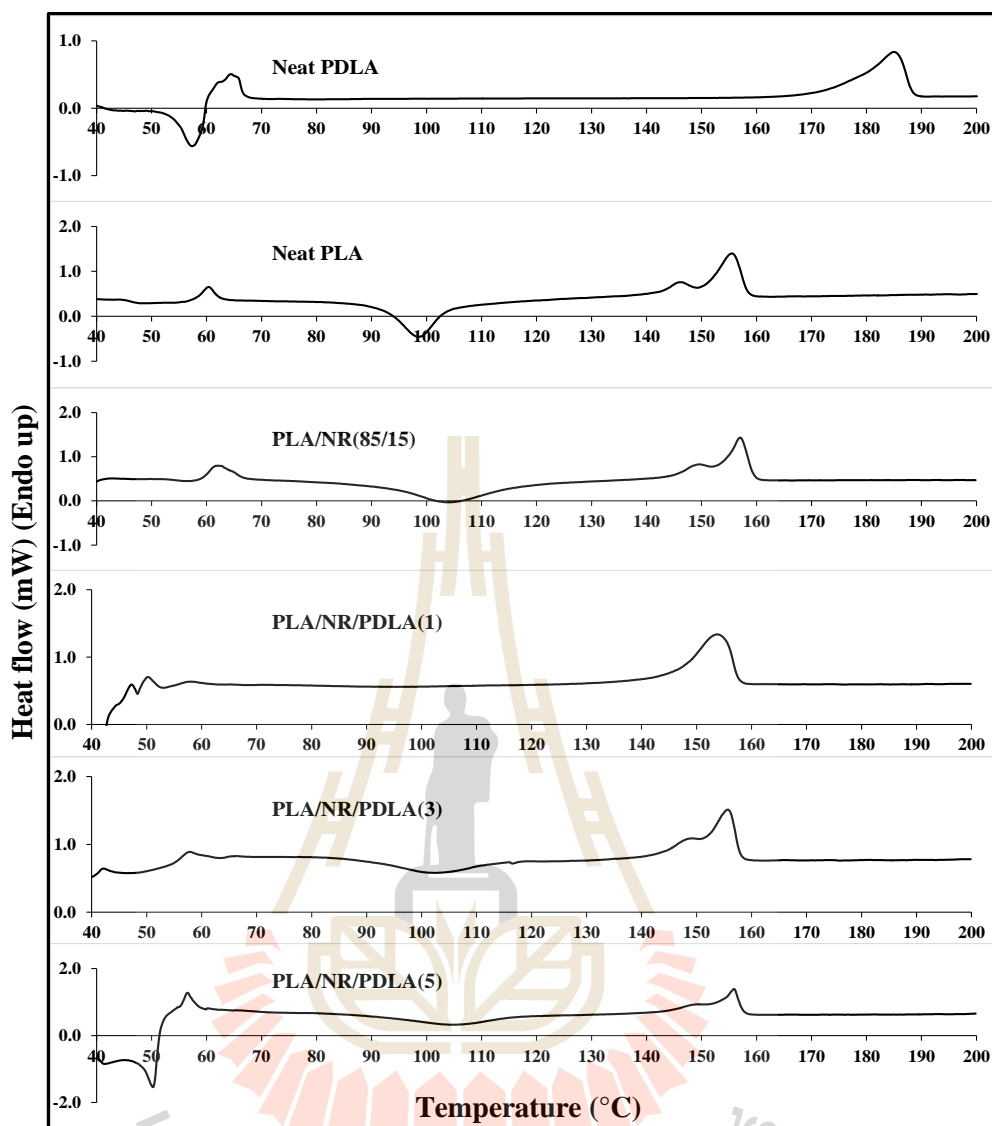


Figure 4.15 DSC thermograms of PLA, PLA/NR(85/15) and PLA/NR/PDLA blend with various contents of PDLA (the first heating, heating rate 5°C/min).

Table 4.4 DSC first heating results of PLA, PLA/NR(85/15) and PLA/NR/PDLA blends.

sample	T_g (°C)	T_{cc} (°C)	T_{m1} (°C)	T_{m2} (°C)	ΔH_c (J/g)	ΔH_m (J/g)	X_c (%)
PDLA	N/A	N/A	N/A	185	N/A	73.23	78.24
PLA	60.8	98.6	146.2	155.6	25.16	26.47	1.40
PLA/NR(85/15)	60.7	104.1	149.6	157	25.16	26.89	1.85
PLA/NR/PDLA(1)	N/A	N/A	153.8	N/A	N/A	24.32	25.98
PLA/NR/PDLA(3)	N/A	102.4	149.1	155.7	18.96	20.49	1.63
PLA/NR/PDLA(5)	N/A	104.8	148.1	155.9	15.91	17.38	1.57

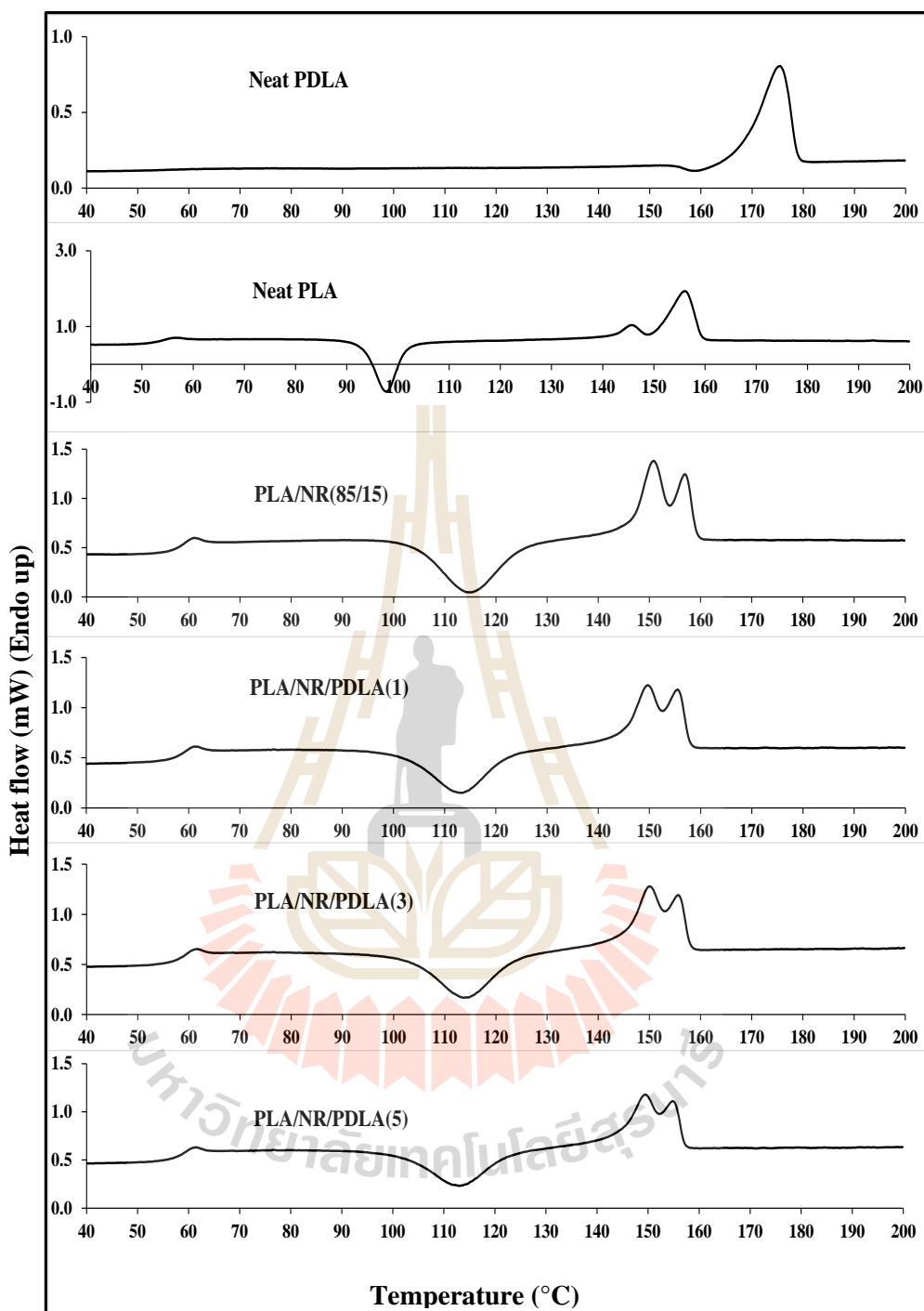


Figure 4.16 DSC thermograms of PLA, PLA/NR(85/15) and PLA/NR/PDLA blend with various contents of PDLA (the second heating, heating rate 5 °C/min).

Table 4.5 DSC second heating results of PLA, PLA/NR(85/15) and PLA/NR/PDLA blends.

sample	T _g (°C)	T _{cc} (°C)	T _{m1} (°C)	T _{m2} (°C)	ΔH _c (J/g)	ΔH _m (J/g)	X _c (%)
PDLA	N/A	N/A	N/A	175.4	N/A	62.07	66.31
PLA	53.9	97.7	145.6	156	27.14	32.06	5.26
PLA/NR(85/15)	59.4	114.8	150.9	156.9	23.89	25.01	1.23
PLA/NR/PDLA(1)	59.3	112.9	149.8	155.5	16.06	19.64	3.82
PLA/NR/PDLA(3)	59.6	113.8	150.1	155.6	18.96	20.49	1.63
PLA/NR/PDLA(5)	59.3	112.9	149.5	154.8	16.22	17.37	1.23

4.2.5 WAXS patterns of PLA, PDLA and the blends

Figure 4.18 shows the WAXS patterns of film sample of neat PDLA, neat PLA, PLA/NR(85/15) and PLA/NR/PDLA blend with various PDLA contents. The neat PDLA showed a large amorphous scattering background with small diffraction peaks at 2θ at approximately 16.3° . This suggested that low crystalline phase. The WAXS patterns of neat PLA and PLA/NR(85/15) blend exhibited a broad diffraction peak centered at $2\theta \approx 15^\circ$. The PLA did not show any characteristic peak, which indicates that the structure is amorphous. The WAXS pattern of PLA/NR/PDLA(1) had a weaker diffraction peak at 2θ of 10.5° , 18.5° and 23.8° , which correspond to the PLA stereocomplex crystallites (Tsuji and Ikada, (1990); Wei et al., (2014); Pholharn, Srithep, and Morris, (2017)). These diffraction peaks become sharper with increasing PDLA content in the blend. This suggested that the number of stereocomplex crystallite increased with increasing PDLA content. The stereocomplex crystallites enhanced the crystallization of PLA by providing heterogeneous nucleation site. However, in the current work the increase in number of stereocomplex crystallites in the blend containing higher amount of PDLA did not improve the X_c of PLA phase in PLA/NR/PDLA(3) and PLA/NR/PDLA(5). This could be because the stereocomplex crystallite formed in PLA/NR/PDLA blend acted as a cross-linking point of PLA chain. Therefore, the cross-linking point hindered chains movement and crystal growth of PLA (Wei et al., (2014); Rahman et al., (2009)). The network structure developed uniformly as the SC crystallite increased

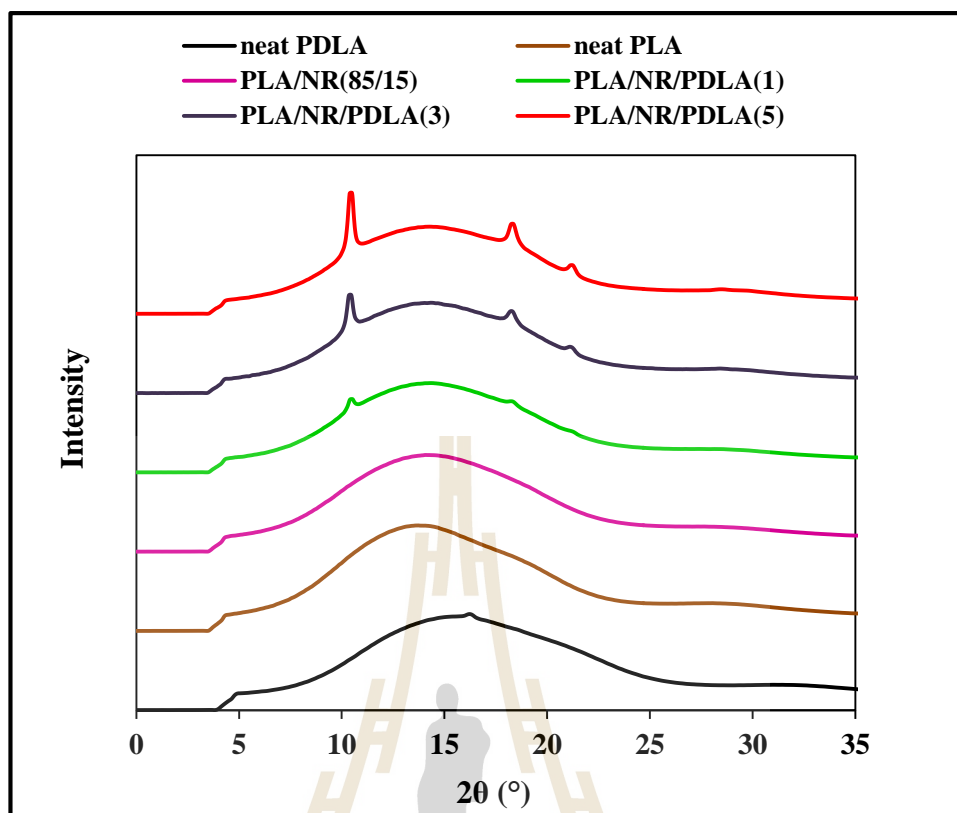


Figure 4.17 WAXS patterns of PDLA, PLA, PLA/NR(85/15) and PLA/NR/PDLA blend with various contents of PDLA.

4.3 Effect of annealing time on mechanical, thermal and morphological properties of PLA/NR/PDLA blends

To observe the effect of annealing treatment on the properties of the blends, the blend specimens were annealed in an air oven at 100°C for 10, 30 and 60 minutes.

4.3.1 Mechanical properties

4.3.1.1 Tensile Properties

Tensile stress-strain curves of PLA and PLA blends before and after annealing are shown in Figure 4.18. Stress-strain curves of PLA before and after annealing showed a rigid and brittle polymer. The ductility of PLA/NR(85/15) and PLA/NR/PDLA blends was decreased after annealing. It might be because of the spherulite size of PLA and PLA/NR/PDLA blends was increased after annealing (Han, Han and Dong (2013)). Figure 4.19 and 4.20 presents the tensile strength and Young's modulus of PLA, PLA/NR and PLA/NR/PDLA blends before and after annealing respectively. Tensile strength and modulus of annealed neat PLA was significantly decreased. This may be because of spherulite size increased after annealing (Park, Todo and Arakawa (2005) and Han, Han and Dong (2013)). When the spherulite size increased, interspherulitic connections will be weaker (Pang et al., (2008) and Han, Han and Dong (2013)). Tsuji and Ikada (1995) also found that the modulus of PLLA was decreased with the large spherulite formed. The modulus and tensile strength of PLA/NR and PLA/NR/PDLA blends were not significantly changed after annealing treatment.

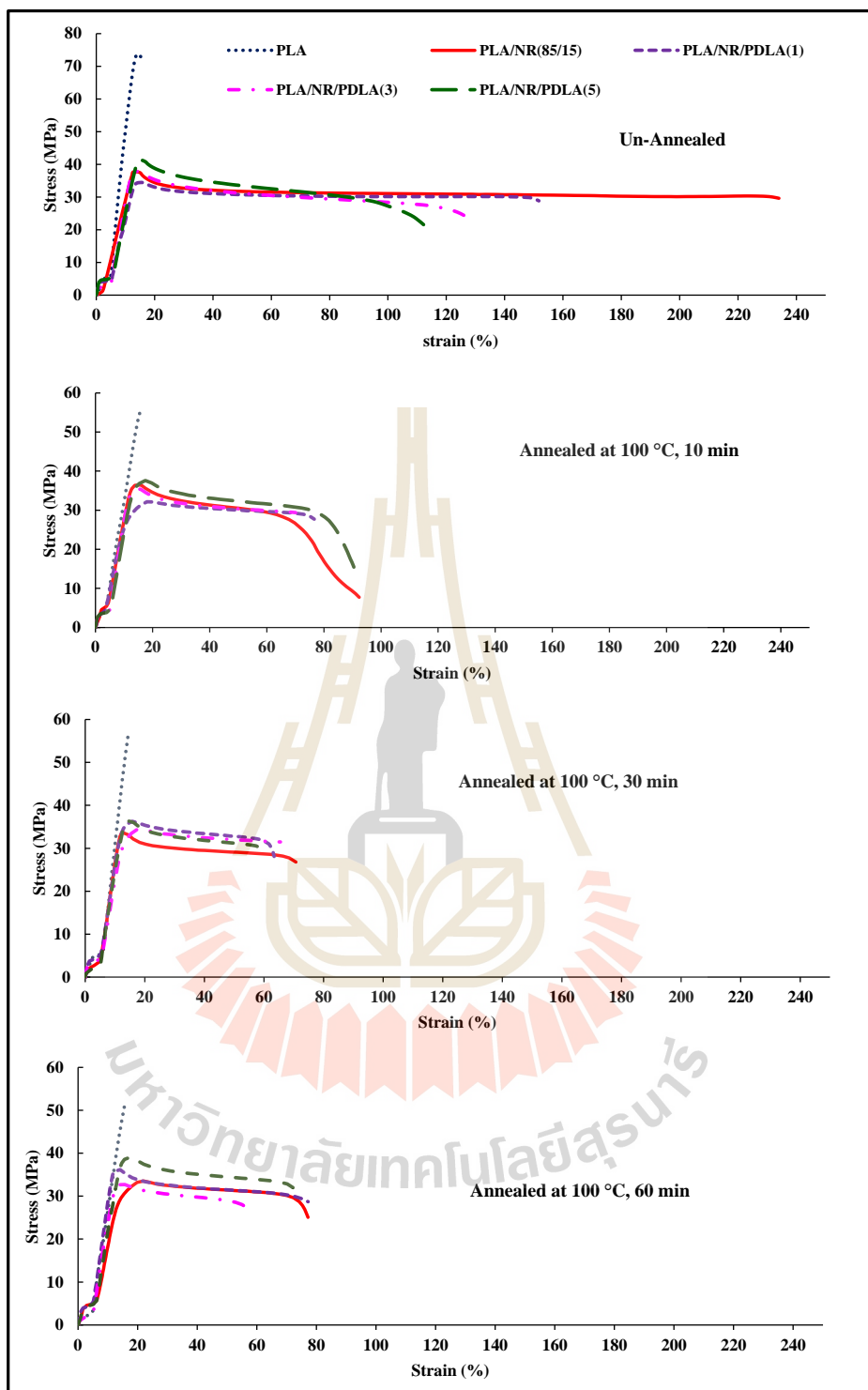


Figure 4.18 Stress-strain curve of PLA, PLA/NR(85/15), PLA/NR/PDLA blends before and after annealing treatment.

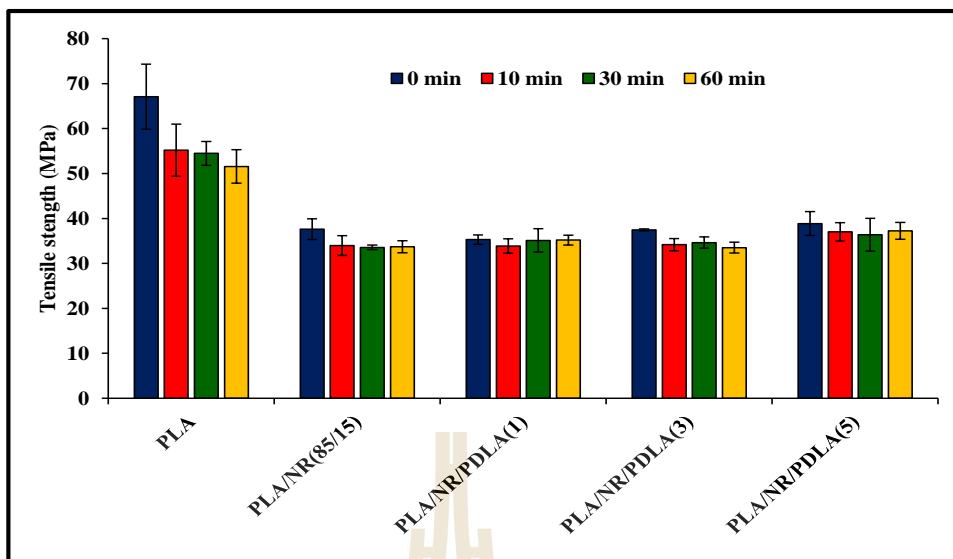


Figure 4.19 Tensile strength of PLA, PLA/NR(85/15), PLA/NR/PDLA blends before and after annealing treatment.

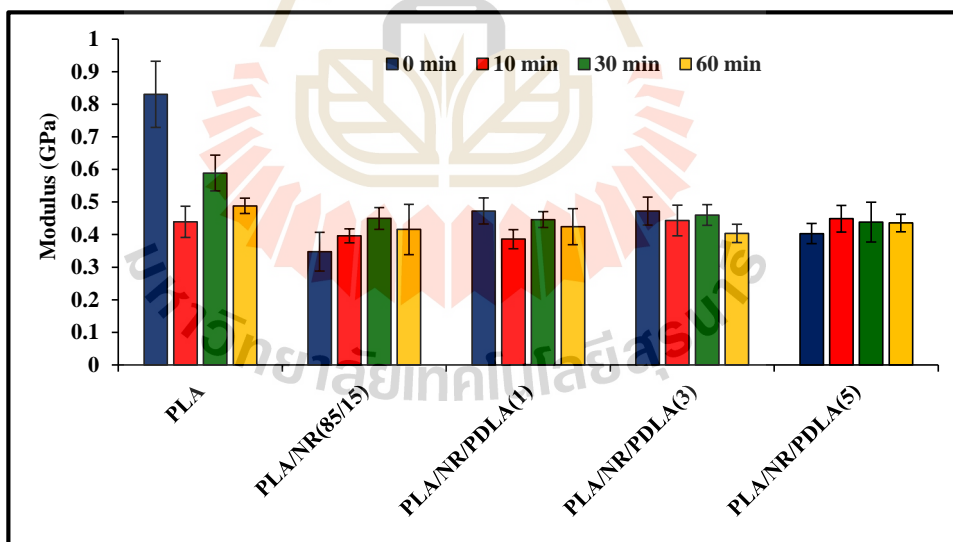


Figure 4.20 Modulus of PLA, PLA/NR(85/15), PLA/NR/PDLA blends before and after annealing treatment.

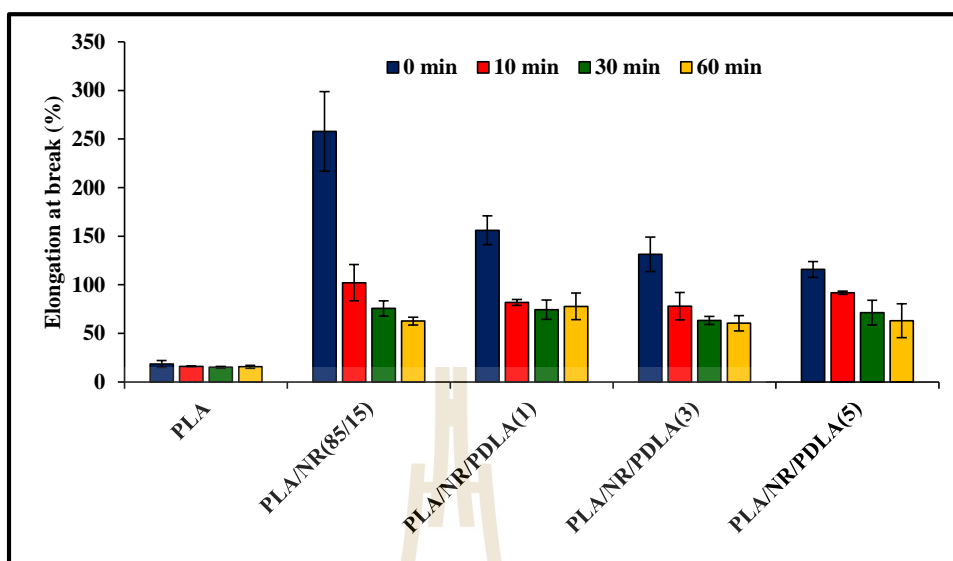


Figure 4.21 Elongation at break of PLA, PLA/NR(85/15), PLA/NR/PDLA blends before and after annealing treatment.

Elongation at break of PLA, PLA/NR and PLA/NR/PDLA blends after annealing treatment is shown in Figure 4.21. Neat PLA displayed a low elongation at break before and after annealing treatment due to its inherent brittleness. The elongation at break of PLA/NR and PLA/NR/PDLA blends decreased obviously with annealing time at 10 min, and then showed slightly decrease from 10 to 60 min. The reduction of elongation at break of all blends might be due to the larger spherulites occurred after annealing treatment. However, elongation at break of all blends was still higher than that of neat PLA, which indicated that NR still had a toughening effect for neat PLA, both before and after annealing treatment.

4.3.1.2 Impact properties

Figure 4.22 presents the unnotched Izod impact strength of PLA, PLA/NR and PLA/NR/PDLA blends before and after annealing treatment. The results showed that unnotched Izod impact strength of PLA/NR and PLA/NR/PDLA(1) blends showed a reduction of impact strength after annealing for 10 min. This may be because spherulite size of the blends was increased after annealing (Han, Han and Dong (2012)) The impact strength decreases with increasing average spherulite size (Li , Schultz and Chan (2015)) However, when the annealed time was increased from 10 min to 30 and 60 min, the unnotched Izod impact strength of PLA/NR and PLA/NR/PDLA(1) was improved. For PLA/NR/PDLA(3) and PLA/NR/PDLA(5), the impact strength was improved after annealing for 10 to 60 min. The improvement in unnotched Izod impact strength of the blends after annealing

The notched Izod impact strength of PLA, PLA/NR and PLA/NR/PDLA blends before and after annealing treatment are shown in Figure 4.23. The notched Izod impact strength of all blends was sharply reduced after annealing treatment. Notch in specimens had a sharp tip and led to stress concentration, and then crack growth passed along the spherulite boundaries with low crack propagation energy. The unnotched and notched Izod impact strength of PLA before and after annealing treatment showed no distinct change.

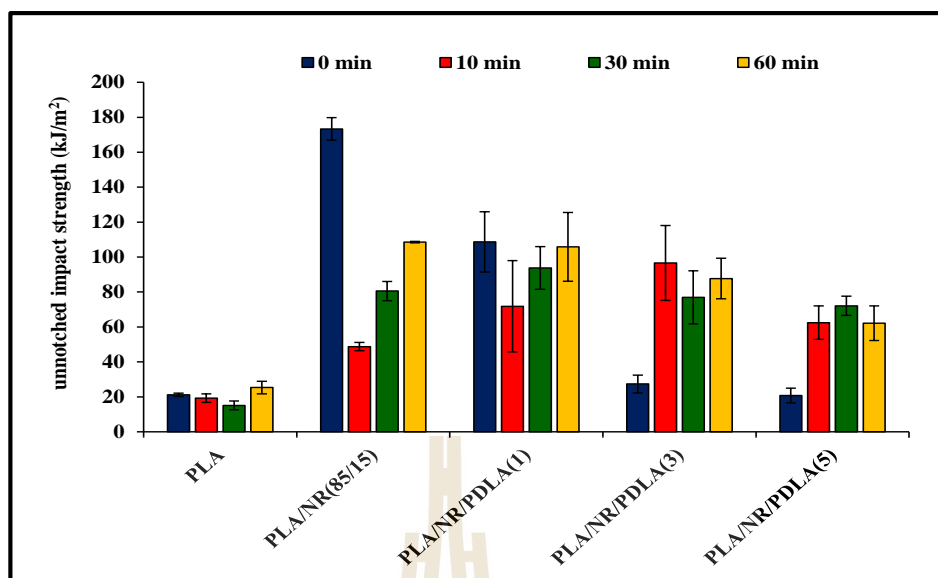


Figure 4.22 Unnotched Izod impact strength of PLA, PLA/NR(85/15), PLA/NR/PDLA blends before and after annealing treatment.

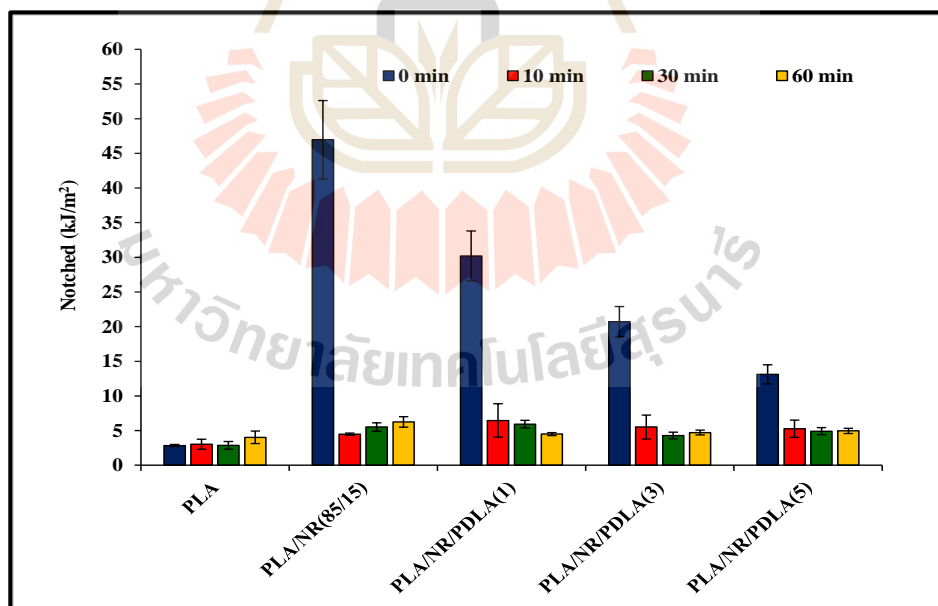


Figure 4.23 Notched Izod impact strength of PLA, PLA/NR(85/15), PLA/NR/PDLA blends before and after annealing treatment.

4.3.3 Heat distortion temperature properties

Figure 4.24 shows the HDTs of neat PLA, PLA/NR and PLA/NR/PDLA blends before and after annealing. The HDT of PLA/NR blend containing 1 wt% PDLA based on the amount of PLA before annealing treatment was the highest. After annealing, HDTs of all samples increased with an increase of the annealed time. This improvement was mainly due to the increase in crystallinity. Nevertheless, after annealing, HDT of PLA/NR/PDLA blends was not higher than that of neat PLA. This could be because the crystallinity of the blends containing PDLA was not higher than that of neat PLA. It was suggested that PDLA did not act as efficiently nucleating agent for PLA/NR(85/15) blend system in the current work.

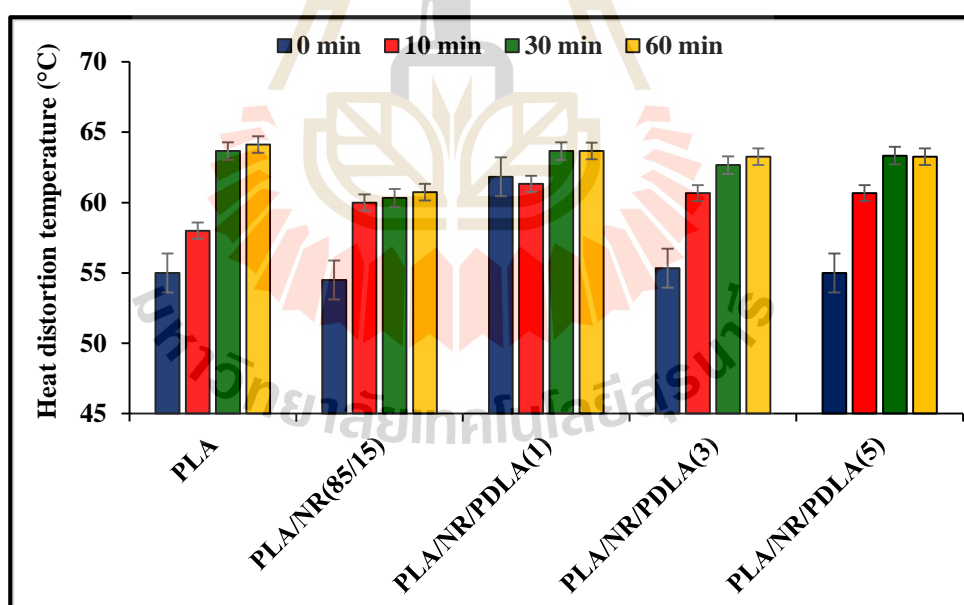


Figure 4.24 HDT of PLA, PLA/NR(85/15), PLA/NR/PDLA blends before and after annealing treatment.

4.3.4 Morphological property

Figure 4.25 (a-d) show SEM micrographs of tensile fractured surface of PLA/NR(85/15) and PLA/NR/PDLA blends before and after annealing. It was observed that the elongated fibrils of the blends after annealing were shorter. This can be used as evidence of a reduction in elongation at break of all the blends.

Figure. 4.26 (a-d), - 4.39 (a-d) show the SEM micrographs of fracture surface of PLA/NR (85/15), PLA/NR/PDLA(1), PLA/NR/PDLA(3) and PLA/NR/PDLA(5) blend before and after annealing treatment. The average particle sizes was calculated according to the equations 4.1. (section 4.2.4). The average NR particle diameter in PLA/NR (85/15) blend are tabulated in Table 4.6. From SEM micrograph and calculated NR particle diameter, the domain NR droplets size increased and showed poor interfacial adhesion when the annealing time was increased. On the other hand, the domain NR droplets size in PLA matrix of PLA/NR/PDLA(1) blend showed no significant change when the annealing time increased, as seen in Figure 4.27. This could be because of the suppressing effect of crystalline of PLA matrix on the coalescence of NR particle in the blend. This was confirmed by the X_c of PLA phase in PLA/NR/PDLA(1) given in Table 4.7. The optimum rubber particle size gave a highest toughness for several polymer. The rubber particle size of 1-5 μm was the more effective toughening agent (Johnsen et al, 2007).

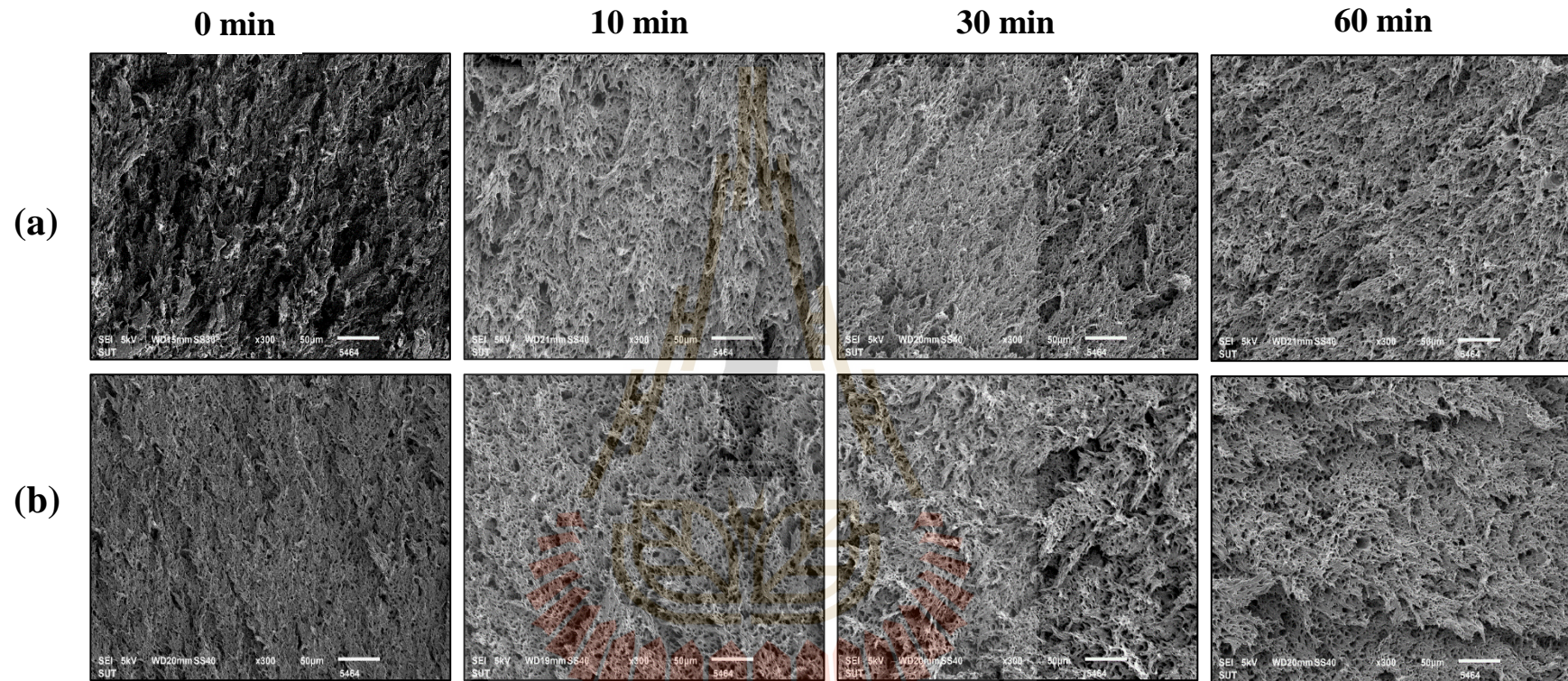


Figure 4.25 SEM micrographs at 300x magnification of tensile fractured surface of (a) PLA/NR(85/15), (b)PLA/NR/PDLA(1), (c) PLA/NR/PDLA(3) and PLA/NR/PDLA(5) blends before and after annealing treatment.

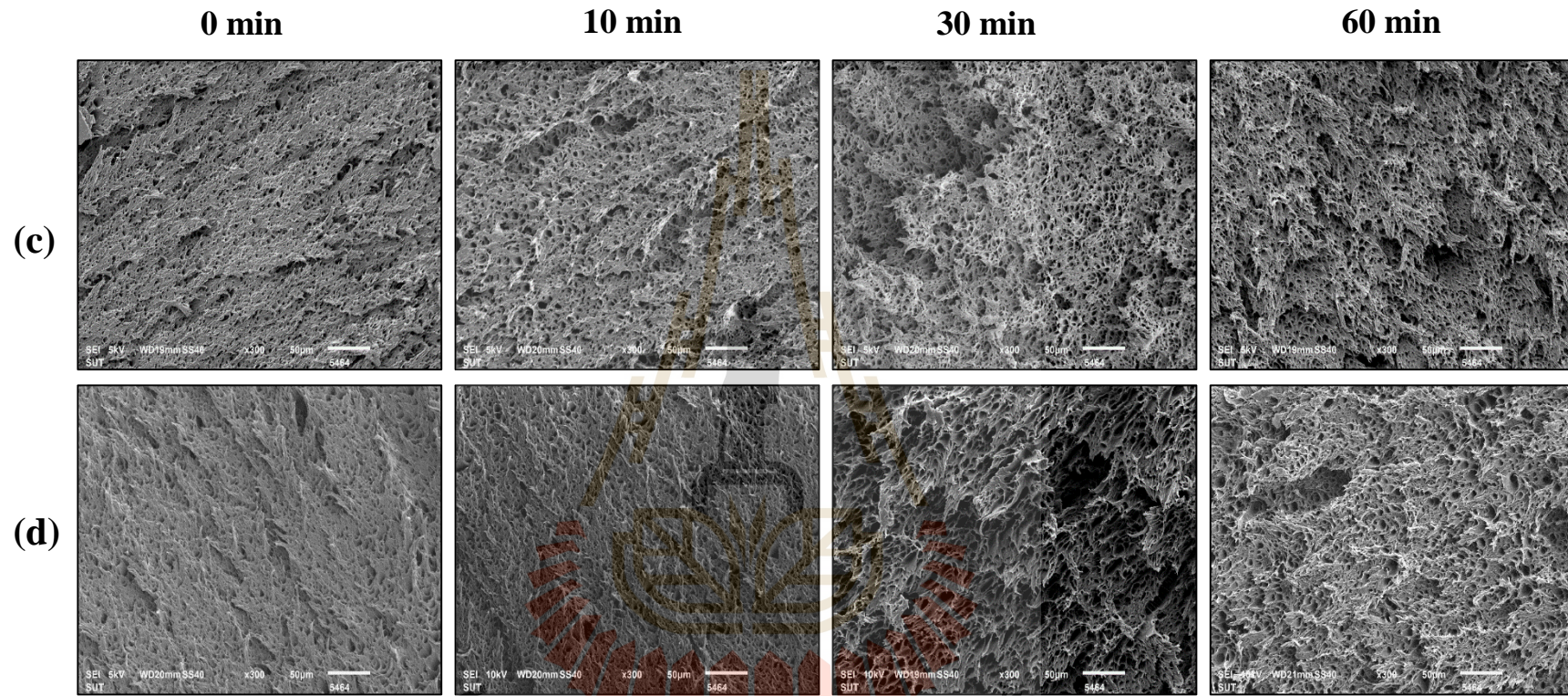


Figure 4.25 SEM micrographs at 300x magnification of tensile fractured surface of (a) PLA/NR(85/15), (b)PLA/NR/PDLA(1), (c) PLA/NR/PDLA(3) and PLA/NR/PDLA(5) blends before and after annealing treatment (continued).

Table 4. 6 Diameters of NR particles in the PLA/NR(85/15) and PLA/NR/PDLA blends before and after annealing treatment.

Samples	Average particle diamete (D_n) (μm)				Minimum particle diameter (μm)				Maximum particle diameter (μm)			
	Annealing time (min)				Annealing time (min)				Annealing time (min)			
	0	10	30	60	0	10	30	60	0	10	30	60
PLA/NR (85/15)	3.03 \pm 1.06	3.69 \pm 1.07	3.52 \pm 1.34	3.31 \pm 1.34	1.08	1.75	1.12	1.11	8.43	8.49	8.58	8.73
PLA/NR/PDLA(1)	3.34 \pm 1.07	2.91 \pm 1.09	3.09 \pm 0.85	3.38 \pm 0.97	1.30	1.00	1.36	1.32	7.65	8.37	5.51	6.75
PLA/NR/PDLA(3)	3.30 \pm 1.00	3.11 \pm 1.14	4.00 \pm 0.99	3.77 \pm 1.11	0.80	1.02	1.66	2.00	8.00	7.41	8.79	8.82
PLA/NR/PDLA(5)	3.54 \pm 1.08	3.69 \pm 1.01	3.41 \pm 0.98	3.80 \pm 1.03	1.71	1.97	1.60	1.99	8.25	7.82	8.91	7.41

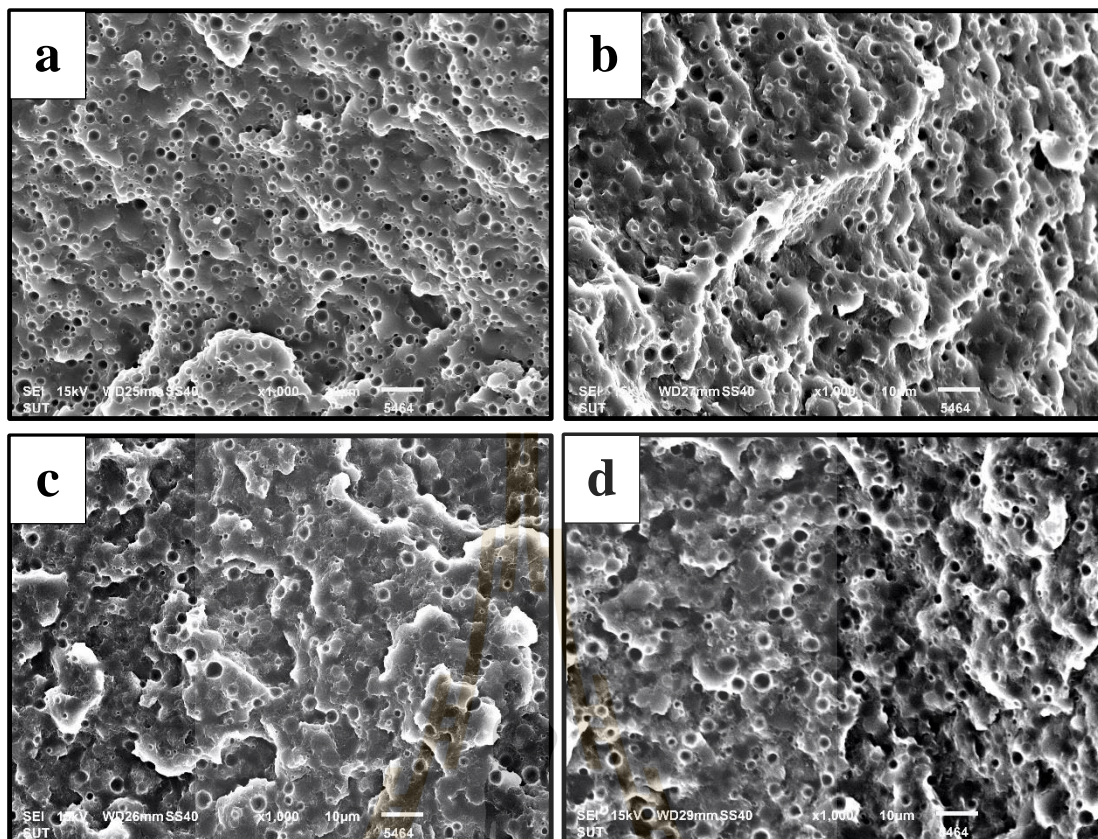


Figure 4.26 SEM micrographs at 1,000x magnification of freeze-fractured surfaces of PLA/NR(85/15) with various annealing time: (a) 0 min, (b) 10 min, (c) 30 min and (d) 60 min.

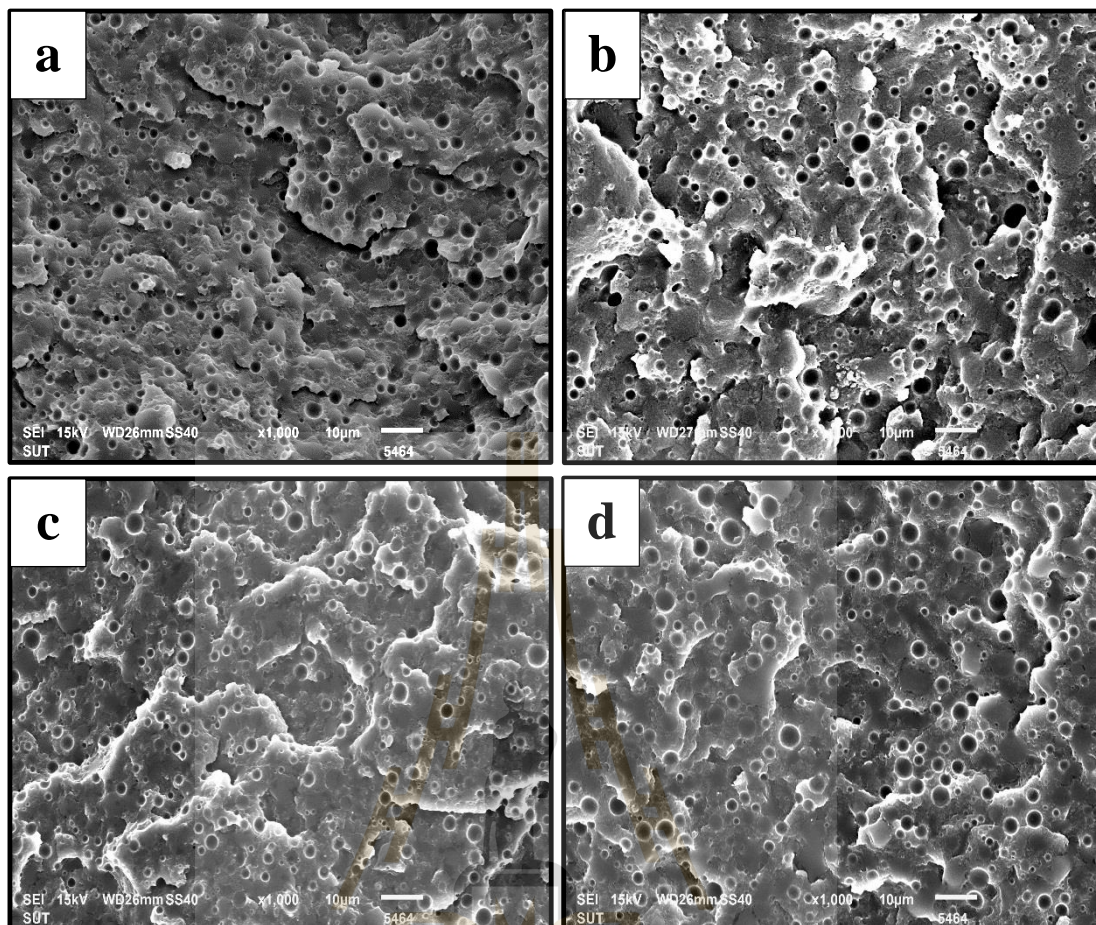


Figure 4.27 SEM micrographs at 1,000x magnification of freeze-fractured surfaces of PLA/NR/PDLA(1) with various annealing time: (a) 0 min, (b) 10 min, (c) 30 min and (d) 60 min.

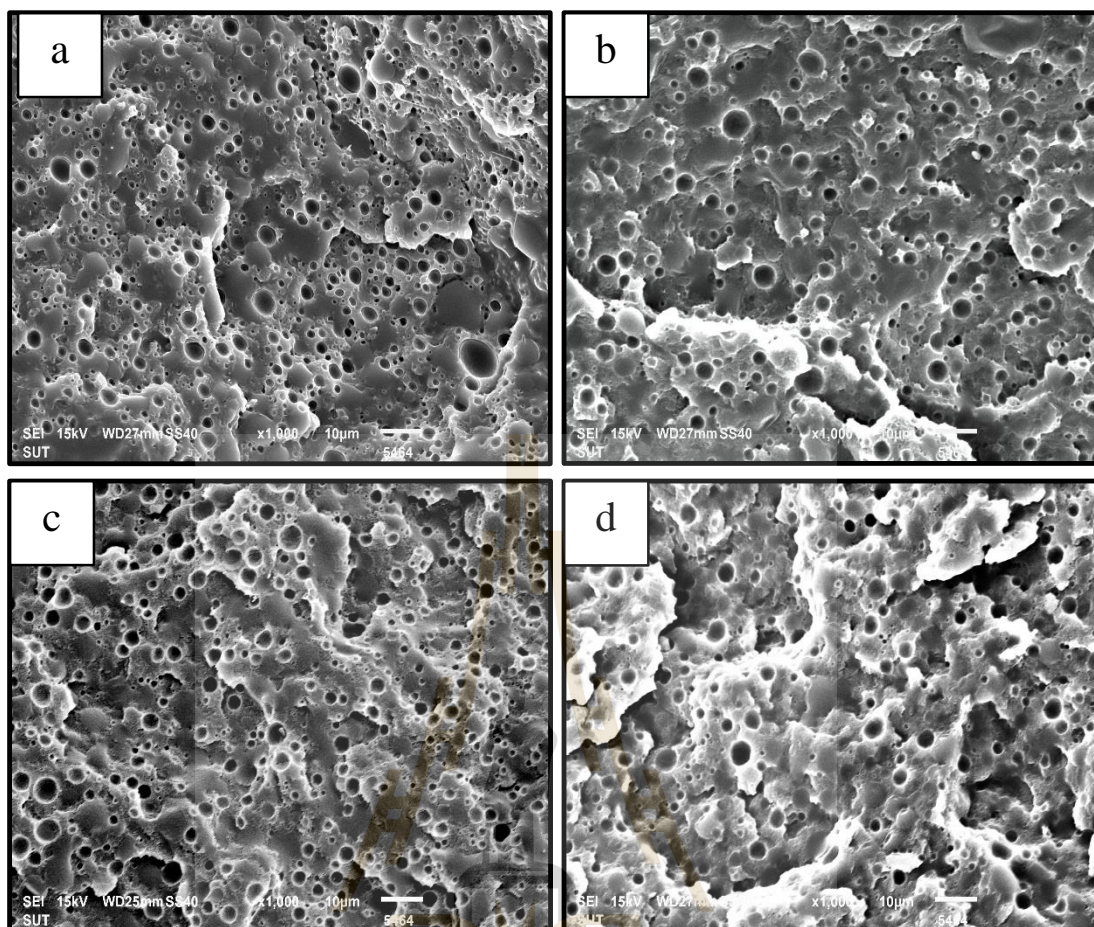


Figure 4.28 SEM micrographs at 1,000x magnification of freeze-fractured surfaces of PLA/NR/PDLA(3) with various annealing time: (a) 0 min, (b) 10min, (c) 30 min and (d) 60 min.

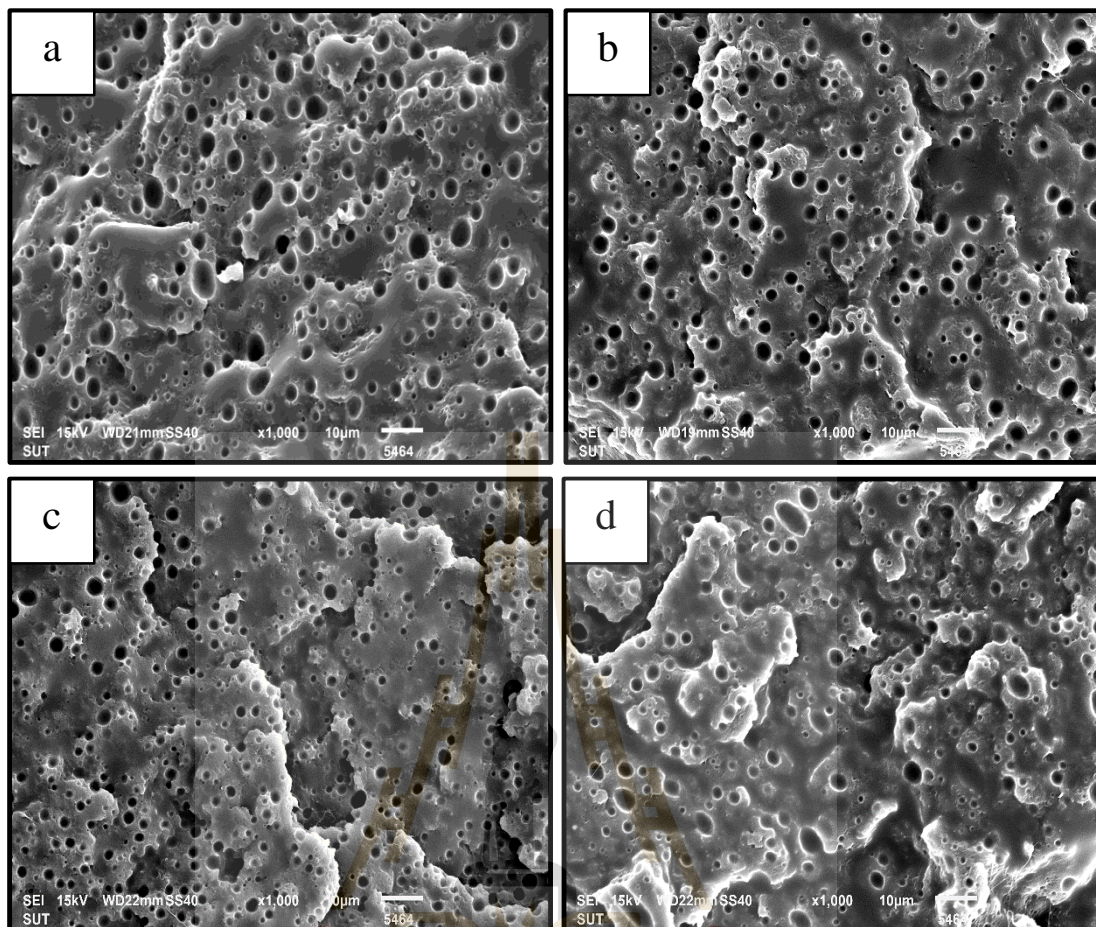


Figure 4.29 SEM micrographs at 1,000x magnification of freeze-fractured surfaces of PLA/NR/PDLA(5) with various annealing time: (a) 0 min, (b) 10 min, (c) 30 min and (d) 60 min.

4.3.5 Thermal properties

Figure 4.30 (a-d) - Figure 4.34 (a-d) and Table 4.7 show the DSC results from first heating scan of PLA, PLA/NR(85/15) and PLA/NR/PDLA blends before and after annealing. The results showed that cold crystallization peak for all the sample disappeared after annealing, indicating that all these samples were completely crystallized during annealing treatment (Narita, Katagiri, and Tsuji., 2011). However, cold crystallization peak of PLA/NR/PDLA(1) blend did not appear before and after annealing. It could be because PLA/NR/PDLA(1) blend was completely crystallized during the sample preparation process. In addition, it was found that degree of crystallinity of PLA/NR/PDLA(1) blend before and after annealing were not significantly changed. Melting temperature (T_m) of PLA/NR(85/15) and PLA/NR/PDLA blends was increased after annealing. The presence of two melting peaks in PLA could be related to the formation of different crystal structures. Melting peak appeared at higher temperature belonged to more perfect crystalline structure (Sarasua et al., 1998). The X_c of neat PLA, PLA/NR(85/15), PLA/NR/PDLA(1), PLA/NR/PDLA(3) and PLA/NR/PDLA(5) blends before annealing was 1.36, 1.80, 25.25, 1.83 and 1.57%, respectively. In general, the degree of crystallinity of all samples increased as an increase of annealing time. In this study, the test specimens of the blends were annealed at 100°C. The maximum crystallinity of PLA, PLA/NR(85/15) and PLA/NR/PDLA blends was obtained from annealing treatment at 10 minutes.

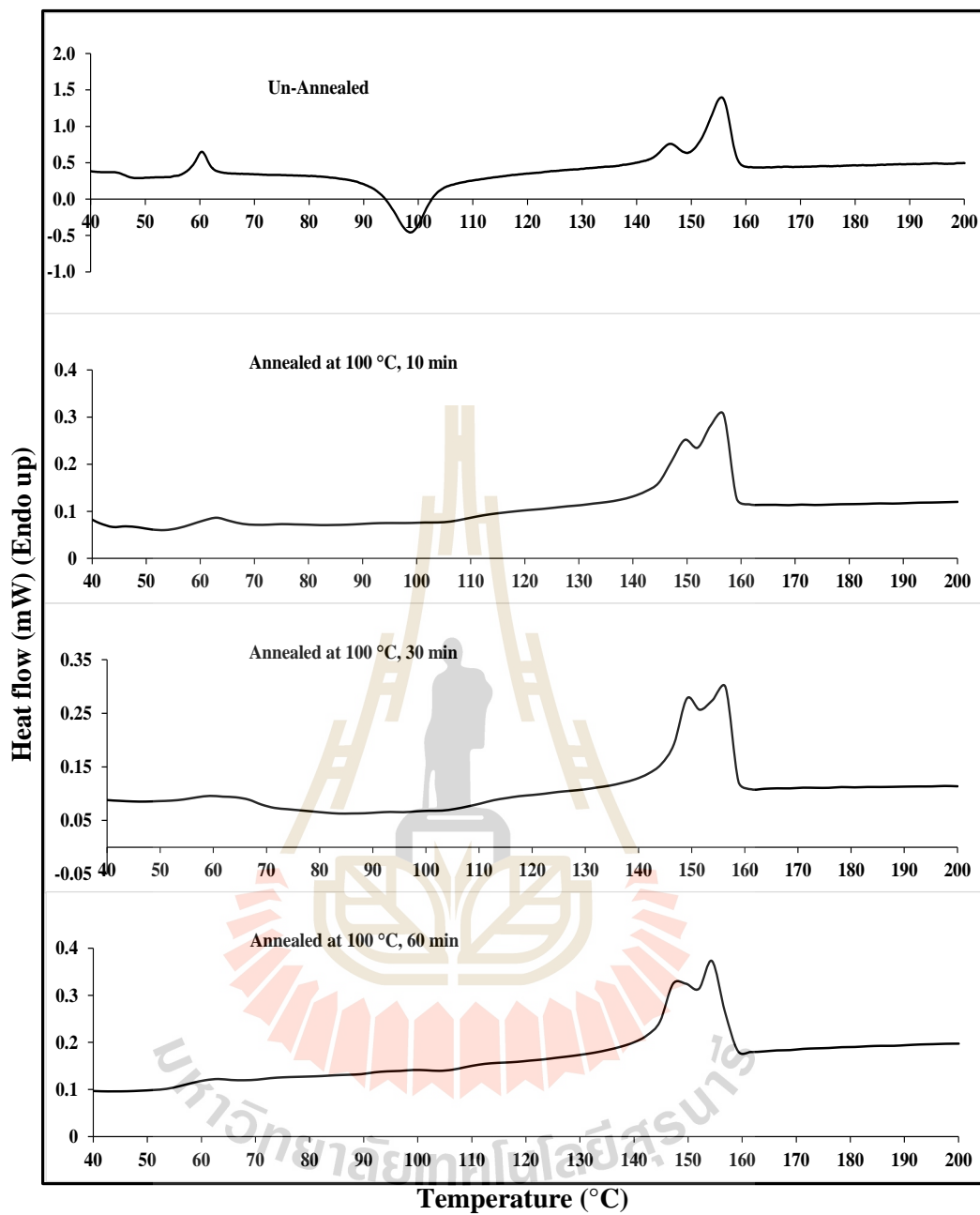


Figure 4.30 DSC thermograms of neat PLA with various annealing time
(the first heating, heating rate 5°C/min)

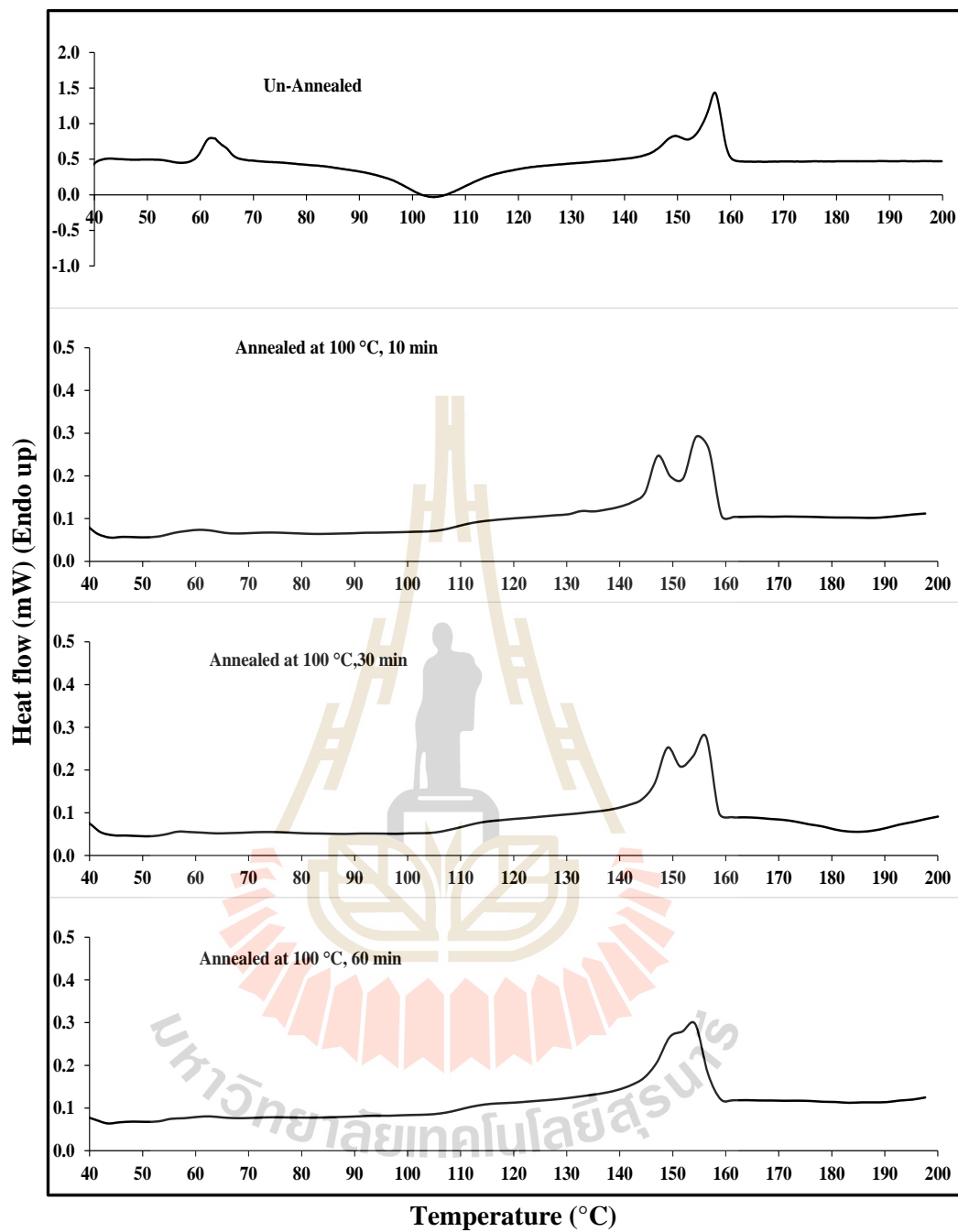


Figure 4.31 DSC thermograms of PLA/NR(85/15) with various annealing time (the first heating, heating rate 5°C/min).

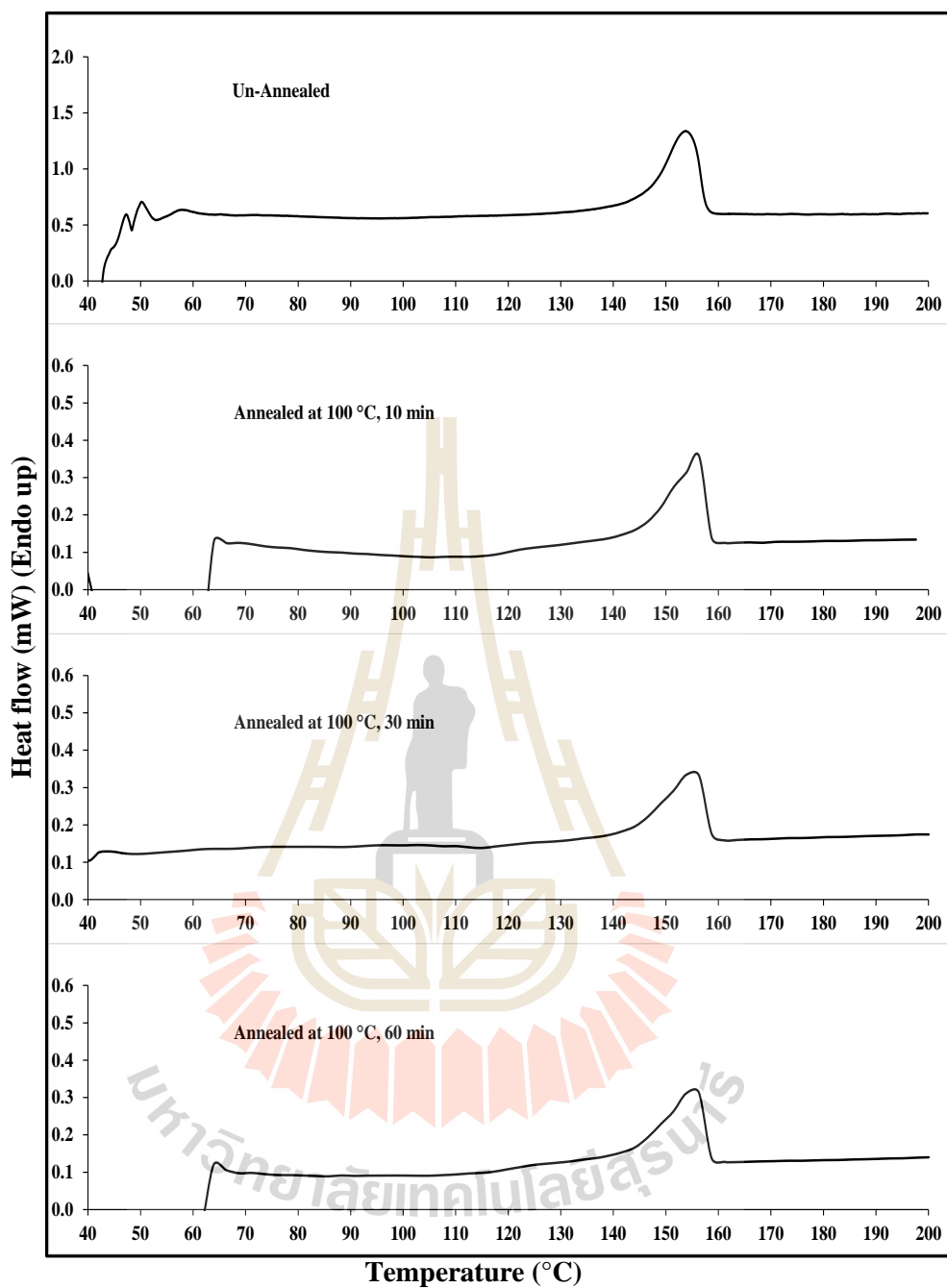


Figure 4.32 DSC thermograms of PLA/NR/PDLA(1) with various annealing time (the first heating, heating rate 5°C/min).

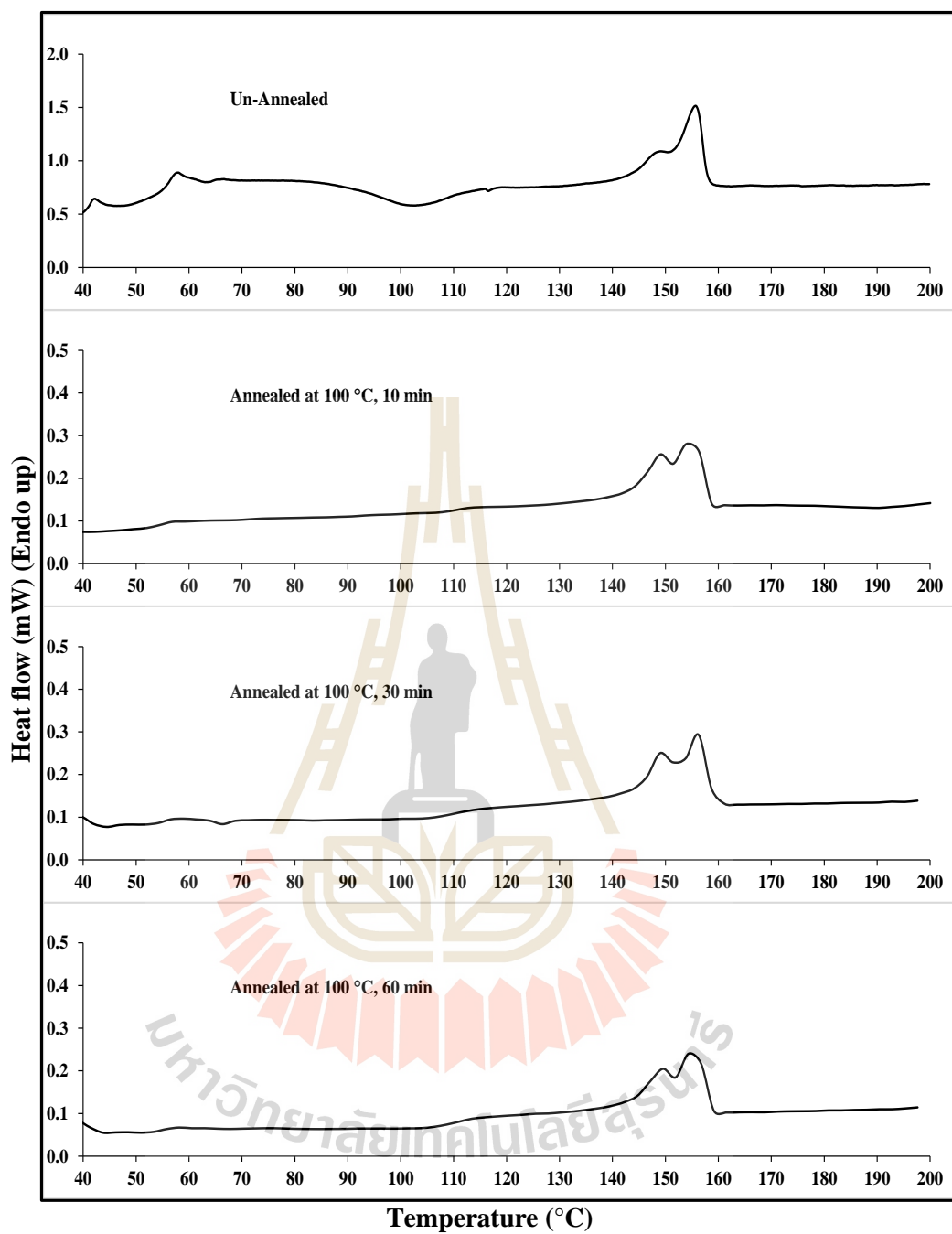


Figure 4.33 DSC thermograms of PLA/NR/PDLA(3) with various annealing time (the first heating, heating rate 5°C/min).

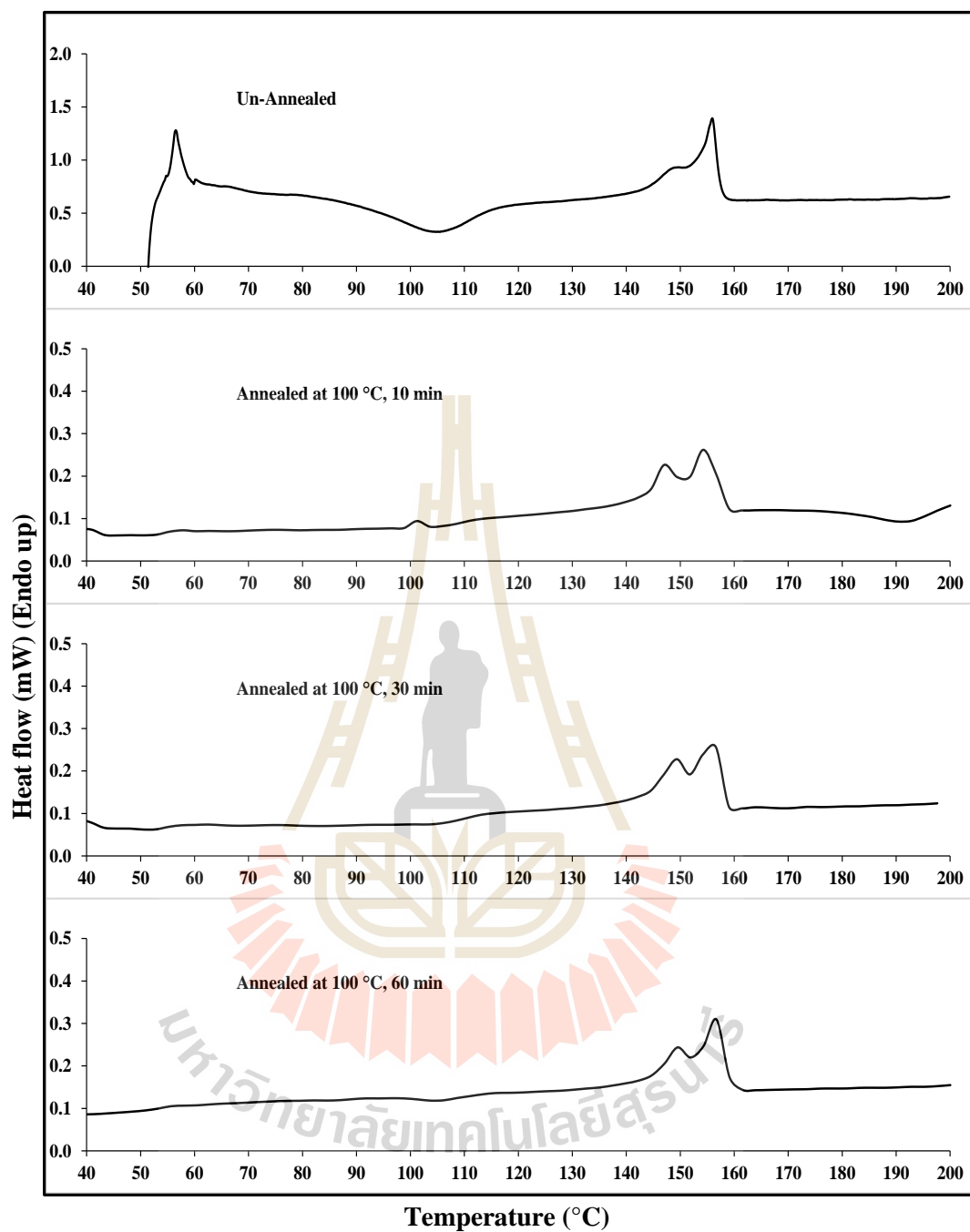


Figure 4.34 DSC thermograms of PLA/NR/PDLA(5) with various annealing time (the first heating, heating rate 5°C/min).

Table 4.7 DSC first heating results of PLA, PLA/NR/PDLA blends before and after annealing treatment.

Sample	Annealing time (min)	First heating					
		T _g (°C)	T _{cc} (°C)	T _m (°C)	ΔH _c (J/g)	ΔH _m (J/g)	X _c
PLA	0	60.8	98.6	146.2/155.6	25.16	26.47	1.40
	10	63.1	–	149.1/156.1	0	24.14	25.79
	30	-	–	149.4/155.7	0	25.61	27.36
	60	-	–	148.2/154.9	0	27.07	28.92
PLA/NR (85/15)	0	60.7	104.1	149.6/157.0	25.16	26.89	1.85
	10	-	–	147.8/155.7	0	24.74	26.43
	30	-	–	149.4/155.7	0	24.55	26.23
	60	-	–	150.8/154.8	0	24.15	25.80
PLA/NR/PDLA(1)	0	-	–	153.8	0	24.32	25.98
	10	-	–	156.4	0	21.94	23.44
	30	-	–	155.4	0	21.35	22.81
	60	-	–	155.2	0	21.79	23.28
PLA/NR/PDLA(3)	0	-	102.4	149.1/155.7	18.96	20.72	1.88
	10	-	–	149.2/155.3	0	19.89	21.25
	30	-	–	149.5/156.4	0	19.7	21.05
	60	-	–	149.1/155.6	0	17.93	19.16
PLA/NR/PDLA(5)	0	-	104.8	148.1/155.9	15.91	17.38	1.57
	10	-	–	147.4/154.8	0	18.36	19.62
	30	-	–	148.7/155.9	0	18.61	19.88
	60	-	–	149.4/157	0	18.57	19.84

CHAPTER V

CONCLUSIONS

Polymer blends of poly(lactic acid) (PLA) and natural rubber (NR) at the ratios of 95/5, 90/10, 85/15 and 80/20 (wt%) were prepared and tested. Impact strength of PLA was found to be dramatically improved with the addition of 15 wt% NR [PLA/NR(85/15)]. At this content, unnotched and notched Izod impact strength were 167.22 and 54.31 kJ/m², which were higher than those of neat PLA about 7 and 10 times, respectively. However, tensile strength and Young's modulus of the blends decreased with increasing NR content. The HDT slightly decreased as NR content increased. The decrease of HDT of PLA/NR blend could be resulted from soft NR phase. SEM micrographs showed that PLA/NR blends were immiscible.

Effect of PDLA content on mechanical, thermal and HDT properties of PLA/NR(85/15) blend was then studied. The amount of PDLA added into PLA/NR(85/15) blend was 1, 3 and 5 wt% based on the amount of PLA in the blend. When 1 wt% of PDLA was incorporated into PLA/NR(85/15) blend [PLA/NR/PDLA(1)], the HDT of the blend was significantly improved. On the other hand, the impact strength and elongation at break of PLA/NR(85/15) blend decreased with an increase of PDLA content. Nevertheless, with an exception of unnotched Izod impact strength, the values were still higher than those of neat PLA. Hence, the addition of PDLA at 1 wt% based on PLA content into PLA/NR blend led to the blend with higher impact strength and HDT compared to neat PLA. From DSC first heating scan results, cold crystallization temperature (T_{cc}) of the blends, with the exception of the value of

PLA/NR/PDLA(1), was higher than neat PLA. Melting temperature (T_m) of PLA in the blend was also shifted to higher temperature. T_{cc} of PLA phase did not found in PLA/NR/PDLA(1). Crystallinity of PLA phase in PLA/NR(85/15), PLA/NR/PDLA(1) and PLA/NR(85/15) blend with 3 wt% [PLA/NR/PDLA(3)] and 5 wt% [PLA/NR/PDLA(5)] PDLA were 1.80, 25.25, 1.83 and 1.57%, respectively. From DSC second heating scan results, glass transition temperature (T_g) of PLA phase was increased with adding NR into PLA. T_{cc} of PLA/NR/PDLA blends were lower than that of PLA/NR(85/15). T_g and T_m of PLA in the blends did not significantly change with adding PDLA. Crystallinity of PLA phase in PLA/NR(85/15), PLA/NR/PDLA(1), PLA/NR/PDLA(3) and PLA/NR/PDLA(5) were 1.23, 3.82, 1.63 and 1.23%, respectively. SEM micrographs revealed the increment in average diameter of NR particles in the blend containing PDLA. WAXS patterns of PLA/NR (85/15) blend containing PDLA exhibit scattering peaks of stereocomplex crystallite at 2θ of 10.5° , 18.5° and 23.8° . These diffraction peaks become sharper with increasing PDLA content.

The PLA, PLA/NR(85/15) and PLA/NR/PDLA blends specimens were annealed in an air oven at 100°C for 10, 30 and 60 min. After annealing, it was found that the unnotched impact strength of PLA, PLA/NR(85/15) and PLA/NR/PDLA(1) was decreased, whereas impact strength of PLA/NR(85/15) blend with 3 and 5 wt% PDLA was improved. The tensile strength, Young's modulus, elongation at break and impact strength of the blends after annealing treatment tended to decrease. HDTs and degree of crystallinity of PLA, PLA/NR and PLA/NR/PDLA blends increased as an increase of annealing time. SEM micrographs showed the domain NR droplets size in

the blends tended to increase and showed poor interfacial adhesion when the annealing time was increased.



REFERENCES

- Ahmed, J., Varshney, S, K., Janvier, F. (2014). Rheological and thermal properties of stereocomplexed polylactide films. **Journal of Thermal Analysis and Calorimetry**. 115(3): 2053–2061.
- Auras, R., Lim, L-T., Selke, S. E. M., Tsuji, H. (2010). Poly(lactic acid) : synthesis, structures, properties, processing, and applications. **John Wiley and Sons: New Jersey**. 3-4.
- Almeida, A, S., Tavares, M, I, B., Silva, E, O., Cucinelli Neto, R. P., Moreira L, A. (2012). Development of hybrid nanocomposites based on PLLA and low-field NMR characterization. **Polymer Testing**. 31: 267–275.
- Barham, P. J., Keller, A. (1978). The relationship between microstructure and mode of fracture in polyhydroxybutyrate. **Journal of Polymer Science Part B: Polymer Physics**. 24(1): 69–77.
- Battegazzore, D., Bocchini, S. (2011). Crystallization kinetics of poly(lactic acid)-talc composites. **eXPRESS Polymer Letters**. 5 (10): 849-858.
- Bitinis, N., Verdejoa, R., Cassagnau, P., and Lopez-Manchadoa, M.A. (2011). Structure and properties of polylactide/natural rubber blends. **Materials Chemistry and Physics**. 129: 823– 831.
- Brizzolara, D., Cantow, H. J., Diederichs, K., Keller, E., Domb, A. J. (1996). Mechanism of the atereocomplex formation between enantiomeric poly(lactide)s. **Macromolecules**. 29: 191–197.

- Buzarovska, A., Grozdanow, A. (2012). Biodegradable Poly(L-lactic acid)/TiO₂ Nanocomposites: Thermal Properties and Degradation. **Journal of Applied Polymer Science**. 123 (4): 2187-2193.
- Celli, A., Scandola, M. (1992). Thermal properties and physical ageing of poly (L-lactic acid) **Polymer**. 33(13):2699-2703.
- Chen, G-X., Kim, H-S., Shim, J-H., Yoon, J-S. (2005). Role of epoxy groups on clay surface in the improvement of morphology of poly(l-lactide)/clay composites. **Macromolecules**. 38: 3738-3744.
- Chen, X., Ren, J., Zhang, N., Gu, S., Li, J. (2015). Effects of heat treatment on the thermal and mechanical properties of ramie fabric-reinforced poly(lactic acid) biocomposites. **Journal of Reinforced Plastics and Composites**. 34(1): 28–36.
- El-Hadi, A., Schnabel, R., Straube, E., Muller, G. and Henning, S. (2002). Correlation between degree of crystallinity, morphology, glass temperature, mechanical properties and biodegradation of poly (3-hydroxyalkanoate) PHAs and their blends. **Polymer Testing**. 21: 665–674.
- Feng, Y., Hu, Y., Yin, J., Zhao, G. and W. Jiang: (2013). High impact poly(lactic acid)/poly(ethylene octane) blends prepared by reactive blending. **Polymer Engineering & Science**. 53: 389
- Ge, H., Yang, F., Hao, Y., Wu G., Zhang, H., Dong, L. (2013). Thermal, mechanical, and rheological properties of plasticized poly(L-lactic acid). **Journal of Applied Polymer Science**. 127(4): 2832-2839.

- Guo, X., (2012). **Investigation of poly(lactic acid)/polyoxy methylene blends: crystallization behavior and heat resistance**. M. Sci. thesis, Washington State University, United States.
- Guo, X., Zhang, J., Huang, J. (2015). Poly(lactic acid)/polyoxymethylene blends: Morphology, crystallization, rheology, and thermal mechanical properties. **Polymer**. 69: 103- 109.
- Han, L., Han, C., Dong, L. (2013). Effect of crystallization on microstructure and mechanical properties of poly[(ethyleneoxide)-*block*-(amide-12)] toughened poly(lactic acid) blend. **Polymer International**. 62(2): 295–303.
- Harris, A, M., Lee, E, C. (2008). Improving mechanical performance of injection molded PLA by controlling crystallinity. **Journal of Applied Polymer Science**. 107: 2246–2255.
- Ikada, Y., Jamshidi, K. (1987). Stereocomplex formation between enantiomeric poly(lactides). **Macromolecules**. 20 (4): 904-906.
- Jing, L., Dakai, C., Baozhu, G., Minghao, G., Jie, R. (2011). Crystallization morphology and crystallization kinetics of poly(lactic acid): effect of N-Aminophthalimide as nucleating agent. **Polymer Bulletin**. 67 (5) :775–791.
- Johnsen, B.B., Kinloch, A.J., Mohammed, R.D. Taylor, A.C., Sprenger, S. (2007). Toughening mechanisms of nanoparticle-modified epoxy polymers. **Polymer**. 48: 530-541.
- Jun, W, P., Seung, S, I. (2002). Phase behavior and morphology in blends of poly(L-lactic acid) and poly(butylene succinate). **Journal of Applied Polymer Science**. 86 (3): 647-655.

- Juntuek, P., Ruksakulpiwat, C., Chumsamrong, P., Ruksakulpiwat, Y. (2011). Effect of glycidyl methacrylate-grafted natural rubber on physical properties of polylactic acid and natural rubber blends. **Journal of Applied Polymer Science**. 125, 745–754.
- Kim, K-W., Lee, B-H., Kim H.-J., Sriroth, K., Dorgan, J, R. (2012). Isothermal cold crystallization kinetics of polylactide/-nucleating agents. **Journal of Thermal Analysis and Calorimetry**. 108:1131–1139.
- Kawamoto, N., Sakai, A., Horikohi, T. (2007). Nucleating agent for poly(L lactic acid)-An optimization of chemical structure of hydrazide compound for advanced nucleation ability. **Journal of Applied Polymer Science**. 103 (1): 198-203.
- Lee, B-H., Kim, H-S., Lee, S., Kim, H-J., Dorgan, J, R. (2009). Bio-composites of kenaf fibers in polylactide: Role of improved interfacial adhesion in the carding process. **Composites Science and Technology**. 69: 2573–2579.
- Li, J-Z., Schultz, J. M., Chan, C-M. (2015). The relationship between morphology and impact toughness of poly(L-lactic acid)/poly(ethylene oxide) blends. **Polymer**. 63: 179-188.
- Liao, R., Yang, B. (2007). Isothermal Cold Crystallization Kinetics of Polylactide/Nucleating Agents. **Journal of Applied Polymer Science**. 104: 310-317. 30:2125–2130.
- Lim, M- H., Lee, O-H., Chin, J-E., Ko, H-M., Kim, I-C., Lee, H, B., Im, S-Y., Bai, S. (2008). Simultaneous degradation of phytic acid and starch by an industrial strain of *Saccharomyces cerevisiae* producing phytase and α -amylase. **Biotechnology Letters**. 30:2125–2130.

- Lopez-Rodriguez, N., Lopez-Arraiza, A., Meaurio, E., Sarasua, J. R. (2006). Crystallization, morphology, and mechanical behavior of polylactide/poly(ϵ -caprolactone) blends. **Polymer Engineering & Science**. 46 (9): 1299-1308.
- Murariu, M., Da Silva Ferreira¹, A., Alexandre, M., Dubois, P. (2008). Polylactide (PLA) designed with desired end-use properties: 1. PLA compositions with low molecular weight ester-like plasticizers and related performances. **Polymers for Advanced Technologies**. 19: 636–646.
- Odian, G. (2004). Principles of polymerization. Fourth Edition ed. **John Wiley and Sons: New Jersey**. 47-50.
- Ohlberg, S. M., Roth, J. and Raff, R. A. V. (1959). Relationship between Impact strength and spherulite Growth in Linear Polyethylene. **Journal of Applied Polymer Science**. 1(1): 114-120.
- Pan P., Kai W., Zhu B., Dong T., Inoue Y. (2007). Polymorphous crystallization and multiple melting behavior of poly(L-lactide): Molecular weight dependence. **Macromolecules**. 40: 6898–6905.
- Pang, Y., Dong, X., Liu, K., Han, C. C., Chen, E., and Wang, D. (2008). Ductile–brittle transition controlled by isothermal crystallization of isotactic polypropylene and its blend with poly(ethylene-co-octene). **Polymer**. 49: 4259–4270.
- Park, B-S, Song, J. C., Park, D. H., Yoon, K-B. (2012). PLA/Chain-Extended PEG blends with improved ductility. **Journal of Applied Polymer Science**. 123: 2360–2367.
- Park, S-D., Todo, M., Arakawa, K. (2005). Effects of isothermal crystallization on fracture toughness and crack growth behavior of poly (lactic acid). **Journal of Materials Science**. 40: 1055 – 1058.

- Patel, J., Phillips, P. J. (1973). The young's modulus of polyethylene. **Journal of Polymer Science Part C: Polymer Letters**. 11(12): 771–776.
- Petchwattana, N., Covavisaruch, S., Euapanthasatec, N. (2012) Utilization of ultrafine acrylate rubber particles as a toughening agent for poly(lactic acid). **Materials Science and Engineering A**. 532: 64– 70.
- Pongtanayuta, K., Thongpina, C., Santawiteeb, O. (2013). The effect of rubber on morphology, thermal properties and mechanical roperties of PLA/NR and PLA/ENR blends. **Energy Procedia**. 34: 888–897.
- Prospector materials database. (n.d.). Polylactic Acid (PLA) typical properties. June 9, 2015. Available from: <http://plastics.ulprospector.com/generics/34/c/t/polylactic-acid-pla-properties-processing>.
- Rahman, N., Kawai, T., Matsuba, G., Nishida, K., Kanaya, T., Watanabe, Hiroshi., Okamoto, H., Kato, M., Usuki, A., Matsuda, M., Nakajima, K., and Honma, N. (2009). Effect of Polylactide Stereocomplex on the Crystallization Behavior of Poly(L-lactic acid). **Macromolecules**. 42: 4739–4745.
- Robertson, G, L. (2012). Food Packaging: **Principles and Practice, 3rd Edition**.
- Santos, F, A., Tavares, M, I, B. (2014). Development and characterization of hybrid materials based on biodegradable PLA matrix, microcrystalline cellulose and organophilic silica. **Polímeros**. 24(5): 561-566.
- Sarazin, P., Li, G., Orts, W. J., and Favis, B. D. (2008). Binary and ternary blends of polylactide, polycaprolactone and thermoplastic starch. **Polymer**. 49: 599-609
- Sawpan, M, A., Pickering, K, L., Fernyhough, A. (2011). Improvement of mechanical performance of industrial hemp fibre reinforced polylactide biocomposites. **Composites: Part A**. 42: 310–319.

- Serizawa, S., Inoue, K., Iji, Mi. (2006). Kenaf-fiber-reinforced poly(lactic acid) used for electronic products. **Journal of Applied Polymer Science**. 100: 618–624.
- Shi, Q, F., Mou, H, Y., Li, Q, Y., Wang, J, K., Guo, W, H. (2012). Influence of heat treatment on the heat distortion temperature of poly(lactic acid)/bamboo fiber/talc hybrid biocomposites. **Journal of Applied Polymer Science**. 123: 2828–2836.
- Shih, Y-F., Huang, C-C. (2011). Polylactic acid (PLA)/banana fiber (BF) biodegradable green composites. **Journal of Polymer Research**. 18:2335–2340.
- Silverajah, V, S, G., Nor Ibrahim, A., Zainuddin, N., Yunus, W, M, Z, Wan., Hassan, H, Abu. (2012). Mechanical, thermal and morphological properties of poly(lactic acid)/epoxidized palm olein blend. **Molecules**. 17: 11729-11747.
- Tábi, T., Sajó, I. E., Szabó, F., Luyt, A. S., Kovács, J. G. (2010). Crystalline structure of annealed polylactic acid and its relation to processing. **Express Polymer Letters**. 4 (10): 659–668.
- Tang, Z., Zhang, C., Liu, X., Zhu, J. (2012). The crystallization behavior and mechanical properties of polylactic acid in the presence of a crystal nucleating agent. **Journal of Applied Polymer Science**. 125: 1108–1115.
- Tao, Y., Yan, L., Jie, R. (2009). Preparation and properties of short natural fiber reinforced poly(lactic acid) composites. **Transactions of Nonferrous Metals Society of China**. 19: s651–s655.
- Teng, C-C., Ma, C-C, M., Cheng, B-D., Shi, Y-F., Chen, J-W., Hsiao, Y-K. (2011). Mechanical and thermal properties of polylactide-grafted vapor-grown carbon nanofiber/polylactide nanocomposites. **Composites: Part A**. 42: 928–934.

- Tsuji, H., Ikada, Y. (1995). Properties and morphologies of poly(l-lactide): 1. Annealing condition effects on properties and morphologies of poly(l-lactide). **Polymer** 36(14): 2709–2716
- Tsuji, H., Takai, H., Saha, S.K. (2006). Isothermal and non-isothermal crystallization behavior of poly(l-lactic acid): Effects of stereocomplex as nucleating agent. **Polymer**. 47: 3826–3837.
- Ublekov, F., Badrian J. (2012). Influence of clay content on the melting behavior and crystal structure of nonisothermal crystallized poly(L-lactic acid)/nanocomposites. **Journal of Applied Polymer Science**. 124 (2): 1643-1648.
- Wang, Y., Chiao, S. M., Hung, T-F., Yang, S-Y. (2012). Improvement in toughness and heat resistance of poly(lactic acid)/polycarbonate blend through twin screw blending: Influence of compatibilizer type. **Journal of Applied Polymer Science**. 125: E402–E412.
- Wei, K. C., Nor, A. I., Norhazlin, Z., Mohd, F. A. Rahman., and Buong, W. C. (2013). Impact toughness and ductility enhancement of biodegradable poly(lactic acid)/poly(ϵ -caprolactone) blends via addition of glycidyl methacrylate. **Advances in Materials Science and Engineering**. 2013: 1-8. doi: <http://dx.doi.org/10.1155/2013/976373>.
- Wei, X-F., Bao, R-Y., Cao, Z-Q., Yang, W., Xie, B-H., and Yang, M-B. (2014). Stereocomplex crystallite network in asymmetric PLLA/PDLA blends: formation, structure, and confining effect on the crystallization rate of homocrystallites. **Macromolecules**. 47 (4): 1439–1448.
- Wootthikanokkhan, J., Cheachun, T., Sombatsompop, N., Thumsorn, S., Kaabbuathong, N., Wongta, N., Wong-On, J., Isarankura Na Ayutthaya, S., Kositchaiyong, A. (2013). Crystallization and thermomechanical properties of PLA composites: effects of

- additive types and heat treatment. **Journal of Applied Polymer Science**. 129(1): 215-223.
- Wu, S. (1998). A generalized criterion for rubber toughening: The critical matrix ligament thickness. **Journal of Applied Polymer Science**. 35(2):549-561.
- Xavier, A. M. M. (2010). Study of lactic acid polycondensation and lactide production. **Master Thesis**. University of Porto.
- Xu, W. Q., Grabiec, D., and Nehring, R. J. (2005). Polymer nucleating agents: **Google Patents. US6913829 B2**
- Xu, Y-Q., Qu, J-P. (2009). Mechanical and rheological properties of epoxidized soybean oil plasticized poly(lactic acid). **Journal of Applied Polymer Science**. 112: 3185–3191.
- Yamane, H., Sasai, K. (2003). Effect of the addition of poly(D-lactic acid) on the thermal property of poly(L-lactic acid). **Polymer**. 44: 2569–2575.
- Yokohara, T., Yamaguchi, M. (2008). Structure and properties for biomass-based polyester blends of PLA and PBS. **European Polymer Journal**. 44: 677-685.
- Yu, F., Liu, Tao., Zhao, X., Yu, X., Lu, Ai., Wang, J. (2012). Effects of talc on the mechanical and thermal properties of polylactide. **Journal of Applied Polymer Science**. 125: E99–E109.
- Yu, R-L., Zhang, L-S., Fenga, Y-H., Zhang, R-Y., Zhu, Jin. (2014). Improvement in toughness of poly(lactic acid) by melt blending with bio-based poly(ester)urethane. **Chinese Journal of Polymer Science**. 32 (8): 1099–1110.
- Zhang, K., Hai-Ou, Y., Shi, Y-D., Chen, Y-F., Zeng, J-B., Guo, J., Wang, B., Guo, Z. and Wang, M. (2017). Morphological regulation improved electrical conductivity and electromagnetic interference shielding in poly(L-lactide)/poly(e-caprolactone)/

carbon nanotube nanocomposites via constructing stereocomplex crystallites.

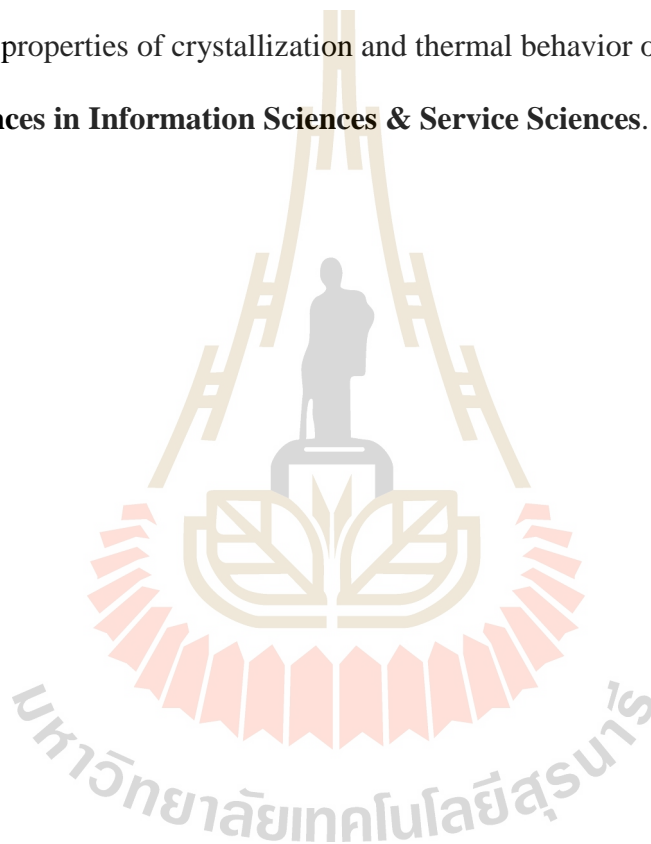
Journal of Materials Chemistry C. 5: 2807—2817.

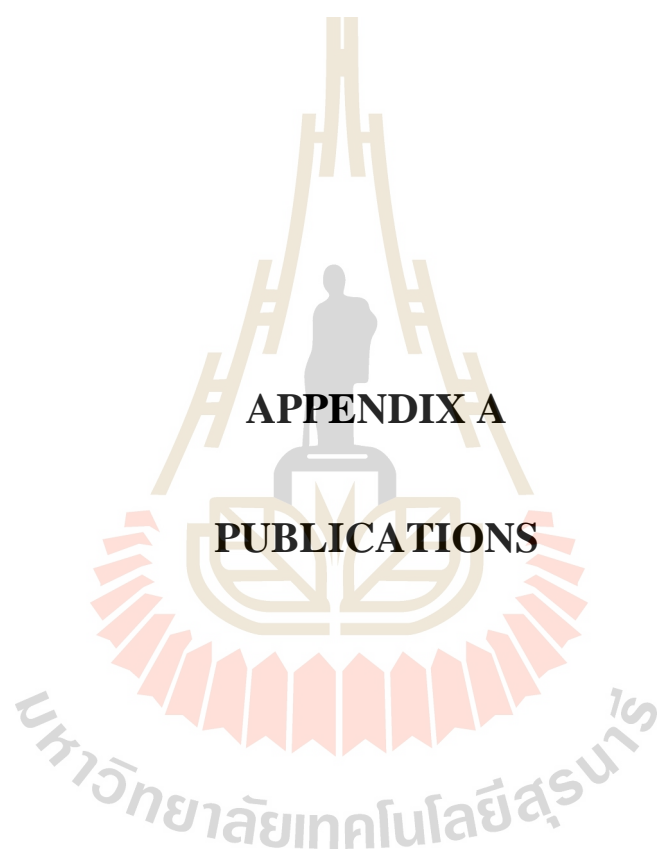
Zhao, Q., Ding, Y., Yang, Biao., Ning, N., Fu, Q. (2013). Highly efficient toughening effect of ultrafine full-vulcanized powdered rubber on poly(lactic acid)(PLA).

Polymer Testing. 32: 299–305.

Zou, J., Wu, J., Li, Z., Wei, Y., Guo Y., Zhang, J. (2012). Effects of poly(d-lactide acid) on the properties of crystallization and thermal behavior of poly(l-lactide acid).

Advances in Information Sciences & Service Sciences. 4(10): 382-392.





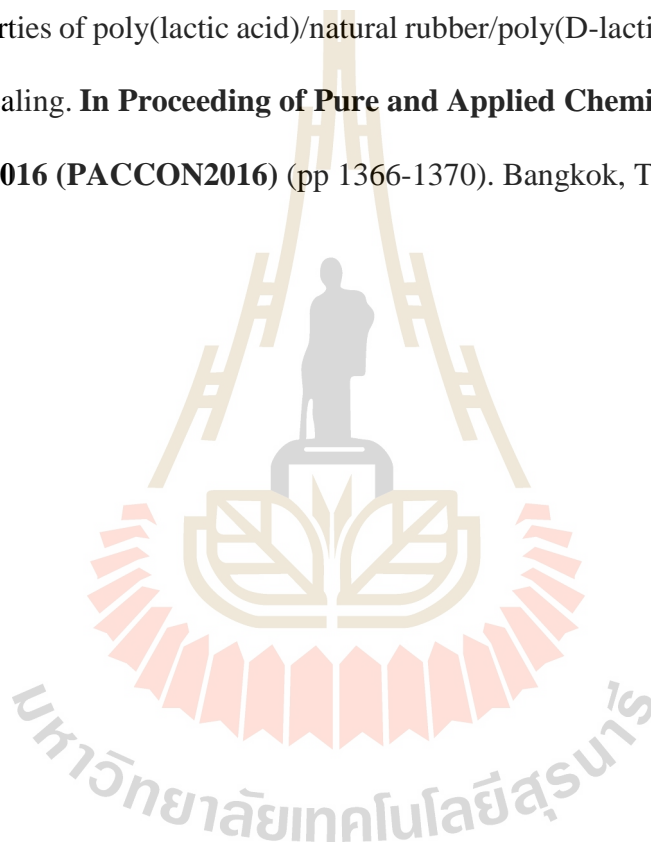
APPENDIX A

PUBLICATIONS

List of Publications

Pongputtipat, W., Ruksakulpiwat, Y and Chumsamrong, P. (2016). Effect of poly(D-lactic acid) on physical of poly (lactic acid)/natural rubber blends. **Suranaree J. Sci. Technol.** 23(2):129-134.

Pongputtipat, W., Ruksakulpiwat, Y and Chumsamrong, P. (2016). Toughness and thermal properties of poly(lactic acid)/natural rubber/poly(D-lactic acid) blends: before and after annealing. **In Proceeding of Pure and Applied Chemistry International Conference 2016 (PACCON2016)** (pp 1366-1370). Bangkok, Thailand.



EFFECT OF POLY(D-LACTIC ACID) ON PHYSICAL PROPERTIES OF POLY(LACTIC ACID)/NATURAL RUBBER BLENDS

Wachirabhorn Pongputtipat^{1,2}, Yupaporn Ruksakulpiwat^{1,2} and Pranee Chumsamrong^{1,2*}

Received: November 05, 2015; Revised: February 05, 2016; Accepted: March 24, 2016

Abstract

In this study, poly(lactic acid) (PLA) was melt blended with a natural rubber (NR) at the ratios of 95/5, 90/10, 85/15, and 80/20 by weight. It was found that the impact strength and elongation at break of PLA/NR blends increased with increasing NR content up to 5 wt%. While tensile strength and Young's modulus decreased. The most significant improvement in Izod impact strength and elongation at break was found for the blend containing 15 wt% NR. Therefore, PLA/NR at a ratio of 85/15 wt% was chosen to study the effect of poly(D-lactic acid) (PDLA) on mechanical properties and heat distortion temperatures (HDT) of PLA/NR blend. The amount of PDLA applied was 1, 3, and 5 percent by weight based on PLA content in the blend. The results showed that impact strength and elongation at break of PLA/NR blend decreased with increasing amount of PDLA. However, the values were still higher than those of pure PLA. HDT of the blend with 1 wt% PDLA based on PLA content was improved in comparison to that of PLA/NR blend and pure PLA.

Keywords: Poly(lactic acid), Poly(D-lactic acid), natural rubber, HDT

Introduction

Poly(lactic acid) (PLA) is a biodegradable polymer derived from renewable resources. PLA provides good strength and easy processability with perfect degradable in most products. However, PLA suffers from low heat distortion temperature (HDT), because its T_g is only 54-60°C and low toughness. Hence, PLA is not suitable for some applications, for example, microwavable trays and hot-fill applications. To achieve high toughness PLA,

¹ School of Polymer Engineering, Institute of Engineering, Suranaree University of Technology, Nakhon Ratchasima 30000, Thailand. E-mail: pthongnoi@sut.ac.th

² Center for Petroleum, Petrochemicals, and Advanced Materials, Chulalongkorn University, Bangkok 10330, Thailand.

* Corresponding author

natural rubber (NR) has been one of desirable impact modifiers for PLA (Bitinis *et al.*, 2011; Bitinis *et al.*, 2012; Juntuek *et al.*, 2011; Pongtanayut *et al.*, 2013). The rubber particles behave as stress concentrators enhancing the fracture energy absorption of brittle polymers and ultimately result in a material with improved toughness (Pongtanayut *et al.*, 2013). NR exhibits a unique combination of toughness, flexibility and biodegradability that together with its low cost makes it an ideal candidate to improve the brittleness of PLA. HDT of a polymeric material is an index of its heat resistance towards applied load. There are several ways to improve HDT of PLA such as blending with a high thermal stability polymer, addition of high thermal stability filler. Moreover, the easy way to increase the HDT value of polymer is to increase the crystallinity of PLA. Interestingly, in the 1980s, it was found that an equivalent mixture of poly (L-lactic acid) (PLLA) and poly(D-lactic acid) (PDLA) formed a stereocomplex. The stereocomplex has a melting temperature, T_m , of 230°C that was approximately 50°C higher than the T_m of either PLLA or PDLA (Ikada *et al.*, 1987). This significant increase in melting temperature was due to the strong van der Waals interactions in the stereocomplex crystalline structure (Brizzolara *et al.*, 1996). Tsuji *et al.* investigated the isothermal and non-isothermal crystallization behavior of PLLA blend with a small amount of PDLA (0.1–10 wt%). The higher PDLA content was in PLLA matrix, the faster crystallization rate was gained, which revealed that PDLA was an effective nucleating agent for PLLA. The stereocomplex crystallites were consistent

with the increased content of the PDLA (Tsuji *et al.*, 2006). Therefore, in the present work, PLA was blended with NR first in order to obtain high toughness PLA. High toughness and high HDT blend was expected to achieve after the addition of PDLA.

Materials and Methods

Materials

Poly(lactic acid) (PLA, 4043D) was supplied from Nature works LLC. Poly (D-lactic acid) (PDLA) was provided by Department of Chemistry, Chiang Mai University. Natural rubber (STR 5L) was purchased from Thai Hua Rubber Co., Ltd.

Preparation of Blends

PLA blends were prepared using an internal mixer (Hakke Rheomix) at the temperature of 170°C with a rotor speed of 60 rpm for 10 min. Before mixing, PLA and PDLA were dried in an oven at 70°C for 4 h. The compositions in percentage by weight (wt%) of all blends are shown in Table 1. After mixing in an internal mixer, the blend specimens were prepared by compression molding machine (LabTech, LP20-B) at melting temperature of 170°C.

Mechanical and HDT Analysis

The unnotched and notched Izod impact test were performed according to ASTM D256 using an impact testing machine (Instron). Tensile properties were obtained according to ASTM D638 using an Instron universal testing machine with a load cell of 5 kN and a crosshead speed of 10 mm/min.

Table 1. Blend compositions

Code	PLA (wt%)	NR (wt%)	PDLA (wt%) ^a
PLA	100	-	-
PLA/NR (95/5)	95	5	-
PLA/NR (90/10)	90	10	-
PLA/NR (85/15)	85	15	-
PLA/NR (80/20)	80	20	-
PLA/NR/PDLA (1)	84.15	15	0.85 (1) ^a
PLA/NR/PDLA (3)	82.45	15	2.55 (3) ^a
PLA/NR/PDLA (5)	80.75	15	4.25 (5) ^a

^a wt% of PDLA based on the amount of PLA in the blends.

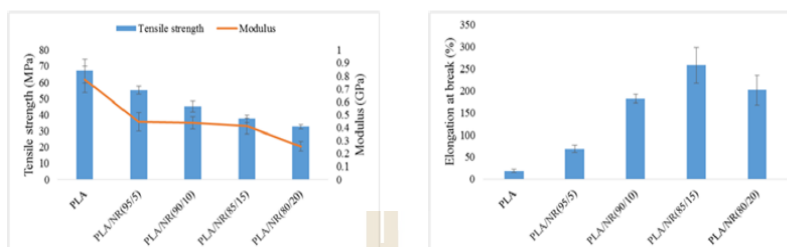


Figure 1. Tensile strength and Young's modulus of PLA, PLA/NR blends at various NR contents

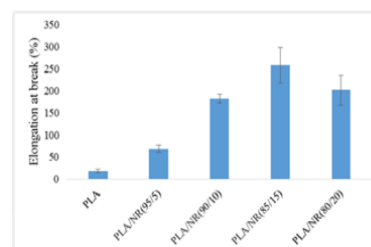


Figure 2. Elongation at break of PLA, PLA/NR blends at various NR contents

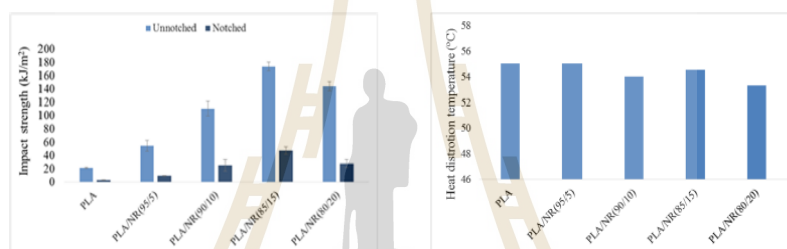


Figure 3. Izod impact strength of PLA, PLA/NR blends at various NR contents

Figure 4. Heat distortion temperatures of PLA, PLA/NR blends at various NR contents

The heat distortion temperature of PLA, and PLA/NR, PLA/NR/PDLA blends was measured using a HDT/VICAT manual heat deflection tester (model HDV1). The dimension of the test bars was 127 mm × 13 mm × 3 mm and the test procedure was conformed to the ASTM D648 standard. The loading pressure was 0.455 MPa (66 psi) and samples were heated at a rate of 2°C/min from room temperature.

Results and Discussion

Effect of NR Content on Mechanical Properties and HDT of PLA

Figure 1 shows the tensile strength and Young's modulus of PLA, PLA/NR blends at various NR contents. Modulus and tensile strength of PLA/NR decreased with increasing NR content. The reduction in these mechanical properties was due to the result of the rubbery nature of NR. Also, the reduced PLA phase in

the blend and the poor interfacial adhesion between PLA and NR may be the reasons for a decrease in tensile strength and Young's modulus (Xu *et al.*, 2014). Elongation at break of PLA and PLA/NR blends is shown in Figure 2. Elongation at break was increased from 18.54% for neat PLA to 257.85% for PLA/NR (85/15).

Figure 3 shows the unnotched and notched Izod impact strength of PLA, PLA/NR blends at various NR contents. Notched condition was designed to reduce the toughness of materials. In the other words, the notched condition gives much lower absorbed energy to the samples (Tjong *et al.*, 1996). Hence, Notch specimen is better measure the resistance of the polymer to crack propagation and we can determine how resistant the specimen absorbs energy when given some defects on it. The unnotched and notched Izod impact strength of neat PLA were 20.70 and 2.91 kJ/m², respectively. Impact strength of PLA/NR blends increased with increasing NR content up to 15 wt%. When

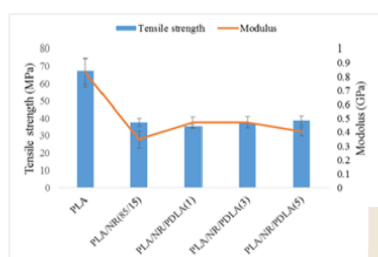


Figure 5. Tensile strength and Young's modulus of PLA, PLA/NR(85/15) and PLA/NR/PDLA blends

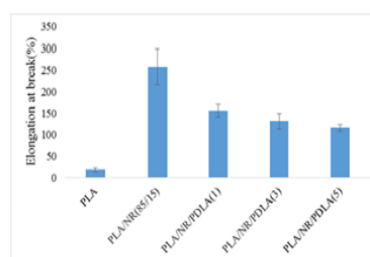


Figure 6. Elongation at break of PLA, PLA/NR (85/15) and PLA/NR/PDLA blends

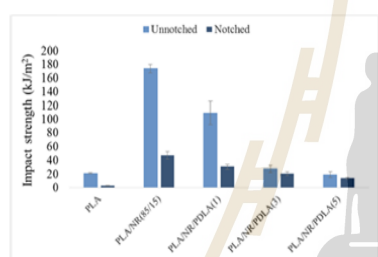


Figure 7. Izod impact strength of PLA, PLA/NR(85/15) and PLA/NR/PDLA blends

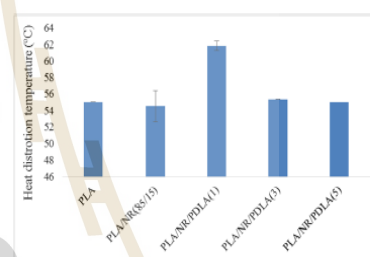


Figure 8. HDT of PLA, PLA/NR (85/15) and PLA/NR/PDLA blends

NR content was 15 wt%, unnotched and notched izod impact strength of the PLA/NR blend were 167.22 and 54.31 kJ/m², respectively. When NR content was increased to 20 wt%, unnotched and notched Izod impact strength of PLA/NR blend were decreased to 139.09 and 28.05 kJ/m², respectively. However, this value was still higher than that of neat PLA. The high flexibility of NR resulted in more energy absorption.

Figure 4 shows the values of heat distortion temperatures for the PLA and PLA/NR blends. Generally, the heat distortion temperature decreased as NR content increased. The decrease of HDT of PLA/NR blend could be resulted from soft NR phase. Furthermore, the incorporation of NR into the PLA decreased stiffness of specimens.

Effect of PDLA Content on Mechanical Properties and HDT of PLA/NR Blend

To study the effect of PDLA content on

mechanical properties of PLA/NR blends, NR content was fixed at 15 wt% according to the highest impact strength of PLA/NR (85/15) blend. The total amount of PLA and PDLA in the blend was kept constant at 85 wt% and the PDLA content in the blends was designed to be 1, 3, and 5 wt% based on the amount of PLA. Therefore, the ratios of PLA to PDLA were 84.15/0.85, 82.45/2.55, and 80.75/4.25 wt% as shown in Table 1.

Figure 5 shows the tensile strength and Young's modulus of PLA, PLA/NR and PLA/NR/PDLA blends at various PDLA contents. Modulus and tensile strength of PLA/NR/PDLA increased with increasing PDLA content. This indicated that PDLA could enhance stiffness of PLA/NR blends (Tsuji and Ikada, 1999; Sarasua *et al.*, 2005).

Elongation at break of PLA, PLA/NR and PLA/NR/PDLA blends is shown in Figure 6. Elongation at break was decreased with an increase in PDLA content. The lowest

Table 2. Tensile strength, modulus, and elongation at break of PLA, PLA/NR and PLA/NR/PDLA blends

Sample	Tensile strength (MPa)	Modulus (GPa)	Elongation at break (%)
PLA	67.11 ± 7.23	0.83 ± 0.10	18.54 ± 3.66
PLA/NR(95/5)	55.15 ± 2.42	0.52 ± 0.07	68.54 ± 8.64
PLA/NR(90/10)	45.15 ± 3.43	0.44 ± 0.04	182.35 ± 9.67
PLA/NR(85/15)	37.63 ± 2.30	0.35 ± 0.06	257.85 ± 40.83
PLA/NR(80/20)	32.65 ± 1.29	0.31 ± 0.04	201.99 ± 33.66
PLA/NR/PDLA(1)	35.30 ± 2.30	0.47 ± 0.03	156.14 ± 14.83
PLA/NR/PDLA(3)	37.44 ± 0.21	0.47 ± 0.04	131.43 ± 17.79
PLA/NR/PDLA(5)	38.87 ± 2.66	0.40 ± 0.03	115.81 ± 8.18

Table 3. Izod impact strength and HDT of PLA, PLA/NR and PLA/NR/PDLA blends

Sample	Izod impact strength (J/m ²)		HDT (°C)
	Unnotched	Notched	
PLA	21.16 ± 0.94	2.85 ± 0.15	55.0
PLA/NR(95/5)	56.19 ± 13.98	9.12 ± 0.83	55.0
PLA/NR(90/10)	110.16 ± 11.15	25.22 ± 8.65	54.0
PLA/NR(85/15)	173.34 ± 6.49	46.95 ± 5.65	54.5
PLA/NR(80/20)	143.94 ± 6.87	27.44 ± 5.99	53.3
PLA/NR/PDLA(1)	108.68 ± 17.22	30.20 ± 3.59	61.8
PLA/NR/PDLA(2)	27.38 ± 5.07	20.71 ± 2.18	55.3
PLA/NR/PDLA(3)	19.18 ± 4.21	13.71 ± 1.38	55.0

elongation at break of 115.81 ± 8.18 % was found for PLA/NR/PDLA(5). However, it was significantly higher than that of pure PLA.

Figure 7 shows the unnotched and notched Izod impact strength of the PLA, PLA/NR and PLA/NR/PDLA blends. The unnotched and notched Izod impact strength were 20.70 and 2.91 kJ/m² for neat PLA and 173.34 and 46.95 kJ/m² for PLA/NR (85/15), respectively. When PDLA was added into PLA/NR blend, unnotched and notched Izod impact strength of PLA/NR/PDLA were decreased. The reduction of impact strength and elongation at break indicated that PLA/NR/PDLA blend was more rigid but less toughness than PLA/NR (85/15).

HDTs for the PLA, PLA/NR and PLA/NR/PDLA blends are shown in Figure 8. The HDT of PLA/NR blend containing 1 wt% PDLA based on the amount of PLA was higher than that of neat PLA. It might be because of high crystallinity and small spherulite size of PLA/NR/PDLA(1) (Tang *et al.*, 2012).

The summaries of tensile strength, modulus, and elongation at break of PLA and

all blends are shown in Table 2. Table 3 shows Izod impact strength and HDT of PLA and all blends.

Conclusions

Impact strength of PLA was found to be dramatically improved with the addition of 15 wt% NR. At this content, unnotched and notched Izod impact strength were higher than those of pure PLA about 7 and 10 times, respectively. However, tensile strength and Young's modulus of the blends decreased with increasing NR content. When 1 wt% PDLA based on PLA content was incorporated into PLA/NR blend, HDT of PLA/NR blend was significantly improved. On the other hand, the impact strength and elongation at break of PLA/NR blend decreased with an increase of PDLA content. Nevertheless, with an exception of unnotched Izod impact strength, the values were still higher than those of neat PLA. Hence, the addition of PDLA at 1 wt% based

on PLA content into PLA/NR blend led to the blend with higher impact strength and HDT compared to neat PLA.

Acknowledgements

Financial support from National Research Council of Thailand and Center of Excellence on Petrochemical and Materials Technology, Chulalongkorn University, Thailand is gratefully acknowledged.

References

- Bitinis, N., Verdejoa, R., Cassagnau, P., and Lopez-Manchadao, M.A. (2011). Structure and properties of polylactide/natural rubber blends. *Mater. Chem. Phys.*, 129(3):823-831.
- Bitinis, N., Sanz, A., Nogales, A., Verdejoa, R., Lopez-Manchadao, M.A., and Ezquerra, T.A. (2012). Deformation mechanisms in polylactic acid/natural rubber/organoclay bionanocomposites as revealed by synchrotron X-ray scattering. *Soft Matter*, 8(34):8990-8997.
- Brizzolara, D., Cantow, H.J., Diederichs, K., Keller, E., and Domb, A.J. (1996). Mechanism of the stereocomplex formation between enantiomeric poly(lactide)s. *Macromolecules*, 29(1):191-197.
- Ikada, Y., Jamshidi, K., Tsuji, H., and Hyon, S.H. (1987). Stereocomplex formation between enantiomeric poly(lactides). *Macromolecules*, 20(4):904-906.
- Juntuek, P., Ruksakulpiwat, C., Chumsamrong, P. and Ruksakulpiwat, Y. (2011). Effect of glycidyl methacrylate-grafted natural rubber on physical properties of polylactic acid and natural rubber blends. *J. Appl. Polym. Sci.*, 125(1):745-754.
- Pongtanayut, K., Thongpin, C., and Santawitee, O. (2013). The effect of rubber on morphology, thermal properties and mechanical properties of PLA/NR and PLA/ENR blends. *Energy Procedia.*, 34:888-897.
- Tang, Z., Zhang, C., Liu, X., and Zhu, J. (2012). The crystallization behavior and mechanical properties of polylactic acid in the presence of a crystal nucleating agent. *J. Appl. Polym. Sci.*, 125(2): 1108-1115.
- Tjong, S.C., Chen, J.S., and Liu, S.L. (1996). Structural properties and impact fracture behavior of injection molded blends of liquid crystalline copolyester and modified poly(phenylene oxide). *Polymer Eng. Sci.*, 36(6):797-806.
- Tsuji, H. and Ikada, Y. (1999). Stereocomplex formation between enantiomeric poly(lactic acid)s. XI. Mechanical properties and morphology of solution-cast films. *Polymer*, 40(25):6699-6708.
- Tsuji, H., Takai, H., and Saha, S.K. (2006). Isothermal and non-isothermal crystallization behavior of poly (l-lactic acid): Effects of stereocomplex as nucleating agent. *Polymer*, 47(11):3826-3837.
- Sarasua, J.R., Arraiza, A.L., Balerdi, P., and Maiza, I. (2005). Crystallinity and mechanical properties of optically pure polylactides and their blends. *Polym. Eng. Sci.*, 45(5):745-753.
- Xu, C., Yuan, D., Fu, L., and Chen, Y. (2014). Physical blend of PLA/NR with co-continuous phase structure: Preparation, rheology property, mechanical properties and morphology. *Polymer Testing*, 37:94-101.

Toughness and thermal properties of poly(lactic acid)/natural rubber/poly(D-lactic acid) blends: Before and after annealing

Wachirabhorn Pongputtipat,^{1,2} Yupaporn Ruksakulpiwat,^{1,2} Pranee Chumsamrong*^{1,2}

¹School of Polymer Engineering, Institute of Engineering, Suranaree University of Technology, Nakhon Ratchasima 30000, Thailand

²Center of Excellence on Petrochemical and Materials Technology, Chulalongkorn University, Bangkok 10330, Thailand

*e-mail: pthongnoi@sut.ac.th

Abstract:

From our study, it was found that impact strength and elongation at break of PLA significantly improved by blending with 15 weight percent (wt%) natural rubber (NR). However, heat distortion temperature (HDT) of the blend was slightly decreased. Poly(D-lactic acid) (PDLA) that could act as nucleating agent for PLA¹ was then added to PLA/NR (85/15 wt%) blend in an amount of 1, 3 and 5 wt% based on PLA content. The impact strength of PLA/NR/PDLA blends was tended to reduce with an increase of PDLA content but it was still higher than that of pure PLA. HDT of PLA/NR blend was enhanced after the addition of 1 wt% PDLA. The crystallinity and thermal transitions of PLA/NR/PDLA blends were examined using differential scanning calorimeter (DSC). It was found that crystallinity of the blends was higher than pure PLA and the melting temperature (T_m) of PLA in the blend was also shifted to higher temperature. To observe the effects of annealing treatment on the properties of the blends, the blend specimens were annealed in an air oven at 100 °C for 10, 30 and 60 minutes. Impact strength, crystallinity and HDT of PLA/NR/PDLA blends after annealing were investigated and found that the values were significantly changed.

1. Introduction

Nowadays, biodegradable thermoplastic poly(lactic acid) (PLA) has been widely used in industrial applications, such as in automotive, in medical applications and especially in food packaging applications. It exhibits the environmental friendliness, good clarity, high strength and modulus. However, the drawbacks of PLA are the poor toughness and low heat distortion temperature (HDT). Thus, in order to broaden the applications of PLA, material properties has to be improved. The improvement of toughness can be done by adding the rubber material into polymer matrix.²⁻⁵ The rubber particles behave as stress concentrators enhancing the fracture energy absorption of brittle polymers and ultimately result in a material with improved toughness.⁵ HDT of PLA is very low and is known to be around T_g of PLA (55–60 °C), because the

crystallinity is very low under practical molding conditions due to the low crystallization rate of PLA at a high cooling rate.⁶⁻⁹ There are several methods to improve HDT of PLA such as the addition of crystal nucleating agent, blending PLA with a high HDT polymer and the addition of natural fiber and inorganic filler. In the work of Tang et al., PLA was blended with ethylenebis(hydroxy stearamide) (EBH) crystal nucleating agent, which showed significant increase in crystallinity and HDT.¹⁰ Wang et al. blended PLA with PC and used epoxy as a compatibilizer and tetra-n-butylammonium bromide (TBAB) as a catalyst. The HDT of PLA/PC/EP blends increased with an increase of compatibility of the blend.¹¹ Shi et al. compounded PLA with bamboo fiber and talc. The HDT of composites increased when transcrystallization occurred. Trans-

crystallization was observed in PLA composite with loading BF and talc simultaneously.¹²

One interesting attribute of PLA is the ability of enantiomeric blends of PLLA and PDLA to form a stereocomplex with high crystal stability and crystalline ability.¹³ The stereocomplex has a melting temperature ($T_m=230$ °C) that was approximately 50°C higher than the T_m of either PLLA or PDLA.¹⁴ This significant increase in melting temperature was due to the strong van der Waals interactions in the stereocomplex crystalline structure.¹⁵

In this work, the effects of PDLA content and annealing treatment on the toughness and thermal properties of PLA, toughened by NR was studied. Crystallinity of PLA matrix was expected to be increase after the addition of PDLA and after annealing process. There for, PLA with high toughness and HDT could be obtained.

2. Materials and Methods

2.1 Materials

Poly(lactic acid) (PLA, 4043D) was supplied from Nature works LLC. Poly (D-lactic acid) (PDLA) was provided by Department of Chemistry, Chiang Mai University. Natural rubber (STR 5L) was purchased from Thai Hua Rubber Co., Ltd.

2.2 Preparation of blends

PLA blends were prepared using an internal mixer (Hakke Rheomix) at the temperature of 170 °C with a rotor speed of 60 rpm for 10 min. Before mixing, PLA and PDLA were dried in an oven at 70 °C for 4 h. The compositions in percentage by weight (wt%) of all blends are shown in Table 1. After mixing in an internal mixer, the blend specimens were prepared by compression molding machine (LabTech, LP20-B) at melting temperature of 170 °C. To observe the effects of annealing treatment on the properties of the blends, compression molded HDT bars and impact bars will be annealed in an air oven at 100 °C for 10, 30 and 60 min.

2.3 Characterization of impact and thermal properties of PLA and PLA blends

The unnotched Izod impact test was performed according to ASTM D256 in Izod mode using an impact testing machine (Instron).

Table 1. Blend compositions.

Code	PLA (wt%)	NR (wt%)	PDLA (wt%)
PLA	100	-	-
PLA/NR (85/15)	85	15	-
PLA/NR/PDLA (1)	84.15	15	0.85 (1) ^a
PLA/NR/PDLA (3)	82.45	15	2.55 (3) ^a
PLA/NR/PDLA (5)	80.75	15	4.25 (5) ^a

^awt% of PDLA based on the amount of PLA in the blends

The heat distortion temperature of PLA, PLA/NR and PLA/NR/PDLA blends was measured using a HDT/VICAT manual heat deflection tester (model HDV1). The dimension of the test bars was 127 mm × 13 mm × 3 mm and the test procedure was conformed to the ASTM D648 standard. The loading pressure was 0.455 MPa (66 psi) and samples were heated at a rate of 2 °C/min from room temperature.

Differential scanning calorimeter (Netzsch, DSC 204F1) was used to determine degree of crystallinity (X_c), cold crystallization (T_{cc}), and melting temperature (T_m). All samples were heated from 25-200 °C at the rate of 5 °C/min (the first heating). The following equation was used to calculate the degree of crystallinity within the samples:

$$\% \text{Crystallinity} = X_c = 100 \times \frac{\Delta H_m - \Delta H_c}{\Delta H_m^\infty}$$

where ΔH_m is the measured endothermic enthalpy of melting and ΔH_c is the cold crystallization exothermic enthalpy during the heating scans. The theoretical melting enthalpy of 100% crystalline PLA was taken to be $\Delta H_m^\infty = 93.6$ J/g.¹⁰

3. Results & Discussion

3.1 Impact strength of PLA, PLA/NR and PLA/NR/PDLA blends

Figure 1 presents the impact strength of PLA, PLA/NR and PLA/NR/PDLA blends before and after annealing. The amount of PDLA applied were 1, 3 and 5 wt% based on PLA content in the blend. The results showed that unnotched Izod impact strength before annealing of PLA/NR(85/15) blend was 167.22 kJ/m², whereas it was only 20.70 kJ/m² for pure PLA. After the addition of PDLA, the decrease in impact strength with increasing PDLA content was obtained. The reduction of impact strength indicated that PLA/NR/PDLA blend was more rigid but less toughness than PLA/NR (85/15) blend. After annealing, the impact strength of all blends was still higher than that of PLA. This suggested that NR still showed a toughening effect for PLA under annealing. PLA/NR and PLA/NR/PDLA(1) blends showed a reduction of impact strength after annealing for 10 min. However, when the annealed time was increased from 10 min to 30 and 60 min, the impact strength of PLA/NR and PLA/NR/PDLA(1) was improved. This might be due to longer annealing time resulting in a change of crystal structure and rubber particle size in the blends.¹⁶ On the other hand, impact strength of PLA/NR/PDLA(3) and PLA/NR/PDLA(5) was improved after annealing. The crystallinity, crystal structure and the size of rubber particle in PLA/NR/PDLA(3) and PLA/NR/PDLA(5) blends might be at the optimum.¹⁶

3.2 Thermal properties of PLA, PLA/NR and PLA/NR/PDLA blends

Table 2 shows the DSC results from first heating scan of PLA, PLA/NR and PLA/NR/PDLA blends before and after annealing. The results showed that cold crystallization peak for all the samples disappeared after annealing, indicating that all these samples were completely crystallized during annealing

treatment.^{17,18} However, cold crystallization peak of PLA/NR/PDLA(1) disappeared before and after annealing. It might be because PLA/NR/PDLA(1) was completely crystallized during the sample preparation process. In addition, it was found that degree of crystallinity of PLA/NR/PDLA- (1) before and after annealing were not significantly changed. Melting temperature (T_m) of PLA/NR and PLA/NR/PDLA blends was increased after annealing. The presence of two melting peaks in PLA could be related to the formation of different crystal structures. Melting peak appeared at higher temperature belongs to more perfect crystalline structure.¹⁹ The degree of crystallinity (%XC) of neat PLA, PLA/NR and PLA/NR/PDLA blends are listed in Table 2. The %XC of neat PLA, PLA/NR, PLA/NR/PDLA(1), PLA/NR/PDLA(3) and PLA/NR/PDLA(5) blends before annealing are 1.36, 1.80, 25.25, 1.83 and 1.53 %, respectively. In general, the degree of crystallinity of all samples increased as an increase of annealing time. However, the degree of crystallinity of PLA/NR and PLA/NR/PDLA blends was constant after annealing for 10 minutes.

Figure 2 shows the HDTs of the PLA, PLA/NR and PLA/NR/PDLA blends before and after annealing. The HDT of PLA/NR blend containing 1 wt% PDLA based on the amount of PLA before annealing treatment was the highest. After annealing, HDTs of all samples increased with an increase of the annealing time. This improvement is mainly due to the increase in crystallinity. Nevertheless, after annealing, HDT of PLA/NR/PDLA blends was not higher than PLA.

4. Conclusion

Impact strength of PLA was found to be significantly improved with the addition of 15 wt% NR. At this content, unnotched Izod impact strength were higher than those of pure PLA about 7 times. The impact strength of PLA/NR/

PACCON Proceedings 2016: Polymer Chemistry (POL-3477)

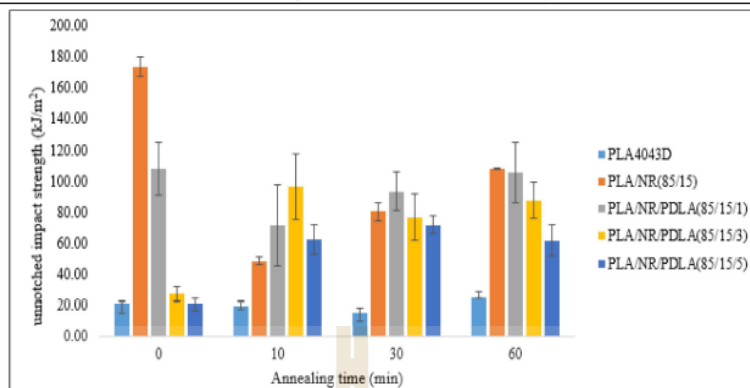


Figure 1. Unnotched Izod impact strength of the PLA, PLA/NR and PLA/NR/PDLA blend.

Table 2. DSC data of PLA, PLA/NR/PDLA blends before and after annealing treatment.

code	Annealing time (min)	First heating				
		Tc (°C)	Tm(°C)	ΔHc (J/g)	ΔHm(J/g)	%Xc
PLA	0	98.6	146.2/155.6	25.16	26.47	1.40
	10	-	149.1/156.1	0	24.14	25.79
	30	-	149.4/155.7	0	25.61	27.36
	60	-	148.2/154.9	0	27.07	28.92
PLA/NR(85/15)	0	104.1	149.6/157.0	25.16	26.89	1.85
	10	-	147.8/155.7	0	24.74	26.43
	30	-	149.4/155.7	0	24.55	26.23
	60	-	150.8/154.8	0	24.15	25.80
PLA/NR/PDLA(1)	0	-	153.8	0	24.32	25.98
	10	-	156.4	0	21.94	23.44
	30	-	155.4	0	21.35	22.81
	60	-	155.2	0	21.79	23.28
PLA/NR/PDLA(3)	0	102.4	149.1/155.7	18.96	20.72	1.88
	10	-	149.2/155.3	0	19.89	21.25
	30	-	149.5/156.4	0	19.7	21.05
	60	-	149.1/155.6	0	17.93	19.16
PLA/NR/PDLA(5)	0	104.8	155.9	15.91	17.38	1.57
	10	-	147.4/154.8	0	18.36	19.62
	30	-	148.7/155.9	0	18.61	19.88
	60	-	149.4/157	0	18.57	19.84

PDLA blends was reduced with an increase of PDLA content.

However, it was still higher than that of pure PLA. After annealing, it was found that impact strength of PLA, PLA/NR and PLA/NR/PDLA(1) was decreased, whereas impact strength of

PLA/NR/PDLA(3) and PLA/NR/PDLA(5) was improved. HDTs and degree of crystallinity of PLA, PLA/NR and PLA/NR/PDLA blends increased as an increase of annealing time.

PACCON Proceedings 2016: Polymer Chemistry (POL-3477)

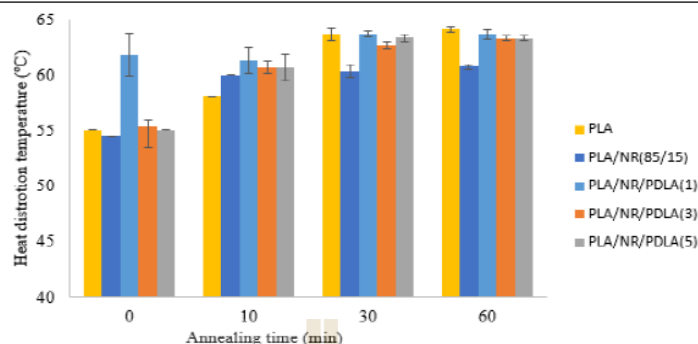


Figure 2. HDTs of PLA, PLA/NR and PLA/NR/PDLA blends.

Acknowledgements

The authors would like to thank National Research Council of Thailand and Center of Excellence on Petrochemical and Materials Technology, Chulalongkorn University, Thailand for the financial support.

References

- Shi, X.; Zhang, G.; Phuong, T. V.; Lazzeri, A. *Molecules* **2015**, *20*, 1579–1593.
- Bitinis, N.; Verdejo, R.; Cassagnau, P.; Lopez-Manchado, M. A. *Mater. Chem. Phys.* **2011**, *129*, 823–831.
- Juntuek, P.; Ruksakulpiwat, C.; Chumsamrong, P.; Ruksakulpiwat, Y. *J. Appl. Polym. Sci.* **2011**, *125*, 745–754.
- Bitinis, N.; Verdejo, R.; Cassagnau, P.; Lopez-Manchado, M. A. *Soft Matter* **2012**, *8*, 8990–8997.
- Pongtanayut, K.; Thongpin, C.; Santawitee, O. *Energy Procedia* **2013**, *34*, 888–897.
- Tsuji, H.; Ikada, Y. *Polymer* **1995**, *36*, 142709–2716.
- Baiardo, M.; Frisoni, G. *J. Appl. Polym. Sci.* **2003**, *90*, 1731–1738.
- Jiang, L.; Zhang, J. *Polymer* **2007**, *48*, 7632–7644.
- Liu, H.; Zhang, J. *Macromolecules* **2011**, *44*, 1513–1522.
- Tang, Z.; Zhang, C.; Liu, X.; Zhu, J. *J. Appl. Polym. Sci.* **2012**, *125*, 1108–1115.
- Wang, Y.; Chiao, S. M.; Hung, T-F.; Yang, S-Y. *J. Appl. Polym. Sci.* **2012**, *125*, E402–E412.
- Shi, Q. F.; Mou, H. Y.; Li, Q. Y.; Wang, J. K.; Guo, W. H. *J. Appl. Polym. Sci.* **2012**, *123*, 2828–2836.
- Chen, G-X.; Kim, H-S.; Shim, J-H.; Yoon, J-S. *Macromolecules* **2005**, *38*, 3738–3744.
- Ikada, Y.; Jamshidi, K. *Macromolecules* **1987**, *20*, 904–906.
- Brizzolara, D.; Cantow, H. J.; Diederichs, K.; Keller, E.; Domb, A. *J. Macromolecules* **1996**, *29*, 191–197.
- Meng, W.; Zhiqiang, W.; Ke, W.; Qin, Z.; Qiang, F. *Polymer* **2014**, *55*, 6409–6417.
- Narita, J.; Katagiri, M.; Tsuji, H. *Macromol. Mater. Eng.* **2011**, *296*, 887–893.
- Hu, Y.; Hu, Y.; Topolkarayev, V.; Hiltner, A.; Baer, E. *Polymer* **2003**, *44*, 5681–5689.
- Sarasua, J.-R.; Prud'homme, R. E.; Wisniewski, M.; Borgne, A. L.; Spassky, N. *Macromolecules* **1998**, *31*, 3895–3905.

BIOGRAPHY

Miss Wachirabhorn Pongputthipat was born on April 14, 1988 in Udon Thani, Thailand. She finished high school from Prakhonchai Pittayakhon School in 2006. She graduated her Bachelor's Degree in Science and Rubber Technology from Ubon Ratchathani University (UBU) in 2011. After that, she then continued her Master's degree in Polymer Engineering at School of Polymer Engineering, Institute of Engineering, Suranaree University of Technology. During her master's degree study, she gave oral presentations in the topic of **“Effect of poly(D-lactic acid) on physical of poly (lactic acid)/natural rubber blends”** in the 41th Congress on Science and Technology of Thailand (STT 41) in Nakhon Ratchasima, Thailand and **“Toughness and thermal properties of poly(lactic acid)/natural rubber/poly(D-lactic acid) blends: before and after annealing”** in the Pure and Applied Chemistry International Conference 2016 in (PACCON2016) Bangkok, Thailand.

มหาวิทยาลัยเทคโนโลยีสุรนารี